

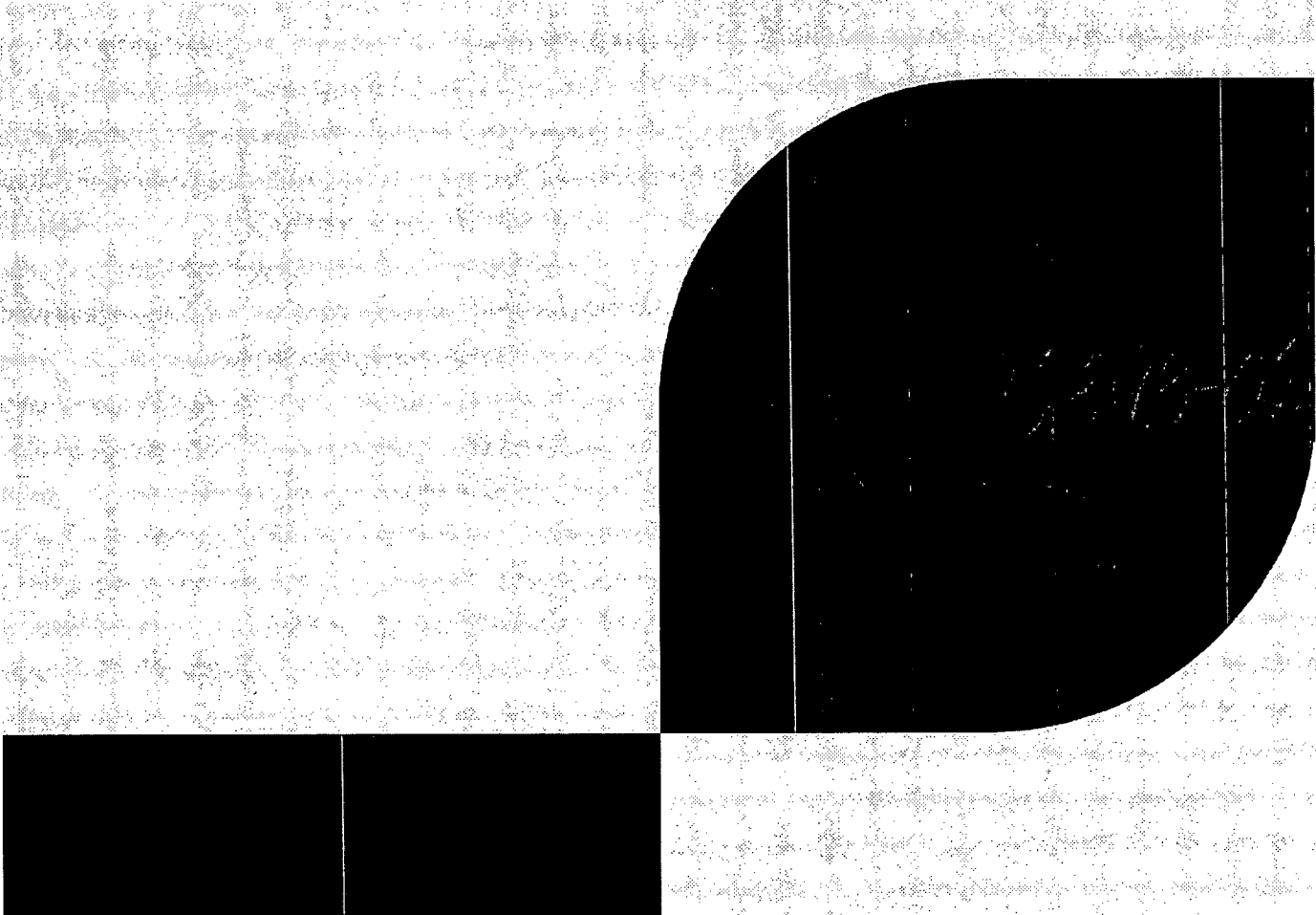
**Enclosure 5**

**AREVA Report ANP-3113(NP)**

**Monticello Nuclear Plant Spent Fuel Storage Pool Criticality Safety Analysis  
for ATRIUM™ 10XM Fuel  
Revision 0**

**Non-Proprietary**

**150 pages follow**



ANP-3113(NP)  
Revision 0

Monticello Nuclear Plant  
Spent Fuel Storage Pool Criticality  
Safety Analysis for ATRIUM™ 10XM Fuel

August 2012



# Controlled Document

AREVA NP Inc.

ANP-3113(NP)  
Revision 0

**Monticello Nuclear Plant  
Spent Fuel Storage Pool Criticality Safety Analysis for  
ATRIUM™ 10XM Fuel**

sj

# Controlled Document

AREVA NP Inc.

ANP-3113(NP)  
Revision 0

Copyright © 2012

AREVA NP Inc.  
All Rights Reserved

# Controlled Document

Monticello Nuclear Plant Spent Fuel Storage Pool  
Criticality Safety Analysis for ATRIUM™ 10XM Fuel

ANP-3113(NP)  
Revision 0  
Page i

## Nature of Changes

Item	Page	Description and Justification
1.	All	This is the initial release.

# Controlled Document

## Contents

1.0	Introduction .....	1-1
2.0	Summary and Conclusions.....	2-1
3.0	Regulatory Criticality Safety Criteria and Guidance .....	3-1
4.0	Fuel and Storage Array Description.....	4-1
4.1	Fuel Assembly Design .....	4-1
4.2	Fuel Storage Racks .....	4-1
5.0	Calculation Methodology .....	5-1
5.1	Area of Applicability .....	5-2
6.0	Modeling Options and Assumptions .....	6-1
6.1	Geometric Modeling of the High Density Boral Rack.....	6-1
6.1.1	Single Cell Model Description .....	6-1
6.1.2	Explicit Storage Cell Model Description.....	6-2
6.1.3	Explicit Rack Model Description .....	6-2
6.1.4	Reactivity Comparison of the Boral Rack Models.....	6-2
6.2	Fuel Assembly Modeling .....	6-3
6.3	Co-Resident Fuel Racks .....	6-3
6.4	General CASMO-4 Modeling Assumptions .....	6-4
7.0	Criticality Safety Analysis.....	7-1
7.1	Definition of the Reference Bounding and REBOL Lattices.....	7-2
7.2	Storage Array Reactivity .....	7-3
7.3	Arrays of Mixed BWR Fuel Types .....	7-3
7.4	Other Conditions.....	7-4
7.4.1	Assembly Rotation .....	7-4
7.4.2	Assembly Lean .....	7-4
7.4.3	Blister Formation.....	7-5
7.5	Normal Fuel Handling .....	7-5
7.6	Accident Conditions .....	7-6
7.7	Manufacturing and Other Uncertainties.....	7-9
7.8	Determination of Maximum Rack Assembly k-eff ( $k_{95/95}$ ) .....	7-10
8.0	References.....	8-1
Appendix A	Sample CASMO-4 Input .....	A-1
Appendix B	Reactivity Comparison for Assemblies Used in the Monticello Reactor.....	B-1
Appendix C	KENO V.a Bias and Bias Uncertainty Evaluation .....	C-1
Appendix D	CASMO-4 Qualification for In-Rack Modeling .....	D-1

# Controlled Document

## Tables

2.1	Criticality Safety Limitations for ATRIUM 10XM Fuel Assemblies Stored in the Monticello Plant Spent Fuel Storage Pool.....	2-4
3.1	Compliance with Interim Staff Guidance Document DSS-ISG-2010-01 Rev. 0.....	3-5
4.1	ATRIUM 10XM Fuel Assembly Parameters.....	4-3
4.2	Fuel Storage Rack Parameters.....	4-4
6.1	Comparison of Modeling Options for the Boral Rack.....	6-8
6.2	Impact of Channel Thickness on In-Rack Reactivity.....	6-9
6.3	Co-Resident Storage Rack Comparison.....	6-9
6.4	In-Rack $k_{\infty}$ Sensitivity to In-core Depletion Fuel Temperature.....	6-10
6.5	In-Rack $k_{\infty}$ Sensitivity to In-core Depletion Power Density.....	6-11
6.6	In-Rack $k_{\infty}$ Sensitivity to In-Core Controlled Depletion.....	6-12
7.1	Summary of CASMO-4 Maximum In-Rack Reactivity Results.....	7-12
7.2	Summary of KENO V.a Maximum In-Rack Reactivity Results.....	7-13
7.3	Manufacturing Reactivity Uncertainties.....	7-14

## Figures

2.1	Overview of the Monticello SFP Criticality Safety Analysis.....	2-6
2.2	ATRIUM 10XM Reference Bounding Assembly.....	2-7
4.1	Representative ATRIUM 10XM Fuel Assembly.....	4-6
4.2	Monticello Spent Fuel Pool Layout.....	4-7
4.3	Schematic Representation of a Section of High Density Storage Rack.....	4-8
4.4	High Density Boral Storage Rack Geometry.....	4-9
6.1	Single Cell Model for the High Density Boral Rack.....	6-13
6.2	Explicit Geometry Model for High Density Boral Rack.....	6-14
6.3	Schematic of Rack to Rack Interfaces.....	6-15
6.4	Impact of Void History Depletion on In-Rack $k_{\infty}$ .....	6-16
7.1	Evaluated Assembly Rotation Cases.....	7-15
7.2	Limiting Accident (Missing Boral Plate).....	7-16

# Controlled Document

## Nomenclature

AEC	Atomic Energy Commission
BAF	bottom of active fuel
BOL	beginning of life
BORAL	neutron absorber composed of boron dispersed within aluminum
BWR	boiling-water reactor
EALF	the energy of the average lethargy causing fission
FPM	fuel preparation machine
GDC	general design criteria
GWd	energy unit, giga-watt-day
H/X	moderating ratio, atomic ratio of hydrogen (H) to fissile isotopes (X)
ISG	interim staff guidance document (Reference 7)
k-eff	effective neutron multiplication factor (aka k-effective)
k <sub>∞</sub>	infinite lattice neutron multiplication factor (aka k-infinity)
LUA	lead use assembly
PLR	part-length fuel rod
NCS	nuclear criticality safety
NRC	Nuclear Regulatory Commission, U.S. (also USNRC)
RAI	request for additional information
REBOL	reactivity-equivalent at beginning of life (fresh fuel, no Gd <sub>2</sub> O <sub>3</sub> )
SFP	spent fuel pool
TAF	top of active fuel
%TD	percent of theoretical density
[ ]	Square brackets enclose information that is proprietary to AREVA.



# Controlled Document

## 1.0 Introduction

This report presents the results of a criticality safety evaluation performed for the Monticello spent fuel storage pool. The previous Nuclear Regulatory Commission (NRC) approved criticality safety evaluation is identified as Reference 1. In this report, a reference bounding assembly has been defined to bound the reactivity of all past and current fuel assembly types delivered to the Monticello Nuclear Plant. This reference bounding assembly is based on an AREVA NP Inc. (AREVA) ATRIUM™\* 10XM fuel assembly. This analysis demonstrates that with the reference bounding assembly the pool k-eff remains below the 0.95 k-effective acceptance criterion established by the NRC.

---

\* ATRIUM is a trademark of AREVA NP.

## 2.0 Summary and Conclusions

Criticality safety calculations have been performed and are documented herein for the Monticello Nuclear Plant spent fuel storage pool. Figure 2.1 provides an overview of the various steps involved in this criticality safety analysis. The analysis flow in this figure begins at the bottom with the evaluation of the existing fuel inventory and ends at the top with the calculation of an array k-eff that meets the regulatory acceptance criterion of 0.95.

This criticality safety analysis is based on the use of a reference fuel assembly design that is bounding for (i.e., more reactive than) all fuel designs previously used or planned to be used at the Monticello Nuclear Plant. The KENO V.a code was used for all calculations that do not require fuel depletion. The CASMO-4 code is used to compare lattice  $k_{\infty}$  values at peak reactivity conditions. The results of these comparisons are used to define the reference bounding lattices and the reactivity-equivalent at beginning of life (REBOL) lattices that are used in KENO V.a. CASMO-4 is also used in defining a portion of the gadolinia manufacturing uncertainty. Benchmarking against criticality experiments is included for the KENO V.a code and justification for the use of the CASMO-4 code is also provided. More detail on methodology and code benchmark / justification is provided in Chapter 5 and Appendices C and D.

The calculations documented herein demonstrate that the ATRIUM 10XM reference bounding assembly design has been selected to be more reactive in an in-rack configuration than any of the current or past fuel assembly designs used in the Monticello reactor. These comparisons are based upon actual GE 7x7, GE 8x8, GE 9x9, and GE 10x10 lattice geometries and enrichments as detailed in Appendix B.\* This criticality safety analysis shows that future ATRIUM 10XM assemblies meeting the storage requirements established in Table 2.1 can be safely stored with these previously manufactured assemblies.

The reference bounding assembly is defined with two U-235 enrichment / gadolinia concentration zones separated by the ATRIUM 10XM geometry transition at [ ] inches. The bottom enrichment and gadolinia zone is defined to extend up to this transition boundary and contains [ ] fuel rods. The top enrichment / gadolinia zone extends from this geometric transition

---

\* Various LUAs were also evaluated.

# Controlled Document

boundary to the top of the fuel assembly and contains [ ] fuel rods. These axial zones are illustrated in Figure 2.2. Two REBOL lattices have been defined to represent the lattices of the reference bounding assembly in KENO calculations. The neutron multiplication factors of the REBOL lattices have been increased by greater than or equal to 0.010  $\Delta k$  to address all uncertainties associated with defining these reactivity equivalent lattices.

*This analysis includes manufacturing uncertainties for the ATRIUM 10XM fuel design and the fuel storage racks. In addition to the manufacturing uncertainties; code modeling uncertainties, reactivity increases due to accident or other conditions, and a one-sided tolerance multiplier are used to determine the 95/95 upper limit k-eff. The conditions and uncertainties assumed in this analysis are described in the various sections of Chapter 7.*

This analysis demonstrates that the reference ATRIUM 10XM fuel assembly does not exceed an array k-eff of 0.95 in the Monticello spent fuel storage pool. As defined in Table 2.1, ATRIUM 10XM fuel that contains equivalent or less enrichment and equivalent or higher  $Gd_2O_3$  concentrations in the fuel zones depicted in Figure 2.2 can be safely stored in the Monticello spent fuel storage pool. In addition, ATRIUM 10XM fuel that contains more enrichment and/or lower  $Gd_2O_3$  concentrations than the reference assembly design can be safely stored provided each zone of the assembly is less reactive than the corresponding zone of the reference bounding assembly design (i.e., less than 0.8825 in-rack k-infinity for both zones in accordance with Table 2.1). This can be established using the storage rack model of the CASMO-4 lattice physics code as described in Appendix A.

This analysis supports the storage of channeled and unchanneled fuel assemblies including assemblies with the AREVA advanced fuel channel. Additionally, there is no limitation for bundle orientation or position in the storage cell since these are accounted for in the analysis.

To assure that the actual reactivity will always be less than the calculated reactivity, the following conservatisms have been included:

- The results are based on a moderator temperature of 4 °C (39.2 °F), which gives the highest reactivity for the limiting rack in the fuel storage pool. The non-limiting rack was also evaluated at its limiting temperature condition.
- Fuel assemblies are assumed to contain the high reactivity reference bounding lattices for the entire length of the assembly (i.e., natural uranium blankets are not modeled).

# Controlled Document

- Each lattice in each fuel assembly in the storage rack is assumed to be at its lifetime maximum reactivity level. There is no assumption of a specific burnup profile for the discharged assemblies. In other words, this is a peak reactivity analysis that does not take credit for lower reactivity conditions associated with burnup past the maximum reactivity.
- The minimum Boron-10 areal density is used when modeling the Boral.
- The most limiting orientation or position of each assembly in its rack cell is accounted for in the analysis.
- Neutron absorption in fuel assembly structural components (i.e., spacers, tie plates, etc.) is neglected.
- The maximum reactivity value includes all significant manufacturing and calculational uncertainties.
- The 0.010  $\Delta k$  uncertainty value applied when the REBOL lattice is defined is treated as a bias - introducing significantly more conservatism than if it had been treated as an uncertainty.\*
- The fuel array is modeled as being infinite in all dimensions.
- An adder has been included to account for significant Boral blistering. (At this time there is no evidence of blistering within the Monticello Boral racks).
- The bias from the KENO V.a benchmark (Appendix C) has been increased to also bound trending conditions that were shown to be statistically insignificant.

This analysis demonstrates that all fuel assemblies previously delivered to the Monticello Nuclear Plant can be safely stored in the spent fuel storage pool. Future ATRIUM 10XM fuel designs that meet the design requirements specified in Table 2.1 or that can be shown to be less reactive (on a lattice basis) than the reference bounding assembly can be safely stored in the Monticello spent fuel pool. The k-eff determined herein for the reference assembly, including all uncertainties, biases, manufacturing tolerances and worst accident or other loading conditions is 0.928 (as detailed in Section 7.8 and Figure 2.1).

---

\* As applied in this evaluation a  $k_{95/95}$  value of 0.928 is produced. If the 0.010  $\Delta k$  uncertainty were not applied to the REBOL lattices and then treated as an additional uncertainty term in Section 7.8, the  $k_{95/95}$  value would decrease to 0.922.

**Table 2.1 Criticality Safety Limitations for ATRIUM 10XM Fuel Assemblies Stored in the Monticello Plant Spent Fuel Storage Pool**

**ATRIUM 10XM Fuel Configuration**

The ATRIUM 10XM fuel configuration is provided in Table 4.1.

**Fuel Channels**

Fuel may be stored with or without fuel channels.

**Fuel Design Limitations for Enriched Lattices\***

The fuel may be stored in the spent fuel storage pool provided the enriched lattices are not more reactive than the reference bounding lattices. This can be demonstrated by meeting either of the following two requirements:

1. The U-235 enrichment and gadolinia loading levels must meet the requirements specified below and shown graphically in Figure 2.2. The dimensions represent fuel column height above the bottom of active fuel (BAF) and below the top of active fuel (TAF).

Above [    ]	Maximum Lattice Average Enrichment, wt% U-235	4.70
	Minimum Number of Rods containing Gd <sub>2</sub> O <sub>3</sub>	8
	Minimum wt% Gd <sub>2</sub> O <sub>3</sub> in these Gd Rod	3.5
At and below [    ]	Maximum Lattice Average Enrichment, wt% U-235	4.70
	Minimum Number of Rods containing Gd <sub>2</sub> O <sub>3</sub>	8
	Minimum wt% Gd <sub>2</sub> O <sub>3</sub> in these Gd Rod	3.919

These eight gadolinia rods cannot be loaded on the perimeter of the lattice or adjacent to the water channel. An equivalent<sup>†</sup> of 2 gadolinia rods must be loaded along each side. Gadolinia is not required in natural Uranium blankets and there are no restrictions on the number, concentration, or placement of any additional gadolinia rods.

Or,

2. The lattice average enrichment is less than 5.0 wt% U-235, and the  $k_{\infty}$  of each enriched lattice does not exceed the following in-rack  $k_{\infty}$  values at any point during its lifetime. (The CASMO-4 storage rack model that must be used for this calculation is defined in Appendix A and the transition between top and bottom lattice geometries occurs at [    ] inches from the bottom of the fueled length.)

Zone	Lattice Geometry	Distance from BAF	Max. in-rack $k_{\infty}$
2	10XMLCT [    ]	[    ] to TAF	0.8825
1	10XMLCB [    ]	0" to [    ]	0.8825

\* These requirements describe the reference bounding lattices shown in Figure 2.2 and Table 7.1.

† Two face adjacent gadolinia rods count as a single rod.

# Controlled Document

Monticello Nuclear Plant Spent Fuel Storage Pool  
Criticality Safety Analysis for ATRIUM™ 10XM Fuel

ANP-3113(NP)  
Revision 0  
Page 2-5

---

**Table 2.1 Criticality Safety Limitations for ATRIUM 10XM Fuel Assemblies Stored  
in the Monticello Plant Spent Fuel Storage Pool** *(Continued)*

**Spent Fuel Storage Rack**

The spent fuel storage rack design parameters and dimensions are provided in Table 4.2.

# Controlled Document

Monticello Nuclear Plant Spent Fuel Storage Pool  
Criticality Safety Analysis for ATRIUM™ 10XM Fuel

ANP-3113(NP)  
Revision 0  
Page 2-6

---

[

]

**Figure 2.1 Overview of the Monticello SFP Criticality Safety Analysis**

# Controlled Document

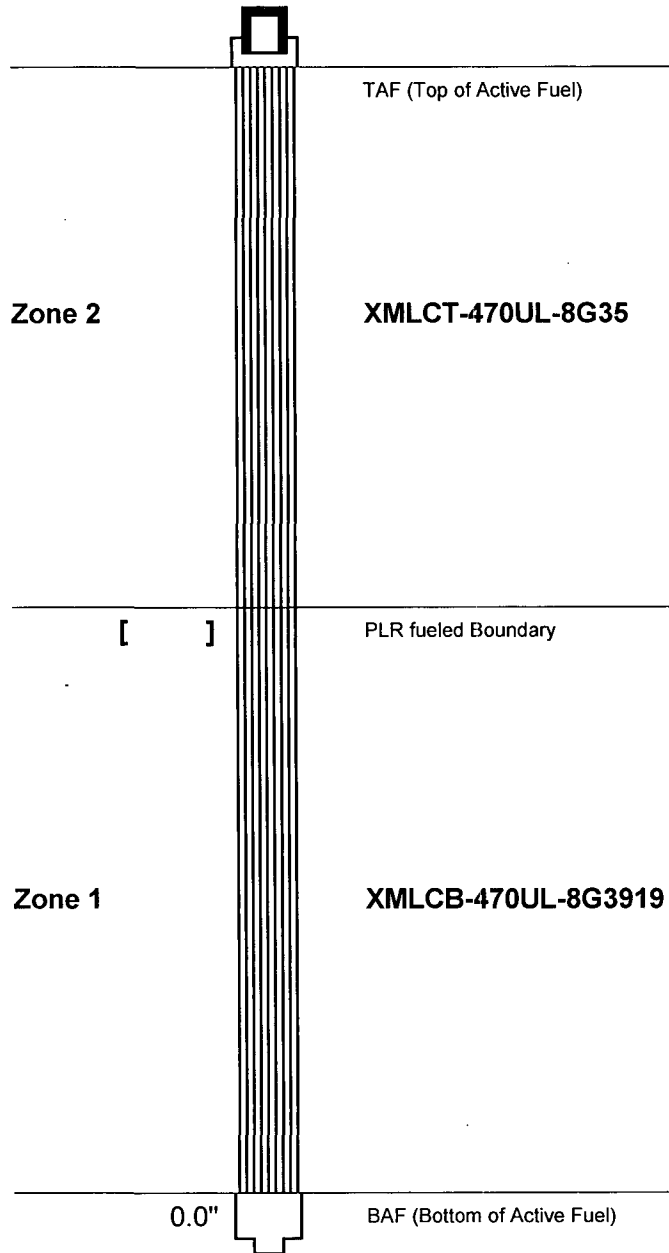


Figure 2.2 ATRIUM 10XM Reference Bounding Assembly



# Controlled Document

## 3.0 Regulatory Criticality Safety Criteria and Guidance

Section 9.1.1 of the Standard Review Plan (Reference 2) identifies the regulatory requirements and associated acceptance criteria considered to be applicable to criticality safety analyses.\* Since this analysis does not support a change in the facility only the requirements specific to the criticality safety analysis apply. The primary requirements relevant to this analysis are General Design Criteria 62 and portions of 10 CFR 50.68, Reference 3.

The Monticello nuclear plant was not designed or licensed to the General Design Criteria (GDC) provided in 10 CFR 50 Appendix A. Instead, Appendix E of the Monticello Updated Safety Analysis Report (USAR) provides a description of conformance to the Atomic Energy Commission's (AEC) Proposed General Design Criteria. For Monticello, the corresponding licensing basis criterion is the AEC Proposed Criterion 66, "Prevention of Fuel Storage Criticality".

AEC Proposed Criterion 66 (similar to GDC 62) specifies that criticality of fuel in handling or storage will be prevented by physical systems or processes with the preference for geometrically safe configurations. There is no physical change being implemented that affects the configuration of the as-licensed spent fuel storage system (i.e., no change to the systems, components, or structures that comprise the spent fuel storage system). The purpose of this analysis is to provide assurance that criticality will not occur within the basis of the existing spent fuel storage configuration for the ATRIUM 10XM fuel design to be provided in the future; therefore, the intent of Criterion 66 (and GDC 62) is met.

10 CFR 50.68 (a) requires that a licensee must either: 1) maintain monitoring systems in accordance with 10 CFR 70.24 to reduce the consequences of a criticality accident, or 2) adhere to the requirements of 10 CFR 50.68(b) to reduce the likelihood that a criticality accident will occur. Monticello complies with the requirements of part (b) of 10 CFR 50.68. The role of this criticality safety analysis in meeting the specific requirements for each of the 10 CFR 50.68(b) requirements is discussed below:

---

\* SRP 9.1.1 is used as the basis for discussion of general requirements for criticality safety analyses in this report. This context does not represent a commitment on the part of the licensee in regard to conformance with this section of the Standard Review Plan.

# Controlled Document

- 1) *Plant procedures shall prohibit the handling and storage at any one time of more fuel assemblies than have been determined to be safely subcritical under the most adverse moderation conditions feasible by unborated water.*

Technical Specification 4.3.1.1(b) requires that a  $k$ -effective of less than or equal to 0.95 must be maintained with unborated water. This analysis establishes the spent fuel pool (SFP) storage requirements that meet this licensing requirement. The criticality aspects of fuel handling are addressed in Sections 7.5 and 7.6, in regard to normal operations and accidents, respectively.

- 2) *The estimated ratio of neutron production to neutron absorption and leakage ( $k$ -effective) of the fresh fuel in the fresh fuel storage racks shall be calculated assuming the racks are loaded with fuel of the maximum fuel assembly reactivity and flooded with unborated water and must not exceed 0.95, at a 95 percent probability, 95 percent confidence level. This evaluation need not be performed if administrative controls and/or design features prevent such flooding or if fresh fuel storage racks are not used.*

This requirement does not apply because this is not a fresh fuel storage criticality analysis. It is also noted that the proposed Technical Specifications will prohibit fuel loading in the fresh fuel storage racks.

- 3) *If optimum moderation of fresh fuel in the fresh fuel storage racks occurs when the racks are assumed to be loaded with fuel of the maximum fuel assembly reactivity and filled with low-density hydrogenous fluid, the  $k$ -effective corresponding to this optimum moderation must not exceed 0.98, at a 95 percent probability, 95 percent confidence level. This evaluation need not be performed if administrative controls and/or design features prevent such moderation or if fresh fuel storage racks are not used.*

This requirement does not apply because this is not a fresh fuel storage criticality analysis. It is also noted that the proposed Technical Specifications will prohibit fuel loading in the fresh fuel storage racks.

- 4) *If no credit for soluble boron is taken, the  $k$ -effective of the spent fuel storage racks loaded with fuel of the maximum fuel assembly reactivity must not exceed 0.95, at a 95 percent probability, 95 percent confidence level, if flooded with unborated water. If credit is taken for soluble boron, the  $k$ -effective of the spent fuel storage racks loaded with fuel of the maximum fuel assembly reactivity must not exceed 0.95, at a 95 percent probability, 95 percent confidence level, if flooded with borated water, and the  $k$ -effective must remain*

# Controlled Document

*below 1.0 (subcritical), at a 95 percent probability, 95 percent confidence level, if flooded with unborated water.*

This criticality safety analysis is being performed specifically to show that this requirement has been met for normal and accident conditions. The applicable requirement is a  $k\text{-effective} \leq 0.95$  at a 95 percent probability with a 95 percent confidence level since Monticello is a boiling-water reactor (BWR) site with unborated water in the SFP. This requirement is also enforced in Section 4.3.1.1(b) of the Technical Specification. The analysis described in this report demonstrates that the calculated  $k_{95/95}$  value meets this requirement.

- 5) *The quantity of SNM, other than nuclear fuel stored onsite, is less than the quantity necessary for a critical mass.*

This requirement does not apply because this analysis only addresses special nuclear material in the form of fuel assemblies in the spent fuel pool.

- 6) *Radiation monitors are provided in storage and associated handling areas when fuel is present to detect excessive radiation levels and to initiate appropriate safety actions.*

This requirement does not apply because this is a criticality analysis only.

- 7) *The maximum nominal U-235 enrichment of the fresh fuel assemblies is limited to five (5.0) percent by weight.*

This criticality safety analysis establishes maximum allowable enrichments below the regulatory requirement and therefore complies with the intent of this requirement.

- 8) *The FSAR is amended no later than the next update which § 50.71(e) of this part requires, indicating that the licensee has chosen to comply with § 50.68(b).*

Compliance with this requirement is the responsibility of the licensee and is not part of this criticality safety analysis.

This criticality safety analysis complies with the intent of all of the applicable sections of 10 CFR 50.68(b).

# Controlled Document

Based upon the discussion above, this analysis complies with the intent of the Proposed AEC General Design Criterion 66 (and GDC 62) as well as 10 CFR 50.68(b).

The USNRC has recently issued document DSS-ISG-2010-01 Revision 0 (Reference 7) that provides interim staff guidance (ISG) for the review of spent fuel criticality safety analyses. Table 3.1 provides a top level summary discussion regarding the compliance of this criticality safety analysis to the ISG document. Where possible, this discussion includes a cross-reference to where specific items identified in the ISG are addressed within this criticality safety analysis report.

The following sources provide additional guidance in meeting the aforementioned regulatory requirements:

- “Guidance on the Regulatory Requirements for Criticality Analysis of Fuel Storage at Light-Water Reactor Power Plants,” also known as the Kopp letter this was issued by the NRC in 1998 (Reference 6).
- “OT Position for the Review and Acceptance of Spent Fuel Storage and Handling Applications,” issued by the NRC in 1978 and amended in 1979 (Reference 5).
- ANSI/ANS American National Standard 8.17-1984 (*Criticality Safety Criteria for the Handling, Storage and Transportation of LWR Fuel Outside Reactors*) issued by the American Nuclear Society, January 1984 (Reference 4).

# Controlled Document

**Table 3.1 Compliance with Interim Staff Guidance Document DSS-ISG-2010-01 Rev. 0**

ISG Section	USNRC Guidance	Compliance with USNRC Guidance	Applicable Sections
IV.1 Fuel Assembly Selection			
	<i>... the staff should review the submittal to verify that it demonstrates that the NCS analysis adequately bounds all designs, including variations within a design.</i>	The lattices of the ATRIUM 10XM reference bounding assembly are demonstrated to be more reactive than the lattices of any previously loaded fuel assembly, including variations due to damaged and modified assemblies.	Appendix B
	<i>...the staff should verify each application includes a portion of the analysis that demonstrates that the fuel assembly used in the analysis is appropriate for the specific conditions.</i>	As discussed above, the ATRIUM 10XM reference bounding assembly is shown to bound all previous designs. Compliance with the requirements listed in Table 2.1 ensures that future ATRIUM 10XM assemblies remain bounded by this evaluation.	Section 2.0 Appendix B
IV.1.a	<i>Use of a single "limiting" fuel assembly design should be assessed, ...</i>	The use of the ATRIUM 10XM reference bounding assembly (and corresponding lattices) is justified as described above.	Section 2.0 Appendix B
IV.2 Depletion Analysis			
	<i>...simulates the use of fuel in a reactor. These depletion simulations are used to create the isotopic number densities used in the criticality analysis.</i>	<p>This evaluation does not directly use the depletion based isotopic number density values in KENO. The CASMO-4 based in-core depletion is used to establish the in-rack lifetime maximum reactivity condition of the reference bounding lattices. Reactivity equivalent at beginning of life (REBOL) lattices are then defined for use in the KENO calculations. The REBOL lattices are defined with a conservative bias to address the uncertainty in the CASMO-4 depletion process and reactivity equivalence method.</p> <p>The definition of the reference bounding and REBOL lattices are described in more detail in Sections 7.0, 7.1, and Appendix B. Appendix D provides details on the treatment of the depletion uncertainty.</p>	Sections 7.0 and 7.1 Appendices B & D

# Controlled Document

**Table 3.1 Compliance with Interim Staff Guidance Document DSS-ISG-2010-01 Rev. 0**  
 (Continued)

ISG Section	USNRC Guidance	Compliance with USNRC Guidance	Applicable Sections
IV.2.a	<p>Depletion Uncertainty</p> <p><i>...an uncertainty equal to 5 percent of the reactivity decrement to the burnup of interest is an acceptable assumption.</i></p> <p><i>...should only be construed as covering the uncertainty in the isotopic number densities...</i></p>	<p>An overall CASMO-4 uncertainty reflecting calculational and depletion based isotopic uncertainties is defined in Section D.4. This value is bounded by the 0.010 Δk bias term applied during the reactivity equivalence calculation. Two independent estimates of the depletion uncertainty were used in this evaluation. One of these methods is consistent with the 5% reactivity decrement described in Reference 7 (except that it includes an additional component for the gadolinia uncertainty).</p>	Appendix D
IV.2.b	<p>Reactor Parameters</p> <p><i>...the staff should verify that each application includes a portion of the analysis that demonstrates that the reactor parameters used in the depletion analysis are appropriate for the specific conditions.</i></p>	<p>Sensitivity comparisons are included in Section 6.4 to show that reasonable parameters have been used in the depletion calculations. The parameters evaluated include:</p> <p style="padding-left: 40px;">Fuel Temperature (Assumption 2, Table 6.4); Moderator Temperature/Void History ( Assumption 3, Figure 6.4); Power Density (Assumption 4, Table 6.5); and Rodded Depletion (Assumption 7, Table 6.6)</p>	Section 6.4
IV.2.c	<p>Burnable Absorbers</p> <p><i>... the staff should verify that each application includes a portion of the analysis that demonstrates that the treatment of burnable absorbers in the depletion analysis is appropriate for the specific conditions.</i></p>	<p>Only integral burnable absorbers have been used in the Monticello reactor and they have been modeled appropriately in Appendix B. The placement of the 8 gadolinia rods in the reference bounding lattices have been selected to produce a high reactivity condition. Table 2.1 requires that all enriched lattices of future ATRIUM 10XM assemblies contain a minimum number of absorber rods with a minimum concentration level or that a CASMO-4 <math>k_{\infty}</math> less than the applicable reference bounding lattice be demonstrated.</p>	Table 2.1 Section 7.1 Appendix B

# Controlled Document

**Table 3.1 Compliance with Interim Staff Guidance Document DSS-ISG-2010-01 Rev. 0**  
 (Continued)

ISG Section	USNRC Guidance	Compliance with USNRC Guidance	Applicable Sections
IV.2.d	Rodded Operation  <i>... the staff should verify that each application includes a portion of the analysis that demonstrates its treatment of rodded operation is appropriate for its specific conditions.</i>	Assumption 7 of Section 6.4 addresses rodded depletion. The use of uncontrolled depletion at rated power conditions is shown to bound depletion at controlled conditions for the ATRIUM 10XM reference bounding lattices.	Section 6.4
IV.3	Criticality Analysis		
IV.3.a	Axial Burnup Profile  <i>...the staff should verify that each application includes a portion of the analysis that demonstrates its treatment of axial burnup profile is appropriate for its specific conditions.</i>	This evaluation uses the lifetime maximum reactivity of each lattice of the reference bounding assembly as discussed in Section 7.0. Therefore, there is no burn-up profile assumption.	Section 7.0
IV.3.b	Rack Model  <i>...the staff should verify that each application includes a portion of the analysis that demonstrates that the rack model analysis used in its submittal is appropriate for its specific conditions.</i>	The modeling of the spent fuel racks have been explicitly addressed in Table 6.3. Comparisons in Table 6.1 demonstrate that the infinite 2x2 model is more reactive than the explicit model. Comparisons in Table 6.1 and Appendix D show that the 2x2 model agrees well with the single cell model used in CASMO-4.	Section 6.1 Appendix D
IV.3.b.i	<i>The dimensions and materials of construction should be traceable to licensee design documents.</i>	The rack dimensions and materials in Table 4.2 were derived from the licensee's design documents.	Section 4.2
IV.3.b.ii	<i>The efficiency of the neutron absorber should be established, especially considering the potential for self-shielding and streaming.</i>	The Boral is modeled using the licensee's design minimum Boron-10 areal density. This value continues to be supported by coupon testing performed as part of Monticello's Boral surveillance program (see response to NRC RAI 3.5.2.1.15-1 in Reference 8).	Section 4.2

# Controlled Document

**Table 3.1 Compliance with Interim Staff Guidance Document DSS-ISG-2010-01 Rev. 0**  
 (Continued)

ISG Section	USNRC Guidance	Compliance with USNRC Guidance	Applicable Sections
IV.3.b.iii	<i>Any degradation should be modeled conservatively, consistent with the certainty with which the material condition can be established.</i>	While no evidence of degradation currently exists for the Monticello racks, a conservative blister model has been developed to account for potential future Boral blistering.	Sections 7.4.3 & 7.8
IV.3.c	<b>Interfaces</b> <i>... the staff should verify that each application includes a portion of the analysis that demonstrates that the interface analysis used is appropriate for its specific conditions.</i>	The original rack and the Boral racks are neutronically isolated by 12 or more inches of water, (see Table 4.2 and Figure 4.2). Therefore, the two rack designs are independent of each other. The scenario where an assembly is misloaded between the two racks has been evaluated in Section 7.6.	Sections 4.2, 6.3, 7.5, and 7.6
IV.3.c.i	<i>Absent a determination of a set of biases and uncertainties specifically for the combined interface model, use of the maximum biases and uncertainties from the individual storage configurations should be acceptable in determining whether the keff of the combined interface model meets the regulatory requirements.</i>	There is sufficient margin between the Boral rack and the original rack to forgo a formal $K_{95/95}$ calculation for the original rack (see Table 6.1 and Table 6.3). Furthermore, since they are neutronically isolated by 12 or more inches of water there is no need to combine rack uncertainties for the limiting Boral rack calculation.	Section 6.3
IV.3.d	<b>Normal Conditions</b> <i>...the staff should verify that each application includes a portion of the analysis that demonstrates that the NCS analysis considers all appropriate normal conditions for its specific conditions.</i>	Translation and orientation variations of the assemblies within the storage racks are considered in Sections 7.4.1 and 7.4.2. The fuel handling considerations for normal conditions are addressed in Section 7.5.	Sections 7.4.1, 7.4.2, and 7.5



# Controlled Document

Monticello Nuclear Plant Spent Fuel Storage Pool  
 Criticality Safety Analysis for ATRIUM™ 10XM Fuel

ANP-3113(NP)  
 Revision 0  
 Page 3-9

**Table 3.1 Compliance with Interim Staff Guidance Document DSS-ISG-2010-01 Rev. 0**  
 (Continued)

ISG Section	USNRC Guidance	Compliance with USNRC Guidance	Applicable Sections
IV.3.e	Accident Conditions  <i>The reviewer should verify all credible accident conditions are addressed.</i>	The accident conditions have been evaluated in Section 7.6.	Section 7.6
IV.4	Criticality Code Validation		
IV.4	<i>The proposed analysis methods and neutron cross-section data should be benchmarked, by the analyst or organization performing the analysis, by comparison with critical experiments. ... The critical experiments ... should include ... configurations having neutronic and geometric characteristics as nearly comparable to those of the proposed storage facility as possible.</i>	The criticality benchmark is shown in Appendix C. Since this is a fresh fuel equivalent evaluation, only critical experiments for fresh fuel have been included in the benchmark data set.	Appendix C
IV.4.a	Area of Applicability  <i>...the staff should verify that applications demonstrate that the validation fully covers the area of applicability for their specific SFP;</i>	The area of applicability is defined by the criticality benchmark comparisons provided in Appendix C. Section 5.1 also provides a summary of this validation and addresses the area of applicability for this Monticello spent fuel storage pool criticality safety analysis.	Section 5.1 Appendix C
IV.4.a.i	<i>The reviewer should verify any validation used for SNF appropriately considers actinides and fission products. NUREG/CR-6979, "Evaluation of the French Haut Taux de Combustion (HTC) Critical Experiment Data," issued September 2008 ...</i>	HTC benchmarks are not included in the validation set since this is a fresh fuel reactivity equivalent evaluation. The treatment of actinides and fission products is part of the CASMO-4 depletion uncertainty addressed in Appendix D.  However, the addendum to Appendix C compares the impact on the KENO bias and uncertainties if appropriate benchmark experiments from the HTC criticals were included. This comparison shows that a more conservative result is obtained without inclusion of the HTC criticals.	Appendix C

# Controlled Document

**Table 3.1 Compliance with Interim Staff Guidance Document DSS-ISG-2010-01 Rev. 0**  
 (Continued)

ISG Section	USNRC Guidance	Compliance with USNRC Guidance	Applicable Sections
IV.4.a.ii	<i>Experiments should be appropriate to the system being analyzed.</i>	The criticality benchmark data shown in Appendix C meets the requirements expressed in the ISG.	Appendix C
IV.4.a.iii	<i>The reviewer should ....{review the selection of benchmark data}</i>	The criticality benchmark dataset has been selected to provide a balanced representation of the spent fuel pool environment. It is shown in Appendix C.	Appendix C
IV.4.a.iv	<i>The reviewer should ensure that the experiments are not all highly correlated, e.g. critical configurations performed with the same fuel rods at the same facility.</i>	The criticality benchmark is shown in Appendix C.	Appendix C
IV.4.b	Trend Analysis <i>...the staff should verify that each application includes a portion of the analysis that demonstrates that the trend analysis used in its validation is appropriate for its specific conditions.</i>	The trending analysis is performed in Appendix C.	Appendix C
IV.4.c	Statistical Treatment <i>...the staff should verify that each application includes a portion of the analysis that demonstrates that the statistical treatment used in its validation is appropriate for its specific conditions.</i>	The benchmark validation suite in Appendix C follows the guidance given in NUREG/CR-6698 with respect to using the variance about the mean, confidence factors, and the treatment of non-normal distributions.	Appendix C

# Controlled Document

**Table 3.1 Compliance with Interim Staff Guidance Document DSS-ISG-2010-01 Rev. 0**  
*(Continued)*

ISG Section	USNRC Guidance	Compliance with USNRC Guidance	Applicable Sections
IV.4.d	<p>Lumped Fission Products</p> <p><i>...the staff should verify that each application that includes lumped fission products includes a portion of the analysis that demonstrates that the lumped fission products used in its validation are appropriate for its specific conditions.</i></p>	<p>The primary components of the Monticello nuclear criticality safety (NCS) analysis include the use of the CASMO-4 code in the definition of the reference bounding and REBOL lattices followed by the actual NCS calculations with KENO V.a (using the defined REBOL lattices). While CASMO-4 does include the use of lumped fission products, they are not credited in the definition of the reference bounding lattices. Therefore, the KENO calculations and <math>k_{95/95}</math> result are conservative since the lumped fission products have been removed.</p>	Section 7.1
IV.4.e	<p>Code-to-Code Comparisons</p> <p><i>...the use of a code-to-code comparison for validating criticality codes is outside the scope of this ISG.</i></p>	<p>Code-to-code comparisons are not used in the validation of KENO V.a - the code used for the criticality analysis.</p> <p>The only use of code-to-code comparisons is for the depletion code, CASMO-4. This use is limited to perturbation calculations used to quantify the CASMO-4 calculational uncertainty relative to KENO V.a.</p>	Appendix C Appendix D
IV.5	Miscellaneous		
IV.5.a	<p>Precedents</p> <p><i>...the staff should verify that for cited precedents, the application includes a portion of the analysis that demonstrates the commonality of the precedent to the submittal, with any differences identified and justified with respect to the use of the precedent.</i></p>	<p>Although not specifically cited, the approach taken in this spent fuel pool criticality safety analysis is similar to a previous SFP criticality analysis recently reviewed and approved by the USNRC (Reference accession numbers ML092810281 and ML101650230).</p> <p>Some changes were incorporated to directly address USNRC concerns identified in the SER accepting the above submittal (ML110250051) and to provide closer compliance to the staff guidance document.</p>	N/A

# Controlled Document

**Table 3.1 Compliance with Interim Staff Guidance Document DSS-ISG-2010-01 Rev. 0**  
 (Continued)

ISG Section	USNRC Guidance	Compliance with USNRC Guidance	Applicable Sections
IV.5.a Continued		Specifically, <ul style="list-style-type: none"> <li>• The criticality benchmark data suite has been modified to remove soluble boron and MOX benchmarks.</li> <li>• The previous submittal content was split between a submitted report and additional answers to USNRC requests for additional information. This information content has been reformatted into a single report.</li> <li>• Differences in modeling, primarily to address differences in the plant specific rack designs.</li> <li>• The CASMO-4 lumped fission products are not credited in the in-rack <math>k_{\infty}</math> values for the reference bounding lattices when the reactivity equivalence comparison is being performed.</li> </ul>	
IV.5.b	References <i>...the NRC reviewer should verify that references cited in the application are used in context and within the bounds and limitations of the references. Any extrapolation outside the context or bounds of the reference should be demonstrated as appropriate.</i>	The MNGP analysis uses references appropriately.	N/A
IV.5.c	Assumptions <i>...applications should explicitly identify and justify all assumptions used in their applications.</i>	Modeling assumptions have been explicitly addressed in the report.	Section 6.0

## 4.0 Fuel and Storage Array Description

A number of different assembly types have previously been loaded in the spent fuel pool with lattice geometries ranging from 7x7 to 10x10. This includes variations in the type and number of water rods and part length fuel rods. The AREVA ATRIUM 10XM fuel product line is planned for use in future reloads. For this reason, the ATRIUM 10XM reference bounding assembly design forms the basis for demonstrating that the maximum k-eff of the spent fuel pool storage array remains less than 0.95.

### 4.1 Fuel Assembly Design

The ATRIUM 10XM fuel assembly is a 10x10 fuel rod array with an internal square water channel offset in the center of the assembly (taking the place of nine fuel rod locations). The assembly contains part-length fuel rods (PLR); therefore, the “top” lattice geometry will apply above the PLR fueled boundary and the “bottom” lattice geometry will apply below the PLR fueled boundary. The ATRIUM 10XM mechanical design parameters are summarized in Table 4.1 and a representation of the ATRIUM 10XM assembly design is provided in Figure 4.1. The ATRIUM 10XM fuel in the Monticello Nuclear Plant uses the AREVA advanced (i.e., thick/thin) fuel channel design.

### 4.2 Fuel Storage Racks

The Monticello spent fuel pool provides the capability of storing a maximum of 2217 fuel assemblies: 20 assemblies in an aluminum I-beam rack (original rack) and 2197 assemblies in the 13x13 high density Boral storage rack modules. The dimensional parameters for these racks are given in Table 4.2 and the pool arrangement is shown in Figure 4.2.

Each high density Boral rack module is composed of alternating or staggered stainless-steel square container tubes. This arrangement results in only one container-tube wall between adjacent fuel assemblies, as illustrated in Figure 4.3 and Figure 4.4. Each container-tube wall has a core of Boral sandwiched between inner and outer surfaces of stainless steel. The Boral core is made up of a central segment composed of a dispersion of boron carbide in aluminum. This central segment is clad on both sides with aluminum. These stainless steel container tubes are closure welded with vent holes to prevent the buildup of hydrogen gas. The

# Controlled Document

completed storage tubes are fastened together by angles welded along the corners and attached to a base plate to form storage modules. These modules are designed to be free standing with low-friction between the module support and pool floor liner.

Note on the Efficacy of Boral: In a water environment, neutron scattering ensures that neutrons approach the Boral from a full range of incident angles. This minimizes the potential for neutron streaming and reduces the significance of self-shielding. In periodic neutron attenuation tests, the Boral coupons in the Monticello spent fuel pool have supported Boron-10 areal densities that are greater than the 0.013 g/cm<sup>2</sup> value used in this evaluation (see the response to NRC RAI 3.5.2.1.15-1 in enclosure 1 of Reference 8).

**Table 4.1 ATRIUM 10XM Fuel Assembly Parameters**

Parameter	Value
<b>Fuel Assembly</b>	
Fuel Rod Array	10x10
Fuel Rod Pitch, in.	[     ]
Number of Full Length Fuel Rods	[   ]
Number of Part Length Fuel Rods	[   ]
Location of Part Length Fuel Rods	See Figure 6.1
Water Channel	1
<b>Fuel Rods</b>	
Fuel Material	UO <sub>2</sub>
Pellet Density, % of Theoretical Density (%TD)	[     ]
Pellet Diameter, in.	[     ]
Pellet Void Volume, %	[     ]
Cladding Material	Zircaloy
Cladding OD, in.	[     ]
Cladding ID, in.	[     ]
<b>Internal Water Channel</b>	
Outside Dimension, in.	[     ]
Inside Dimension, in.	[     ]
Channel Material	Zircaloy
<b>Fuel Channel (standard 100 mil)<sup>†</sup></b>	
Outside Dimension, in.	[     ]
Inside Dimension, in.	[     ]
Channel Material	Zircaloy
<b>Fuel Column Lengths</b>	
Distance from the bottom of the fuel to the top of the fuel in the part length fuel rods, in.	[     ]
Total Fueled Length, in.	[     ]

\* Criticality safety analysis is also valid for lower fuel densities. The analysis uses the effective stack density which is a combination of the pellet density and the pellet void volume.

† The conclusions in this report are also valid for advanced fuel channels (see Section 6.2).

# Controlled Document

**Table 4.2 Fuel Storage Rack Parameters**

Parameter	Value
<b>High Density Boral Racks</b>	
Boral B-10 areal density, g/cm <sup>2</sup>	0.013 minimum
Rack Box OD, in. Box material	6.653 ± 0.04 Stainless steel
Inner rack box wall thickness, in. Box material	0.0355 ± 0.004 Stainless steel
B <sub>4</sub> C plate thickness, in. plate material	0.076 ± 0.005 B <sub>4</sub> C and aluminum clad in two 0.010" aluminum sheets
width, in	6.20 ± 0.03
height, in	146.30
Outer rack box wall thickness, in. Box material	0.090 ± 0.008 Stainless steel
Rack cell pitch, in.	6.563 ± 0.03
Closure plate thickness, in. material	0.125 Stainless steel
Rack to Rack Spacing,* in.	2.33

\* Rack to Rack spacing is the distance from the outside surface of adjacent closure plates. (This value is derived from a 1.875" spacing at the rack module base).



# Controlled Document

**Table 4.2 Fuel Storage Rack Parameters** (Continued)

Parameter	Value
<b>Low Density Original Rack</b>	
Description	10 x 2, <b>I</b> beam and C channel
Material	Aluminum
Depth, in.	6.375
Web thickness, in.	0.1875 & 0.625
Flange thickness, in.	0.1875
Flange width, in.	4.625
Rack cell pitch, in. (rectangular)	6.625 ± 0.090 x 11.875 ± 0.160
Original to Boral Rack Spacing* (minimum), in.	12

\* Rack to Rack spacing is the distance from the outside surface of the original rack to the adjacent closure plate.

# Controlled Document

[



]

**Figure 4.1 Representative ATRIUM 10XM Fuel Assembly**  
(Assembly length and number of spacers has been reduced for pictorial clarity)

# Controlled Document

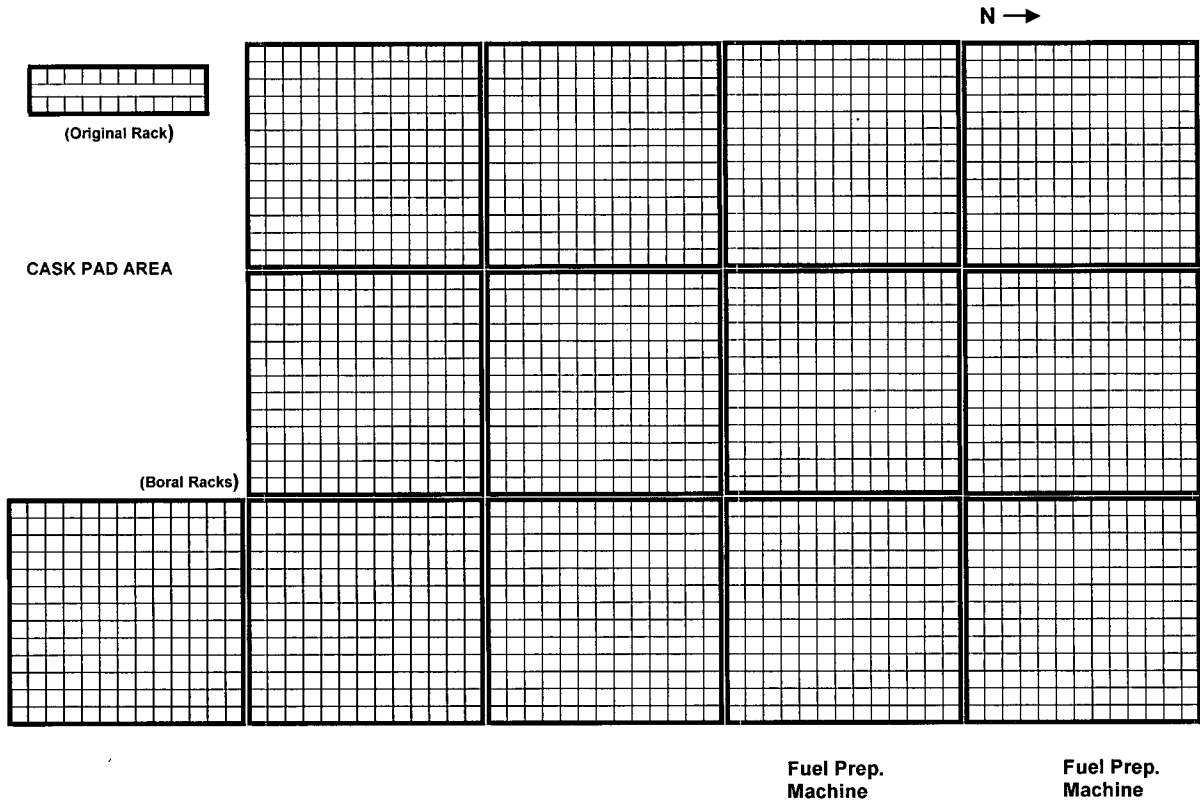


**Figure 4.2 Monticello Spent Fuel Pool Layout**  
(not to scale)

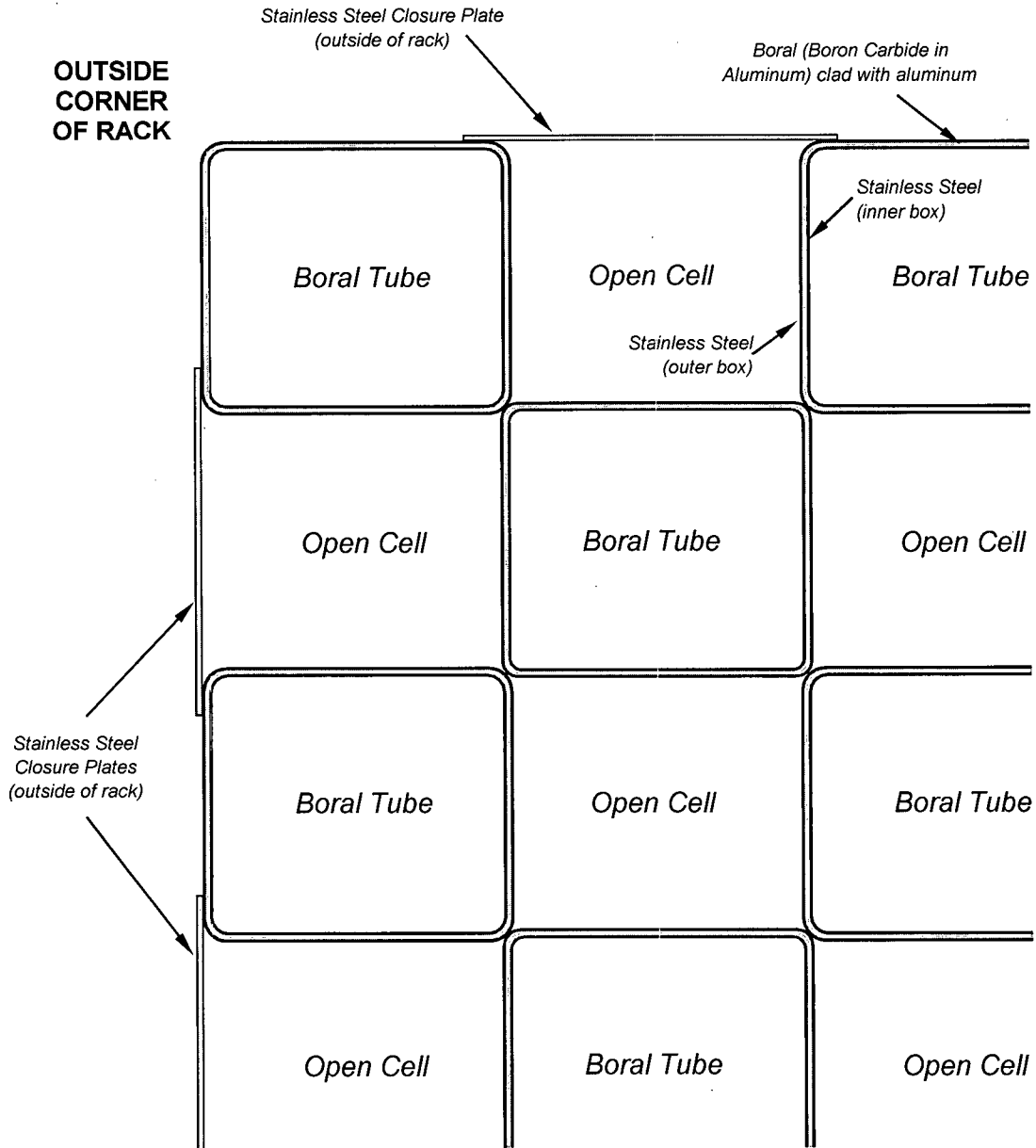


Figure 4.3 Schematic Representation of a Section of High Density Storage Rack  
(not to scale)

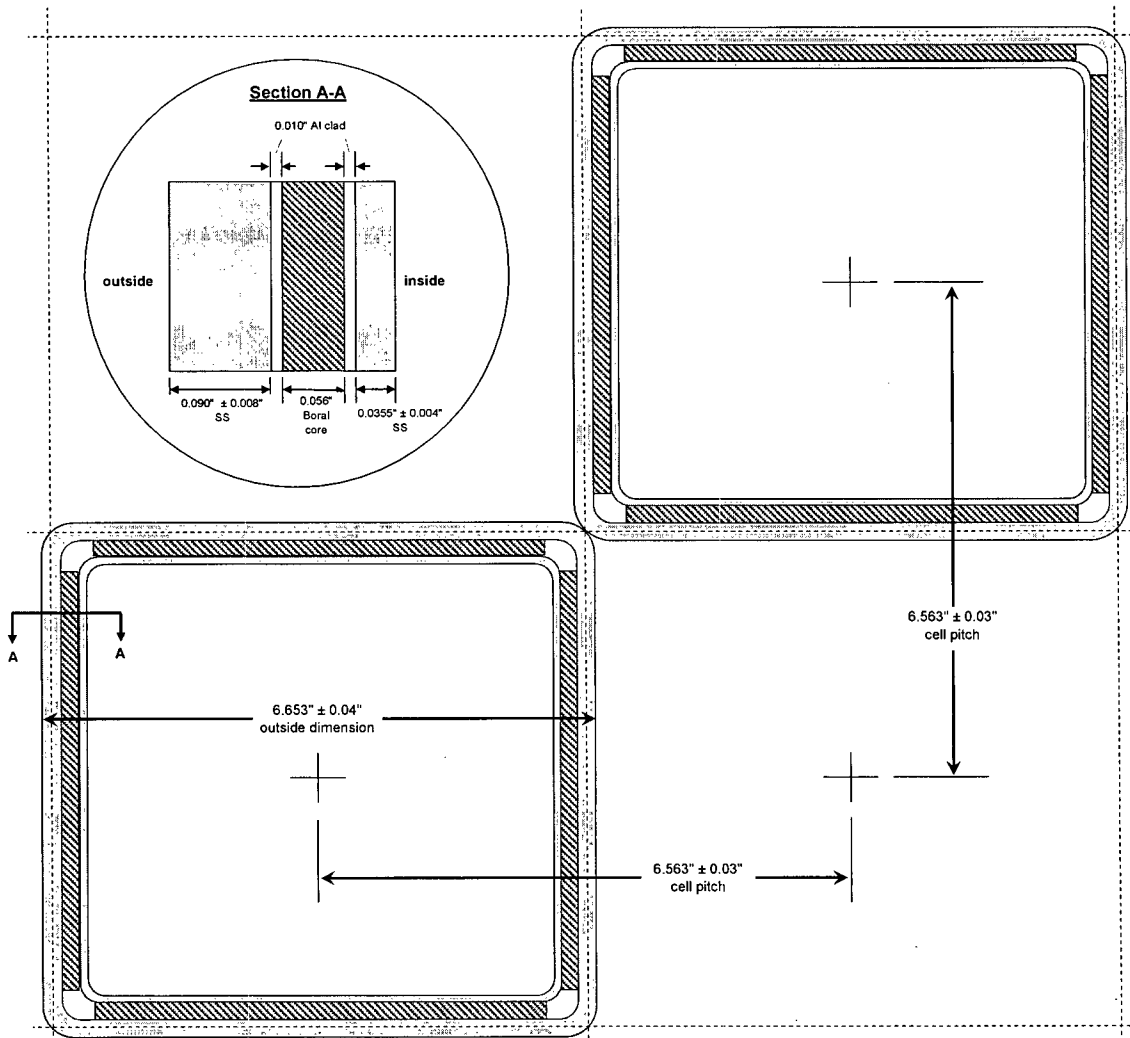


Figure 4.4 High Density Boral Storage Rack Geometry  
(not to scale)

## 5.0 Calculation Methodology

The spent fuel storage criticality safety evaluation is performed with the KENO V.a Monte Carlo code, which is part of the SCALE 4.4a Modular Code System (Reference 9). The SCALE driver module CSAS25 uses the ENDF/B-V 44 energy group data library. It also uses modules BONAMI-2 and NITAWL to perform spatial and energy self-shielding adjustments of the cross sections for use in KENO V.a. AREVA has benchmarked KENO V.a in accordance with NUREG/CR-6698 (Reference 10) using critical experiments related to the storage of fuel assemblies in water - including neutron absorbing materials such as stainless steel and Boral. For applications using the 44 energy group data libraries, a KENO V.a bias magnitude of 0.0075 and a standard deviation of 0.0027 will be used (see Appendix C).

KENO V.a is run on the AREVA scientific computer cluster using the Linux operating system. The hardware and software configurations are governed by AREVA procedures to ensure calculational consistency in licensing applications. The code modules are installed on the system and the installation check cases are run to ensure the results are consistent with the installation check cases that are provided with the code. The binary executable files are put under configuration control so that any changes in the software will require re-certification. The hardware configuration of each machine in the cluster is documented so that any significant change in hardware or operating system that could result in a change in results is controlled. In the event of such a change in hardware or operating system, the hardware validation suite is rerun to confirm that the system still performs as it did when the code certification was performed.

In this analysis the SCALE 4.4a code system is employed to:

- Calculate Dancoff coefficients.
- Calculate absolute k-effective results.
- Evaluate accident conditions, alternate loading conditions, and manufacturing tolerance conditions.

The CASMO-4 code is used when conditions require fuel and gadolinia depletion. CASMO-4 is a multigroup, two-dimensional transport theory code with a rack geometry option that allows typical storage rack geometries to be defined on an infinite lattice basis. This code is used for fuel depletion and relative reactivity comparisons in a manner that is consistent with AREVA's NRC approved CASMO-4 / MICROBURN-B2 methodology (Reference 11). The CASMO-4

# Controlled Document

computer code is controlled by AREVA procedures and the version used in this analysis meets the requirements of Reference 11.

In this analysis CASMO-4 is employed to:

- Perform in-core isotopic depletion at characteristic void history levels, [ ] for bottom geometry lattices and [ ] for top geometry lattices. Use of CASMO-4 for in-core depletion is consistent with its application in EMF-2158(P)(A) (Reference 11).
- Perform in-rack  $k_{\infty}$  assessments to identify the most reactive lattices.
- Define lattices for a reference bounding assembly that represent the maximum reactivity condition supported by the analysis.
- Define the reactivity equivalent at beginning-of-life (REBOL) lattices with fresh fuel and no gadolinia for the subsequent KENO V.a base case criticality calculations. Note that for the REBOL lattices, the U-235 content is manually adjusted upward until the REBOL  $k_{\infty}$  is at least  $0.010 \Delta k$  greater than the lattices of the reference bounding assembly. This  $0.010 \Delta k$  is used to account for all uncertainties associated with defining the REBOL lattices - including calculational and depletion uncertainties of the CASMO-4 code as discussed in Appendix D.
- Evaluate a component of the manufacturing uncertainty for gadolinia content (i.e., the depletion component). This evaluation is needed because changes in gadolinia content affect reactivity more near peak reactivity than at beginning of life.

## 5.1 **Area of Applicability**

Table C.6 in Appendix C shows the ranges of key parameters represented in the KENO V.a benchmark analysis. Parameters such as rectangular lattices of zircaloy clad  $UO_2$  fuel rods in a pool of water with stainless steel and boron are sufficiently general to not require comparison. The remaining parameters are compared in the following table and show that the KENO V.a portion of this analysis has been performed within the range of experimental conditions used in the KENO V.a benchmark.

# Controlled Document

Monticello Nuclear Plant Spent Fuel Storage Pool  
Criticality Safety Analysis for ATRIUM™ 10XM Fuel

ANP-3113(NP)  
Revision 0  
Page 5-3

Parameter	Benchmark Values	Values in this Analysis
Enrichment (wt% U-235)	2.35 to 4.74	3.2 to 3.4
Fuel Rod Pitch (cm)	1.26 to 2.54	1.295
Moderating Ratio (H/X)	110 to >400	113 to 122
Energy of the Average Lethargy Causing Fission (eV)	0.060 to 0.247	0.148 to 0.245

For the CASMO-4 qualification, ATRIUM 10XM fuel lattices were modeled using the Monticello Nuclear Plant limiting storage rack geometry. Therefore, the CASMO-4 calculations performed for this evaluation are within the area of applicability of the comparisons shown in Appendix D.



## 6.0 Modeling Options and Assumptions

The following sections describe the primary modeling simplifications and assumptions used in this analysis including discussion of impact on in-rack reactivity.

### 6.1 *Geometric Modeling of the High Density Boral Rack*

The geometry of the high density spent fuel storage racks includes an arrangement of staggered or alternating Boral tubes, as shown in Figure 4.3 and Figure 4.4. As a minimum, this rack requires an array of 2 tube cells and 2 non-tube cells for explicit modeling. The rack models described below were implemented in KENO V.a and the reactivity results are provided in Table 6.1. These models use infinite periodic boundary conditions in the x, y, and z directions.

#### 6.1.1 Single Cell Model Description

The primary simplifying assumptions can be generally described as follows:

- **Boral Plate:** The Boral plate is modeled as boron-10 only; i.e., the aluminum, carbon, and boron-11 in the core of the plate and the aluminum clad on the outside of the plate are not included in this model. The location of the Boral is shifted to be between storage cells so that half of the actual thickness is assigned to each cell wall. The plate is assumed to extend to the corners of the storage cell (i.e., the water gap in the corners of the Boral tube is not modeled). Neglecting the non-boron-10 components of the Boral is slightly conservative because the neglected materials are relatively weak neutron absorbers. Extending the Boral plate to the corners is expected to have the opposite effect since it introduces a small additional amount of a strong neutron absorber.
- **Stainless Steel Channels:** One half of the total inner and outer stainless steel channels were combined in the model and assumed to make up the inside surface of the storage cell. The impact of this modeling simplification is expected to be minor since the amount of stainless steel is conserved and it still surrounds the Boral plate.
- **Cell Pitch and Water Gaps:** Average cell pitch and average water gap values are used in this model. This helps maintain the accuracy of this simplified model.

This is the model used in the CASMO-4 calculations. Figure 6.1 provides an illustration of the geometry for the single cell model.

## 6.1.2 Explicit Storage Cell Model Description

KENO V.a allows for more detailed modeling of the storage rack geometry than is possible with CASMO-4. The primary modeling changes in comparison to the single cell model are:

- Storage Geometry: The explicit model for KENO V.a is composed of a 2x2 array with two Boral tube storage cells and two open or non-tube cells.
- Boral Plate: The plate is modeled using the nominal width and the corner region is modeled as water. For comparison purposes one solution is provided using Boron-10 only and the second solution models all components of the Boral plate; i.e., Boron, Carbon, and Aluminum.
- Cell Pitch: The average assembly pitch is modeled.

Figure 6.2 provides an illustration of the geometry for the KENO V.a explicit model.

## 6.1.3 Explicit Rack Model Description

The high density Boral storage rack modules have an odd number of rows and columns. For this reason, each module has a Boral tube in each corner. When the racks are placed together, the cells in the adjacent rack have the same geometric configuration (i.e., a Boral cell is face adjacent to another Boral cell and an open cell is face adjacent to another open cell). As shown in Figure 6.3, some cells have two Boral plates between adjacent assemblies and some cells have no Boral material between assemblies. Details associated with the individual storage racks were modeled as described below.

- Storage Geometry: The explicit model from Section 6.1.2 is expanded to a 13x13 array with tube cells in each corner.
- Stainless steel closure plates are approximated for non-tube cells along the perimeter of the rack.
- The nominal rack to rack water gap\* is modeled.

## 6.1.4 Reactivity Comparison of the Boral Rack Models

Table 6.1 provides KENO V.a results for the single cell and more explicit geometry models. Neglecting the single cell model, these results indicate that the explicit 2x2 storage cell model with the Boral modeled as boron-10 only produces the most conservative result. Other conclusions from this comparison are also listed below:

- The single cell model provides a good representation of the reactivity of the Boral rack.
- It is conservative to use a boron-10 only model for the Boral.

---

\* 2.33 inches between the outer surfaces of the closure plates.

# Controlled Document

- It is conservative to neglect the water gaps and closure plates between the storage rack arrays, i.e., the infinite cell model is more conservative than the 13x13 rack model.

The boron-10 only, explicit 2x2 model with periodic boundary conditions in all directions is represented as 0.897 and will be used to represent the reactivity level of the Boral racks. This  $k_{\infty}$  value is about 0.015  $\Delta k$  more reactive than the result from the actual storage rack model (the 13x13 rack model with explicit B4C and finite axial boundary conditions in Table 6.1).

## 6.2 *Fuel Assembly Modeling*

The CASMO-4 modeling of the previously manufactured fuel is performed using the actual lattice dimensions, enrichment, gadolinia loading, and channel type for each specific fuel product line. The KENO V.a in-rack calculations for the limiting ATRIUM 10XM fuel have been performed assuming a uniform 100 mil fuel channel.

A sensitivity calculation was performed with various channel thicknesses with the results summarized in Table 6.2. This analysis shows that in-rack reactivity generally increases with increasing fuel channel wall thickness. The increase in wall thickness results in an increase in channel mass and wall cross-sectional area which in turn results in larger water displacement. The AREVA advanced channel design for ATRIUM 10XM fuel is thicker at the corners with a thinner wall along the sides and has a cross-sectional area that falls between the 80 mil and 100 mil channels. Consequently, an ATRIUM 10XM assembly modeled with a uniform 100 mil fuel channel is more reactive than an assembly without a fuel channel, an assembly with a uniform 80 mil fuel channel, and an assembly with the advanced fuel channel.

Zircaloy has been modeled in KENO as pure zirconium. Neglecting the neutron absorption of the alloying elements (primarily tin, iron, chromium, and nickel) is slightly conservative. In addition, the presence of activated corrosion and wear products (CRUD) is neglected because most of these compounds have higher neutron absorption cross sections than water.

## 6.3 *Co-Resident Fuel Racks*

As shown in Figure 4.2, the Monticello spent fuel pool contains 13 high density Boral racks and one low density original rack. The in-rack  $k_{\infty}$  values for these storage rack types are compared in Table 6.3 with the limiting water temperature specified. This comparison shows that the high density Boral racks are the most limiting finite model.

Review of Section 6.1.4 confirms that the 2x2 Boral infinite cell model is the most limiting overall; therefore, it will be used as the bounding representation of all possible rack configurations in the Monticello spent fuel pool. Based on these comparisons, the 0.897  $k_{95/95}$  result will be used as the primary basis for the  $k_{95/95}$  calculation.

## 6.4 General CASMO-4 Modeling Assumptions

The application of CASMO-4 for in-core fuel depletion is consistent with the NRC approval of EMF-2158(P)(A) (Reference 11). Input for the depletion calculation includes the fuel assembly material and geometry. The ATRIUM 10XM fuel assembly parameters are given Table 4.1. The key fuel pool storage rack parameters are given in Table 4.2. The following general assumptions have been made in regard to CASMO-4 modeling.

Assumption 1: The top of the part length rods in the ATRIUM 10XM assembly, which contain a 6 inch plenum, can be treated as water in the lattice in-core depletion and in the in-rack calculations. The actual content of the 6 inch plenum consists of a stainless steel spring and fill gas. Neglecting the 6 inch plenum is conservative from a criticality stand point because it models a more reactive condition by adding more moderator and neglecting the neutron absorption of the plenum spring material.

Assumption 2: A fuel temperature is assumed for the fuel depletion based on the core average linear heat generation rate. Therefore, consistent fuel temperatures are used for each geometry type. Sensitivity studies were performed to determine the impact of the fuel temperature used in the fuel depletion on the in-rack storage reactivity. The fuel temperature was varied plus and minus 100 °F relative to the base depletion temperature for the reference bounding and limiting lattices. Table 6.4 provides the in-rack results based on in-core depletion at the different temperatures (i.e., the cold in-rack calculations were repeated for the in-core depletions performed at the different temperatures). These results demonstrate that moderator void is much more significant than the depletion fuel temperature.

Assumption 3: The moderator temperature used for in-core depletion is assumed to be at saturated conditions corresponding to the rated dome pressure. The more important parameter in a BWR reactor is the actual moderator density/void level. The in-core depletion calculations are performed at [ ] void history conditions for bottom geometry lattices and [ ] void history conditions for top geometry lattices. Figure 6.4 shows the results of a

# Controlled Document

sensitivity evaluation with respect to the in-core depletion void history and its effect on the maximum in-rack lattice  $k_{\infty}$ . For the reference bounding and limiting lattices the discrete void history conditions evaluated produced (or exceeded)\* the maximum credible  $k_{\infty}$  result.

Assumption 4: The power density used for the fuel depletion is based on the core rated power per unit volume which is consistent with AREVA's standard NRC-approved depletion methodology, Reference 11. Table 6.5 provides the reactivity effect as a function of power density where 100% power density represents the core average power density at rated power. This sensitivity analysis was performed for the reference bounding lattices and the limiting lattices listed in Table B.1 of Appendix B. These results show a small effect on in-rack lattice  $k_{\infty}$  over very large changes in depletion power density. These results also demonstrate that moderator void is much more significant than the depletion power density.

Assumption 5: Modeling the pellet deformation with respect to burnup can be ignored for the in-core depletion and in-rack calculations. Modeling of the pellet deformation does not significantly change the neutronic characteristics of the fuel since the material content is unchanged.

Assumption 6: The spacer (i.e., spacer grid) material can be ignored in the in-core depletion and in-rack calculations. There is no soluble boron in this BWR spent fuel pool, and the spacers will absorb more neutrons than water. Therefore, a more reactive configuration is modeled when the spacer material is neglected.

Assumption 7: The in-core depletion is based upon uncontrolled statepoint conditions. This is appropriate because a bundle is in an uncontrolled state (i.e., the adjacent control blade is not inserted) for the majority of its lifetime, including the time from beginning of life (BOL) to the time when it reaches its lifetime maximum reactivity.

Bundles are physically located in a control cell that is associated with a specific control rod sequence (i.e., A1, A2, B1, or B2); therefore, the potential for controlled operation is limited to the times when the core is operated in that sequence (e.g., one control period in four for a core

---

\* The  $k_{\infty}$  value reported for the top geometry GE14 lattice is based upon 0% void history (see Table B.3). Given that 0% void history is not credible for full power operation in the top of an assembly it would be acceptable to use the [ ] void history value (0.8431). It is conservative to use the [ ] void history value (0.8452) for this lattice.

# Controlled Document

operated with the typical four control rod sequence strategy). Furthermore, the following factors tend to mitigate the amount of controlled depletion: 1) not all available in-sequence control rods are used during a sequence, 2) control rods are typically not fully inserted (they may be in deep, intermediate or shallow positions which leaves the upper lattices in an uncontrolled state), 3) bundles in peripheral and near peripheral core locations are usually not controlled, and 4) the bundles are at a reduced power during the controlled time period which reduces their accumulated burnup while in the controlled state (i.e., they experience a lower burnup rate). The net effect is that a typical bundle will experience controlled depletion for only a fraction of its time from BOL to the exposure that produces its lifetime maximum reactivity.

Potential exceptions to this behavior are: 1) bundles in a power suppression cell, and 2) bundles in a control cell in which the control rod has been declared inoperable. Power suppression is the practice of inserting a control rod to reduce power in suspected leaking fuel bundles. The control rod is typically fully inserted in an inoperable control cell. In either case, the control rod may be inserted for a significant period of time and the bundles around them will have a larger fraction of their lifetime spent in a controlled state. However, this only affects a small population of bundles — four bundles for each affected control cell.

Rodded depletion introduces impacts due to the power gradient imposed by the inserted blade as well as to the assumed power density due to the associated power reduction in the bundle. A sensitivity calculation was performed to determine the impact of in-core controlled depletion on the peak in-rack  $k_{\infty}$  in which both of these parameters were varied. Table 6.6 compares the lifetime maximum  $k_{\infty}$  results for the ATRIUM 10XM reference bounding lattices and the limiting legacy fuel lattices. The results in Table 6.6 are very conservative because no significant number of fuel assemblies will be controlled from BOL to the peak reactivity exposure. These results indicate a reactivity increase for the limiting legacy lattices; however, as shown in Table B.1 there is substantial margin between the reactivity of the legacy fuel lattices and the ATRIUM 10XM reference bounding lattices. The results in Table 6.6 also show that uncontrolled depletion results in a higher in-rack  $k_{\infty}$  for the reference bounding lattices.

Assumption 8: The CASMO-4 model uses a lumped approach for fission products that are not specifically treated. CASMO-4 creates two pseudo nuclides to represent the general behavior of two fission product groups - one non-saturating and one slowly saturating. Any errors in the

# Controlled Document

treatment of these pseudo nuclides becomes part of the depletion uncertainty and is included in the benchmarking and qualification of the CASMO-4 code for in-core depletion, as described in the approved topical report EMF-2158(P)(A) (Reference 11). For this evaluation, the lumped fission products were removed from the reference bounding lattices when the REBOL lattices were defined\*. This modeling adds additional conservatism to the evaluation.

---

\* Note that the lumped fission products were not removed for relative comparison calculations such as Table 6.4, Table 6.5, Table 6.6, Figure 6.4, and comparisons in the Appendices.

# Controlled Document

**Table 6.1 Comparison of Modeling Options for the Boral Rack**

	KENO V.a In-Rack k
<b>Single Cell Model</b>	
	$k_{\infty}$
Rack Model Developed for CASMO-4 (boron-10 only*)	0.8969
<b>2x2 Infinite Array Model</b>	
	$k_{\infty}$
Base (boron-10 only*)	0.8964
Base with Explicit Boral	0.8936
<b>13x13 Rack Model (closure plates and nominal rack spacing)</b>	
	$k$
Base (boron-10 only*)	$k_{\infty} = 0.8870$
Base with 12" water reflector on the top and a 24" concrete reflector on the bottom	$k_{\text{eff}} = 0.8847$
Base with Explicit Boral, 12" top water reflector and a 24" concrete bottom	$k_{\text{eff}} = 0.8819$

**NOTE:** The neutron multiplication values are based upon the limiting water temperature condition, (4 °C for infinite cell conditions or 20 °C for finite rack conditions). These cases produce a KENO standard deviation of about 0.0008.

\* All non-boron-10 materials in the Boral plate are neglected (i.e., modeled as void).



# Controlled Document

**Table 6.2 Impact of Channel Thickness on In-Rack Reactivity**

Fuel Channel Thickness		KENO V.a $k_{\infty}$ Result*
(mil)	(inch)	
100	0.100	0.8950
80	0.080	0.8939
0	0.000	0.8921

**Table 6.3 Co-Resident Storage Rack Comparison**

	KENO V.a In-Rack $k$	Limiting Temperature †
13 x 13 Boral Rack	$k_{\infty} = 0.8870$	20 °C
Low Density Original Rack	$k_{\text{eff}} = 0.8806$	60 °C‡

\* Based on 20 °C moderator temperature.

† Cases were evaluated between 4 °C and 60 °C.

‡ 60 °C is the maximum non-accident water temperature per Section 10.2.2.3 of the Monticello Updated Safety Analysis Report.

# Controlled Document

Monticello Nuclear Plant Spent Fuel Storage Pool  
Criticality Safety Analysis for ATRIUM™ 10XM Fuel

ANP-3113(NP)  
Revision 0  
Page 6-10

**Table 6.4 In-Rack  $k_{\infty}$  Sensitivity to In-core Depletion Fuel Temperature**

[

]

---

\* Includes lumped fission products.

# Controlled Document

Monticello Nuclear Plant Spent Fuel Storage Pool  
Criticality Safety Analysis for ATRIUM™ 10XM Fuel

ANP-3113(NP)  
Revision 0  
Page 6-11

**Table 6.5 In-Rack  $k_{\infty}$  Sensitivity to In-core Depletion Power Density**

[

]

---

\* Includes lumped fission products.

# Controlled Document

Monticello Nuclear Plant Spent Fuel Storage Pool  
Criticality Safety Analysis for ATRIUM™ 10XM Fuel

ANP-3113(NP)  
Revision 0  
Page 6-12

---

**Table 6.6 In-Rack  $k_{\infty}$  Sensitivity to In-Core Controlled Depletion**

[

]

---

\* Includes lumped fission products.

† PD refers to Power Density.

# Controlled Document

Monticello Nuclear Plant Spent Fuel Storage Pool  
Criticality Safety Analysis for ATRIUM™ 10XM Fuel

ANP-3113(NP)  
Revision 0  
Page 6-13

---

[

]

**Figure 6.1 Single Cell Model for the High Density Boral Rack**  
(not to scale – top zone geometry)

# Controlled Document

Monticello Nuclear Plant Spent Fuel Storage Pool  
Criticality Safety Analysis for ATRIUM™ 10XM Fuel

ANP-3113(NP)  
Revision 0  
Page 6-14

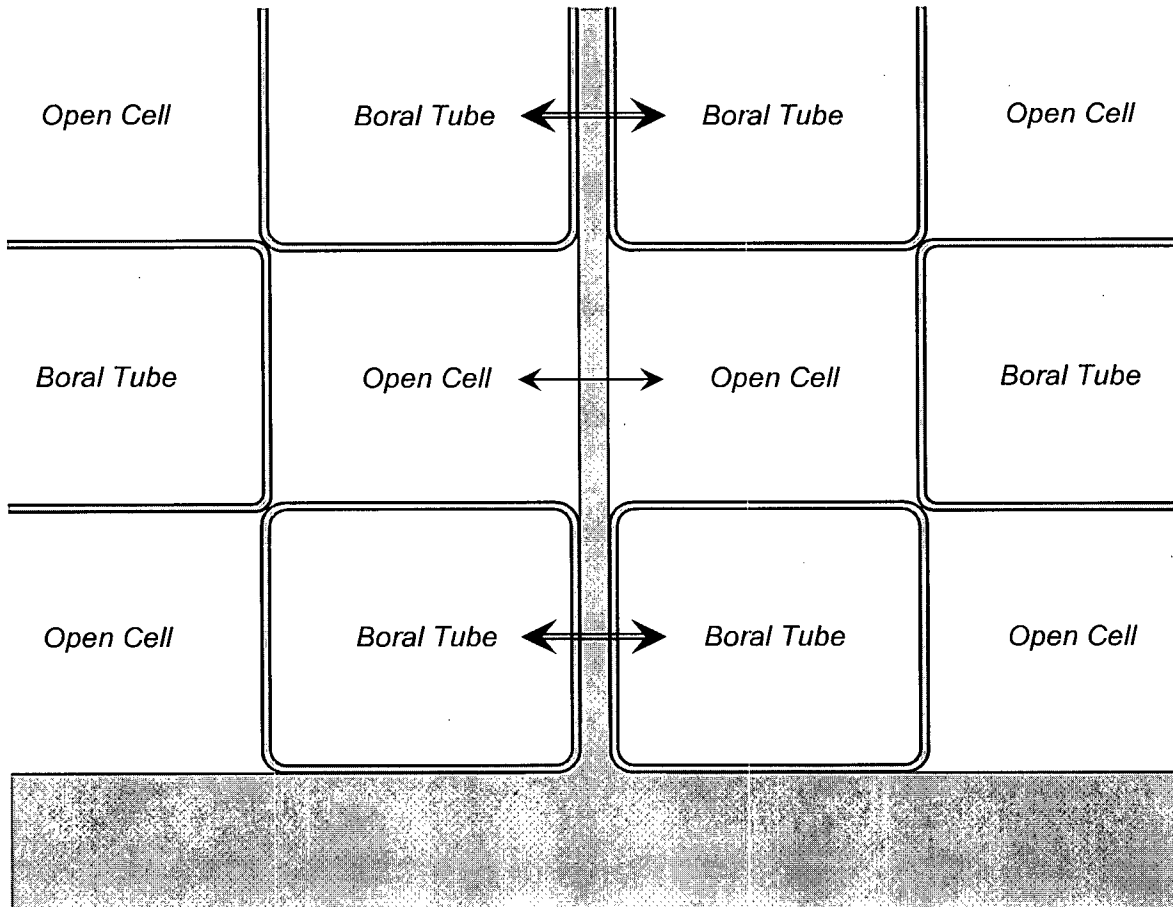
---

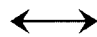

[

**Figure 6.2 Explicit Geometry Model for High Density Boral Rack**  
(not to scale – top zone geometry)

]

# Controlled Document



-  No Boral Plate between cells in adjacent racks
-  Two Boral Plates between cells in adjacent racks

**Figure 6.3 Schematic of Rack to Rack Interfaces**

# Controlled Document

[

]

**Figure 6.4 Impact of Void History Depletion on In-Rack k-infinity**



## 7.0 Criticality Safety Analysis

This criticality safety analysis is based upon an ATRIUM 10XM reference bounding assembly. This reference assembly is comprised of separate top and bottom geometry reference bounding lattices\* and they have been defined to be more reactive than all previously manufactured lattices - as well as future ATRIUM 10XM lattices. The evaluation of the previously manufactured fuel and comparisons to these reference bounding lattices are detailed in Appendix B of this report. The reference bounding ATRIUM 10XM assembly is comprised of two axial zones as described in the following table and as shown graphically in Figure 2.2.

Zone	Lattice Geometry	Distance from BAF	<sup>235</sup> U wt%	No. of Gadolinia Rods	Gadolinia wt%
2	10XMLCT	[ ] to TAF	4.70	8	3.5
1	10XMLCB	0" to [ ]	4.70	8	3.919

The reference bounding lattices are depleted in the reactor core environment to establish the lifetime maximum  $k_{\infty}$  of these lattices in the storage pool environment. The resulting  $k_{\infty}$  values are mainly dependent upon the lattice geometry, the U-235 enrichment level, and the gadolinia concentration; therefore, there is no axial burn-up profile assumption associated with this method.

The actual KENO V.a calculations are based upon reactivity equivalent† at beginning of life (REBOL) lattices that have been designed to be more reactive than the reference bounding lattices and their calculational uncertainties. For this evaluation, a U-235 enrichment level of 3.38 wt% is applied for the top (10XMLCT) geometry and 3.21 wt% is applied for the bottom (10XMLCB) geometry.

\* It is demonstrated in Appendix B that the ATRIUM 10XM reference design in the spent fuel pool geometry is more reactive than the other fuel types used at Monticello.

† The CASMO-4 vs. KENO comparison in Appendix D demonstrates a stable basis for this reactivity equivalence. The 2x2 KENO model used in Appendix D was also established as the maximum  $k_{\infty}$  case in Section 6.1.4.

The final  $k_{95/95}$  evaluation is based upon a number of factors that include the worst credible conditions and uncertainties. Items considered include assembly placement within the storage cell, assembly orientation, manufacturing uncertainties, and accident conditions.

## 7.1 *Definition of the Reference Bounding and REBOL Lattices*

The CASMO-4 lattice depletion calculations are performed at hot operating, uncontrolled, characteristic void history conditions. These void history conditions are [ ] for top geometry lattices and [ ] for the bottom geometry lattices. The calculation results are based upon the nominal fuel design parameters (defined in Table 4.1) and assume a standard 100 mil fuel channel. The location of the 8 gadolinia rods in the reference bounding lattices have been selected to maximize the reactivity of the lattices. Xenon and lumped fission product free restart calculations are performed as a function of exposure and void history to establish the highest in-rack reactivity ( $k_{\infty}$ ) at any time throughout the life of these fuel lattices. The CASMO-4 in-rack  $k_{\infty}$  of the top and bottom zone reference bounding lattices are both 0.8825. These results are summarized in Table 7.1.

The reference bounding and REBOL lattices are based upon a uniform enrichment distribution. A uniform enrichment distribution increases the BWR lattice reactivity because low enriched rods in the corners of the lattice are replaced with rods at an average enrichment level. Relative to a representative top and bottom ATRIUM 10XM lattice design, a uniform enrichment distribution was determined to be more reactive by 0.002 to 0.004  $\Delta k$ . Consequently, the use of these lattices with uniform enrichment distributions conservatively bound the distributed enrichment distributions of expected future lattice designs.

In support of the KENO rack calculations, two REBOL lattices are created corresponding to the top and bottom geometries for the ATRIUM 10XM design. These lattices are defined using a water temperature of 4 °C in the spent fuel pool rack configuration. The top REBOL lattice is defined with a uniform 3.38 wt% U-235 enrichment level, and the bottom REBOL lattice is defined with a uniform 3.21 wt% U-235 enrichment level. These results are also summarized in Table 7.1.

As discussed in the methodology section, an adder of at least 0.010  $\Delta k$  is included in the generation of the REBOL lattices to address CASMO-4 code, geometry, material, and depletion uncertainties. The adequacy of this adder is the primary subject of Appendix D.

## 7.2 *Storage Array Reactivity*

The base storage array reactivity is calculated using KENO V.a as an infinite array of fuel storage cells using the explicit storage cell model as described in Section 6.1.2 and as illustrated in Figure 6.2. This model was shown to be conservative in Section 6.1.4. (KENO V.a results using this model were also shown to trend well with CASMO-4 results in Appendix D)

Each cell is assumed to contain an assembly composed of 3.38 wt% U-235 (top) and 3.21 wt% U-235 (bottom), uniformly enriched REBOL lattices without gadolinia. As discussed earlier, each REBOL lattice is defined to be at least 0.010  $\Delta k$  more reactive than its corresponding reference bounding lattice. A periodic boundary condition is specified for both the x-y plane and for the axial direction. The KENO model assumes a standard 100 mil fuel channel which was shown in Section 6.2 to bound storage with no channel, an 80 mil channel, and the advanced thick-thin channel.

KENO V.a calculations were performed at various temperatures from 4 °C to 60 °C that confirmed that the REBOL assembly is bounded by the 4 °C results. As shown in Table 7.2, the limiting base case KENO k-eff is 0.897. Except as specifically noted, the reactivity values presented in Table 7.1 and Table 7.2 do not include adjustments for uncertainties or KENO V.a code biases. Section 7.8 presents the determination of the upper limit 95/95 reactivity for the storage rack array.

## 7.3 *Arrays of Mixed BWR Fuel Types*

It is shown in Tables B.1 and B.4 that the ATRIUM 10XM reference bounding lattices are more reactive in the in-rack configuration than the limiting lattices of the legacy fuel. Additionally, it is also shown in Appendix B that the other legacy fuel types have significant margin relative to the limiting lattices. It then follows that from a reactivity perspective, the reference bounding ATRIUM 10XM lattices used in this evaluation can conservatively represent past assembly fuel types.

The assembly reactivity limits (either enrichment and gadolinia limitations or direct  $k_{\infty}$  values) defined in Table 2.1 are applicable to all future ATRIUM 10XM fuel assemblies that will be built for the Monticello Nuclear Plant. Therefore, there will not be a more reactive assembly to consider in an accident scenario and an array composed of a mixture of these fuel types will not exceed the reactivity calculated for an array of limiting ATRIUM 10XM assemblies.

## 7.4 *Other Conditions*

The unadjusted reactivity result reported in Table 7.2 is based upon a reference orientation which places the ATRIUM 10XM internal water channel toward the bottom right corner of the storage cell with the assembly centered within the cell as shown in Figure 6.2. The actual position of assemblies in the storage racks will include assembly rotation and lean. In addition, it is possible that blisters could form on the surface of the Boral plates. This deformation of the Boral plate will exclude water and therefore affect the reactivity of the storage racks. These conditions will be evaluated in this section and their worth will be included as a direct adder in the  $k_{95/95}$  equation.

### 7.4.1 Assembly Rotation

The rotational combinations shown in Figure 7.1 and the simple 90°, 180°, and 270° cases were evaluated to determine if the asymmetric nature of the ATRIUM 10XM fuel assembly will produce a more reactive condition than the base case shown in Figure 6.2. The simple 90° rotation case was the most limiting with a  $k_{\infty}$  increase of  $0.001 \pm 0.001 \Delta k$ . This effect will be included in the  $\Delta k_{\text{sys}}$  parameters in the calculation of  $k_{95/95}$  in Section 7.8.

### 7.4.2 Assembly Lean

Each storage cell has a hole in the bottom where the lower tie plate nose piece fits to center the assembly. There is no corresponding mechanism to keep the upper part of the assembly centered; therefore, each assembly has the ability to lean toward a side or corner of the storage cell. The impact of this lean condition was evaluated by assuming the entire bundle can be positioned anywhere within the storage cell. Between 1 and 4 assemblies were moved relative to one another within their cells. The result of this evaluation showed no statistically significant increase relative to the centered position.

# Controlled Document

## 7.4.3 Blister Formation

Under certain conditions, corrosion gases can be trapped within a Boral plate and the aluminum cladding can be deformed to create blisters on the surface of the plate. These blister regions exclude water and can therefore affect the neutron absorption of the Boral storage rack. (As indicated in the response to NRC RAI 3.5.2.1.15-1 in Reference 8, there is no indication of blistering in the Monticello Boral racks). For this analysis a uniform 0.055" void region has been used as a conservative model of this potential blistering condition\*. Calculations indicate that this level of void on all the Boral plates in the pool would increase reactivity by  $0.004 \pm 0.001 \Delta k$ . This effect will be included in the  $\Delta k_{\text{sys}}$  parameters in the calculation of  $k_{95/95}$  in Section 7.8.

## 7.5 **Normal Fuel Handling**

Normal fuel assembly movement is generally described as those movements required to load and unload assemblies into allowable storage locations within the spent fuel pool. The allowed storage locations include the spent fuel pool storage racks and the fuel preparation machines (FPMs).

Fuel movements are accomplished with the use of a refueling bridge with a mast and grapple assembly. Fuel assemblies are grasped and suspended from the mast/grapple assembly with normal lateral movements occurring above the top of the storage cell locations. The base storage array reactivity model assumes an infinite lattice array in both radial and axial dimensions using a periodic boundary condition as addressed in Section 7.2. This infinite array of fuel lattices bounds the case for suspending a single bundle over the rack during normal fuel movements. Loading or unloading an assembly into a storage location requires the raising or lowering of the fuel into the storage cell. This operation is also bound by the base storage array reactivity, which assumes the racks are fully loaded.

The spent fuel storage pool contains two FPMs that allow for the storage of a single assembly within each. Each FPM is neutronicly isolated from the other so interaction between them is

---

\* A uniform void with a 0.055 inch height bounds the condition of having a 1/8 inch high blister with a spherical cross section on every 1.25"x1.25" unit cell on one side of a Boral plate (i.e., 1.25 " diameter blisters with a height of 1/8 inch packed edge to edge). This in turn would be equivalent to each side of the Boral plate having blisters of this size with 50% area coverage.

not considered. It is feasible that an assembly suspended from the refuel bridge can be brought into close proximity to an assembly already located in an FPM. An analysis was performed that considered the additional potential for a misplaced assembly for a total of three (3) assemblies in close proximity. These assemblies are isolated from all other fuel assemblies in the spent fuel pool. For this comparison, three ATRIUM 10XM fuel assemblies with REBOL lattices at 3.5 wt% U-235 were placed together in a triangular pattern. A reactivity optimization search was performed using different assembly spacing and different assembly orientations. In addition, calculations were performed with and without fuel channels and the water temperature was varied from 4 °C to 60 °C. A maximum k-eff of  $0.897 \pm 0.001$  was calculated with unchanneled assemblies at 4 °C.

By coincidence the resulting  $k_{\text{eff}}$  for this configuration is equivalent to the base array reactivity identified in Section 7.2 and used in the  $k_{95/95}$  calculation in Section 7.8. If a  $k_{95/95}$  result were calculated for the fuel handling condition using the REBOL lattices from the main calculation it would be less than the value for the limiting rack (Section 7.8) because:

- this configuration is based on 3.5 wt% U-235 lattices where the REBOL lattices use a lower U-235 enrichment level (3.21 wt% U-235 (Bottom) and 3.38 wt% U-235 (top))
- there are no applicable accident conditions for this configuration
- the manufacturing tolerance value is lower for this application because there are no applicable storage rack, fuel channel, or gadolinia tolerance conditions

Both the misloading of an assembly into a location adjacent to a loaded rack (i.e., a non-allowed storage location) and the dropping of an assembly during fuel movements (i.e., fuel handling accident) are accident conditions which are evaluated in Section 7.6.

## 7.6 **Accident Conditions**

In addition to the nominal storage cell arrangement, accident conditions have also been considered. All  $\Delta k$  values provided in this section are based upon comparative KENO V.a calculations, i.e., only the most limiting scenario will be reflected in the  $k_{95/95}$  calculation in Section 7.8. The following scenarios were evaluated to identify the most limiting accident condition.

- Missing Boral plate in the interior of the rack. (Limiting condition for the Boral rack)
- Boral Storage Racks being forced together.
- Misloaded Bundle Scenarios.

# Controlled Document

- Assembly misloaded between the pool wall and storage rack adjacent to an open cell (no Boral between assemblies)
- Assembly misloaded into the corner region adjacent to 3 racks.
- Assembly misloaded between the fuel preparation machine adjacent to an open cell (no Boral between assemblies)
- Assembly misloaded in the space between the original rack and the Boral rack.
- Dropped assembly lying horizontally across the top of the spent fuel pool.
- Loss of Spent Fuel Pool Cooling. (Limiting condition for the original rack)

The situation where a single Boral plate is missing from an interior storage rack location was evaluated. Since this was the most limiting case, the moderator temperature and assembly position were varied to optimize the worth of the accident. (The use of unchanneled assemblies was considered but was not evaluated because the calculation results indicated an optimum condition occurs when water is between the assemblies and because removal of the fuel channel tends to reduce the reactivity). The most limiting condition occurred at 4 °C with one assembly moved to the edge of the storage cell and the adjacent assembly moved half the distance to the edge of the cell as shown in Figure 7.2. This accident condition has a reactivity worth of  $0.006 \pm 0.001 \Delta k$ . This will be included in the  $\Delta k_{\text{sys}}$  parameters in the calculation of  $k_{95/95}$  in Section 7.8.

It is postulated that 2 or more Boral racks could be forced together during a seismic event. For this situation, the spacing between racks is reduced from 2 or more inches to less than ½ inch. Should this occur, the pool  $k_{\infty}$  is calculated to increase by about  $0.005 \Delta k$ . This accident scenario is less limiting than the optimized missing Boral plate scenario.

The case of a misloaded assembly was investigated by assuming that an assembly was placed on the edge of a Boral storage rack adjacent to an assembly in a non-tube or open storage cell. This misloaded assembly was moved to a location very near the adjacent assembly. The results confirm that this accident scenario increases the system  $k_{\infty}$  by less than  $0.001 \Delta k$ .

As shown in Figure 4.2, a misloaded assembly could be placed in a location where 3 racks meet together. With this geometry, the corner storage cells are all Boral tube cells. As expected, no significant reactivity increase is produced.

It is also possible for an assembly to be in the fuel preparation machine while a second assembly is moved between the fuel preparation machine and the fuel storage rack. This is

# Controlled Document

conservatively modeled as two assemblies placed against each other adjacent to an open cell of the Boral storage rack. The results show a reactivity increase of less than 0.001  $\Delta k$  and confirm that this accident scenario is less limiting than the missing Boral plate scenario.

An assembly might also be placed in the water gap between the Boral rack and the original storage rack. To optimize this condition it is assumed that the misplaced assembly is between an assembly in an open cell of the Boral rack and an assembly in the original rack. Given that the water gap is greater than 12 inches, this scenario produced a reactivity increase of less than 0.001  $\Delta k$  and remains bounded by the missing Boral plate scenario.

For the case of dropping a fuel assembly onto an assembly in the storage rack (i.e., a fuel handling accident in the spent fuel pool), the potential exists for damaging the dropped assembly as well as any other assemblies it contacts. This event has the potential to cause deformation to the affected assemblies, however; the reactivity impact of this deformation on rack reactivity is minimal since it involves only 2-3 assemblies in a localized area. There will also be no significant effect on the array reactivity when the dropped assembly comes to rest in a horizontal or inclined position on top of the storage rack because the dropped assembly will be neutronically isolated from the fuel in the storage cells (greater than 12 inches of water between the dropped assembly and the top of the active fuel zone of the fuel in the storage rack). Finally, similar to the previous discussion for normal fuel handling it is noted that the axial boundary condition used in the KENO model provides an infinitely repeating fuel column. Consequently, the base model conservatively bounds the potential impact of a dropped assembly and no increase in reactivity applies for this event.

For the infinite Boral rack model, the limiting moderator temperature is 4 °C (39.2 °F). Therefore, an increase in the pool water temperature (a loss of spent fuel pool cooling event) will not increase the reactivity of these racks. For the original rack, the water is assumed to be unvoided at 120 °C. This temperature / void condition accounts for the pressure increase applicable to fuel assemblies that are 30 to 40 feet below the surface of the pool. This high temperature condition increases the reactivity of the original rack by 0.008  $\Delta k$ . This reactivity increase will not affect the adjacent Boral racks because there is sufficient water between the original rack and the Boral racks to isolate them from each other. Therefore; this reactivity



increase applies only to the original rack which is much less limiting than the Boral rack (see Table 6.3).

## 7.7 *Manufacturing and Other Uncertainties*

Uncertainties associated with defining bounding REBOL lattices are addressed in Appendix D. Specifically, uncertainties associated with CASMO-4 depletion and modeling capabilities are included within the REBOL definition process (through the requirement for the lattice to have a 0.010 Δk higher reactivity when compared to the corresponding reference bounding lattice). Table 7.1 demonstrates that the requirement for this adder has been met with a minimum difference of 0.0109 Δk for the top lattice.

The manufacturing tolerance values and the calculated reactivity uncertainties for the ATRIUM 10XM fuel are shown in Table 7.3.\* The gadolinia manufacturing uncertainty (gadolinia concentration and gadolinia pellet density) effect on reactivity was evaluated with a combination of KENO V.a and CASMO-4. All other uncertainties reported in Table 7.3 were evaluated with KENO V.a. The ATRIUM 10XM rack calculations are conservatively performed for a minimum B10 areal density, therefore no manufacturing uncertainty is needed for this parameter. BOL dimensions have been assumed, except the fuel rod pitch and channel growth results are based upon conservative spacer and channel growth dimensions.

For the various tolerances which are evaluated with KENO, the k and the standard deviation (s) values are combined consistent with the variance equation listed in Section 4.1.5 of Reference 12:

$$\Delta k^2 = (u^2/\delta x^2)((k - k_{ref})^2 \pm (s_{MC}^2 + s_{MC,ref}^2))$$

where: (k - k<sub>ref</sub>) change in k<sub>eff</sub> induced by change δx on parameter x  
 u standard uncertainty of parameter x  
 δx change in parameter x  
 s<sub>MC</sub> Monte Carlo standard deviation values

---

\* The manufacturing uncertainties for other fuel types in the SFP are not explicitly addressed in this analysis due to the reactivity margin between all existing fuel and the reference bounding lattices. See Appendix B for more detail.

The manufacturing tolerance results have been evaluated using the upper and lower bounds of the full tolerance range; therefore,  $\delta x$  represents a range greater than  $2u$ . Rather than define a single uncertainty interval for this calculation and then multiply it by 2 to reestablish a 95/95 bounding interval,  $u^2/\delta x^2$  is conservatively treated as unity in this calculation.

The Monte Carlo uncertainty values have been added to the limiting case and where  $(k - k_{ref})$  is negative for both the upper and lower bounds of the tolerance interval, a zero value has been used (e.g., the channel thickness, pellet diameter, and Boral sheet width). The adjusted  $\Delta k$  values are the square root of the variance for that particular case. The statistically combined result is the square root of the sum of the variance values.

### 7.8 Determination of Maximum Rack Assembly k-eff ( $k_{95/95}$ )

For the ATRIUM 10XM fuel design with REBOL lattice enrichments of 3.21 and 3.38 wt% U-235, the base case KENO calculated in-rack reactivity from Table 7.2 is 0.897. This k-eff value is used with the following equation to determine the upper limit 95/95 reactivity (also illustrated in Figure 2.1):

$$k_{95/95} = k_{eff} + bias_m + \Delta k_{sys} + (C^2 \sigma_k^2 + C_m^2 \sigma_m^2 + C^2 \sigma_{sys}^2 + \Delta k_{tol}^2)^{1/2},$$

where:

- $k_{eff}$  = Base in-rack reactivity from KENO V.a, (0.897, Table 7.2)
- $bias_m$  = KENO V.a validation methodology bias (0.0075, Appendix C – Section C.8)
- $\Delta k_{sys}$  = Summation of applicable system variables (See the following table and Sections 7.4.1, 7.4.3, and 7.6)
- $C$  = 95% confidence level consistent with KENO V.a (2.0)
- $C_m$  = 95/95 one-sided tolerance multiplier for a sample size of 68 (1.996)
- $\sigma_k$  = k-eff standard deviation from KENO V.a, (0.001, Table 7.2)
- $\sigma_m$  = KENO V.a methodology uncertainty (0.0027, Appendix C – Section C.8)
- $\sigma_{sys}$  =  $(\sigma_{sys1}^2 + \sigma_{sys2}^2 \dots + \sigma_{sys_n}^2)^{1/2}$ , for  $\Delta k_{sys}$  uncertainties. (See the following table and Sections 7.4.1, 7.4.3, and 7.6)
- $\Delta k_{tol}$  = Statistical combination of manufacturing reactivity uncertainties ( [       ] , Table 7.3)

# Controlled Document

The following table provides a summary of the  $\Delta k_{sys}$  and  $\sigma_{sys}$  parameters applicable to this analysis. (The  $\sigma$  values are standard deviation results from KENO).

Description	$\Delta k_{sys}$	$\sigma_{sys}$
Assembly Rotation Effects (Section 7.4.1)	0.001	0.001
Boral Blisters (Section 7.4.3)	0.004	0.001
Limiting Accident (Missing Insert, Section 7.6)	0.006	0.001
Combined Values	0.011	0.0017

The standard deviations and tolerance uncertainties are included as the square root of the sum of the squares since they represent independent events. Solving for  $k_{95/95}$  yields a 95/95 upper limit k-eff that is larger than 0.927 so it is rounded-up to 0.928. The above determination of the upper limit 95/95 k-eff is consistent with the method documented in Reference 6 and allows one to state that at least 95% of the normal population is less than the 95/95 k-eff value calculated with a 95% confidence.

The results demonstrate the postulated configuration with the ATRIUM 10XM REBOL lattices meets the NRC criticality safety acceptance criterion that the array k-eff under the worst credible conditions is  $\leq 0.95$ .

# Controlled Document

**Table 7.1 Summary of CASMO-4 Maximum In-Rack Reactivity Results**

### Reference Bounding Lattices

ATRIUM 10XM geometry, top and bottom lattice geometries explicitly modeled  
 4.70 wt% U-235 uniform enrichment distribution above [ ]  
 4.70 wt% U-235 uniform enrichment distribution at and below [ ]  
 8 gadolinia rods with 3.5 wt% Gd<sub>2</sub>O<sub>3</sub> above [ ]  
 8 gadolinia rods with 3.919 wt% Gd<sub>2</sub>O<sub>3</sub> at and below [ ]  
 Standard 100 mil fuel channel  
 Reflective boundary condition for in-core calculations  
 No xenon or lumped fission products for in-rack calculations  
 Periodic boundary condition for in-rack calculations

Condition	Top Lattice	Bottom Lattice
Maximum In-Rack $k_{\infty}$ , 4°C (39.2°F)	0.8825	0.8825
Exposure, GWd/MTU	10.5	11.5
Void History	[ ]	[ ]

### REBOL Lattices

ATRIUM 10XM geometry, top and bottom lattice geometries explicitly modeled  
 3.38 wt% U-235 uniform enrichment distribution above [ ]  
 3.21 wt% U-235 uniform enrichment distribution at and below [ ]  
 No gadolinia  
 Standard 100 mil fuel channel  
 BOL (zero exposure, no xenon, no fission products)  
 Periodic boundary condition

Condition	Top Lattice	Bottom Lattice
Maximum In-Rack $k_{\infty}$ , 4°C (39.2°F)	0.8934	0.8935
Margin to Reference Bounding Lattice	0.0109	0.0110

# Controlled Document

**Table 7.2 Summary of KENO V.a Maximum In-Rack Reactivity Results**

### Fuel Assembly

ATRIUM 10XM geometry, top and bottom lattice geometries explicitly modeled  
3.38 wt% U-235 uniform enrichment distribution above [ ]  
3.21 wt% U-235 uniform enrichment distribution at and below [ ]  
No gadolinia  
Standard 100 mil Channel  
BOL (zero exposure, no xenon, no fission products)  
Periodic boundary conditions for in-rack x-y plane and the axial direction

### Storage Array Configuration

Explicit 2x2 rack model with infinite periodic boundary conditions  
Assembly centered in cell water volume  
4°C moderator and fuel temperatures

Description	k-eff
In-Rack 4°C (39.2°F) k-eff	0.897 ± 0.001
Maximum $k_{95/95}$ Reactivity (including uncertainties, biases, manufacturing tolerances and worst accident or abnormal loading conditions)	0.928

# Controlled Document

**Table 7.3 Manufacturing Reactivity Uncertainties**  
(Based upon BOL conditions using KENO V.a except as noted.)

[

]

- 
- \* This is a conservative approximation of the spacer growth at peak reactivity exposures.
  - † This is a lifetime maximum value and is assigned to each side of the fuel channel, [ ].
  - ‡ Depletion based adders of [ ] have been added to the gad concentration and gad density cases, respectively.
  - § This calculation was performed using the minimum value so no manufacturing uncertainty is required, see discussion in Section 7.3.

# Controlled Document

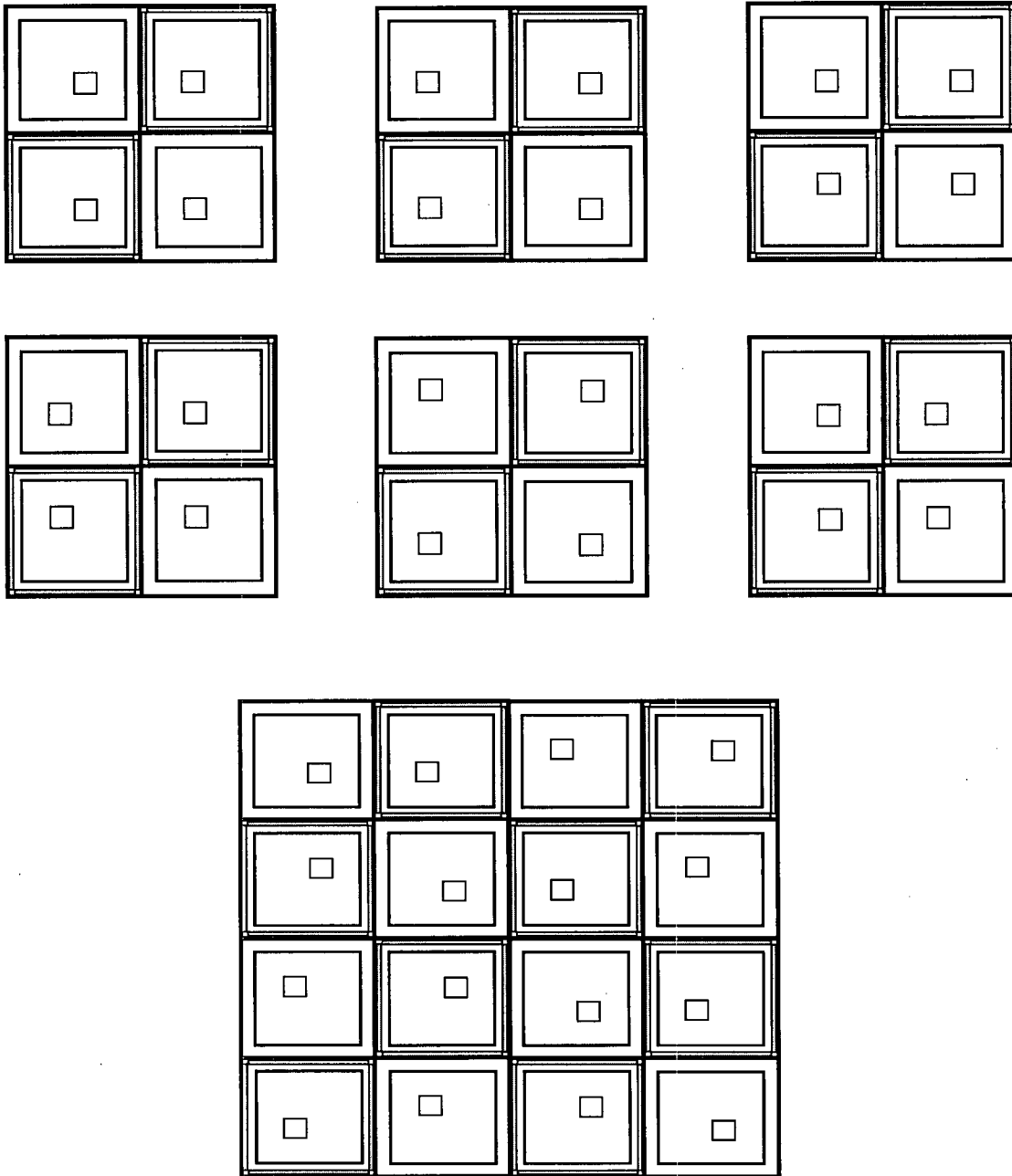


**Figure 7.1 Evaluated Assembly Rotation Cases**

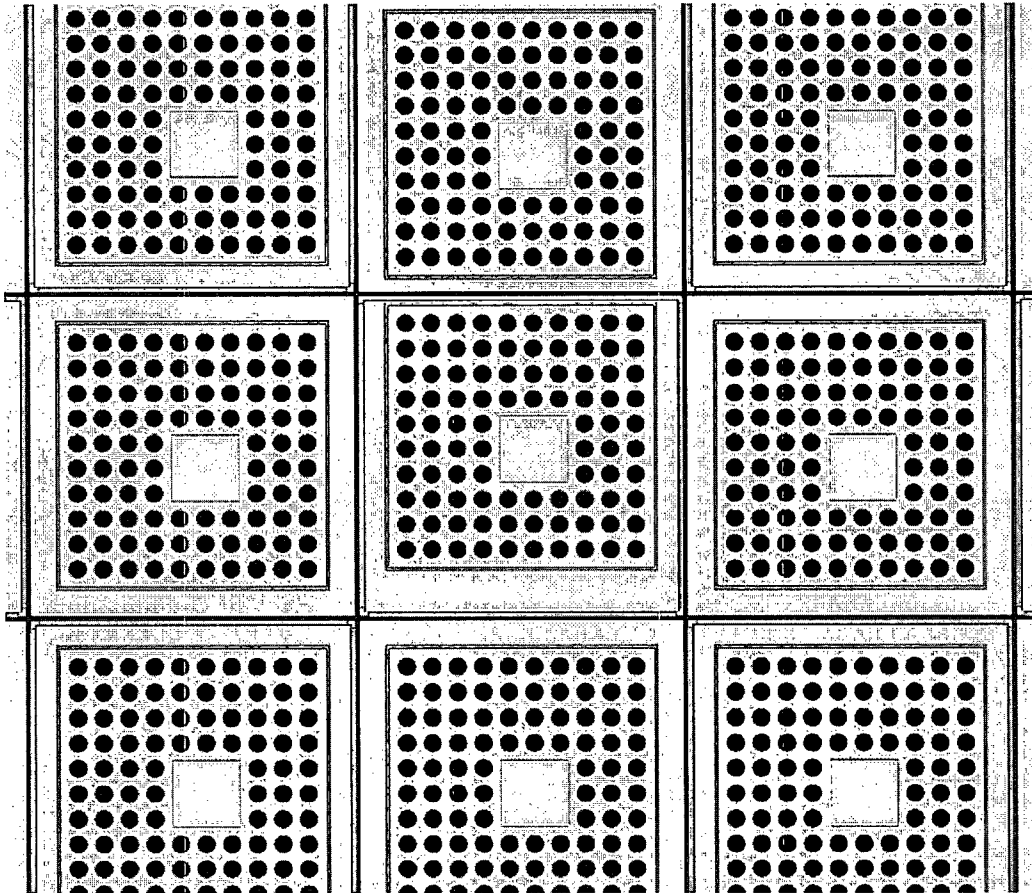


**Figure 7.2 Limiting Accident (Missing Boral Plate)**

(Note that assembly positions have been shifted to maximize the worth of this accident condition. The missing Boral plate is located between the center-top and center cell in the figure.)



# Controlled Document

## 8.0 References

1. Northern States Power Company Docket No. 50-263 Monticello Nuclear Generating Plant Amendment to Provisional Operating License, April 14 1978. (ADAMS # ML020880176)
2. NUREG-0800, *Standard Review Plan for the Review of Safety Analysis Reports for Nuclear Power Plants*, Section 9.1.1 Revision 3 (Criticality Safety of Fresh and Spent Fuel Storage and Handling), U.S. Nuclear Regulatory Commission, March 2007.
3. Code of Federal Regulations, Title 10, Part 50, Section 68, "Criticality Accident Requirements."
4. Criticality Safety Criteria for the Handling, Storage and Transportation of LWR Fuel Outside Reactors, ANSI/ANS American National Standard 8.17-1984, American Nuclear Society, January 1984, (withdrawn 2004).
5. Letter, Brian K. Grimes, Assistant Director for Engineering and Projects Division of Operating Reactors, U.S. Nuclear Regulatory Commission, to All Power Reactor Licensees, "OT Position for the Review and Acceptance of Spent Fuel Storage and Handling Applications," April 14, 1978, as amended by letter, January 18, 1979.
6. Letter, Laurence Kopp (Reactor Systems Branch, NRC) to Timothy Collins, Chief (Reactor Systems Branch-NRC), Subject: "Guidance on the Regulatory Requirements for Criticality Analysis of Fuel Storage at Light-Water Reactor Power Plants," August 19, 1998.
7. Final Division of Safety Systems Interim Staff Guidance, DSS-ISG-2010-01 Revision 0, Staff Guidance Regarding The Nuclear Criticality Safety Analysis For Spent Fuel Pools, (ADAMS # ML110620086).
8. Letter, J. T. Conway (Monticello) to USNRC, "Supplement to Responses to Requests for Additional Information Regarding the Monticello Nuclear Generating Plant License Renewal Application (TAC No. MC6440)," November 17 2005, L-MT-05-114, (ADAMS # ML053250099).
9. NUREG/CR-0200 Revision 6, *SCALE Version 4.4 A Modular Code System for Performing Standardized Computer Analyses for Licensing Evaluation*, Oak Ridge National Laboratory, May 2000.
10. NUREG/CR-6698, *Guide for Validation of Nuclear Criticality Safety Computational Methodology*, Nuclear Regulatory Commission, January 2001.
11. EMF-2158(P)(A) Revision 0, *Siemens Power Corporation Methodology for Boiling Water Reactors: Evaluation and Validation of CASMO-4/MICROBURN-B2*, Siemens Power Corporation, October 1999.

# Controlled Document

Monticello Nuclear Plant Spent Fuel Storage Pool  
Criticality Safety Analysis for ATRIUM™ 10XM Fuel

---

ANP-3113(NP)  
Revision 0  
Page 8-2

12. ICSBEP Guide to the Expression of Uncertainties, Revision 5, V. F. Dean, September 30, 2008. {Distributed with the International Handbook of Evaluated Criticality Safety Benchmark Experiments, Nuclear Energy Agency, NEA/NSC/DOC(95)03, September 2009 Edition.}

# Controlled Document

## Appendix A Sample CASMO-4 Input

Tables A.1 and A.2 provide the CASMO-4 spent fuel storage rack model for the reference bounding lattices defined in this analysis.

ATRIUM 10XM fuel which does not conform to the enrichment and gadolinia requirements described in Table 2.1 can be analyzed for storage in the spent fuel storage racks by adapting the CASMO-4 sample inputs presented in Table A.1 or A.2. Evaluations should be performed with [ ] depletion for bottom geometry lattices and [ ] depletion for top geometry lattices. These calculations will be performed with the NRC approved CASMO-4 code described in EMF-2158(P)(A), (Reference 11 of the main report).

If the lifetime maximum in-rack  $k_{\infty}$  of the new lattices are less than the  $k_{\infty}$  of the corresponding reference bounding lattices (0.8825), the ATRIUM 10XM fuel assembly can be safely stored in the Monticello Nuclear Plant spent fuel storage racks.

# Controlled Document

Monticello Nuclear Plant Spent Fuel Storage Pool  
Criticality Safety Analysis for ATRIUM™ 10XM Fuel

ANP-3113(NP)  
Revision 0  
Page A-2

---

## Table A.1 CASMO-4 Input for ATRIUM 10XM Top Reference Bounding Lattice

[

]

# Controlled Document

Monticello Nuclear Plant Spent Fuel Storage Pool  
Criticality Safety Analysis for ATRIUM™ 10XM Fuel

ANP-3113(NP)  
Revision 0  
Page A-3

---

## Table A.2 CASMO-4 Input for ATRIUM 10XM Bottom Reference Bounding Lattice

[

]

## **Appendix B Reactivity Comparison for Assemblies Used in the Monticello Reactor**

All previously manufactured assemblies used in the Monticello reactor have been evaluated to determine the most limiting lattices on the basis of highest lifetime in-rack  $k_{\infty}$ . The resulting limiting lattices were then used to establish a reference bounding lattice for each geometry zone as well as a corresponding REBOL lattice that is used as the basis for the KENO V.a criticality analysis. Section B.1 provides a comparison of the resulting limiting lattices and their corresponding reference bounding lattices and REBOL lattices.

The Monticello spent fuel pool is described in detail in Section 4 of the main body and contains 13 high density Boral storage racks and 1 low density original rack. The Boral racks represent the limiting storage configuration in the Monticello spent fuel pool (see Table 6.3). Therefore, the Boral rack configuration is used for the  $k_{\infty}$  comparisons in this appendix.

### **B.1 Summary of Lattice In-Rack Reactivity Comparisons**

The screening and calculations performed in Section B.2 of this appendix resulted in the selection of the highest reactivity previously manufactured (or legacy) lattices based upon calculated CASMO-4 in-rack  $k_{\infty}$  values. These limiting as-fabricated lattices are compared to the corresponding ATRIUM 10XM reference bounding lattices and REBOL lattices in Table B.1. This comparison shows that the ATRIUM 10XM reference bounding lattices described in Table 7.1 are more reactive than any of the previously manufactured lattices used in the Monticello reactors. It also shows that the REBOL lattices defined for use in the KENO V.a calculations are more reactive than the reference bounding lattices.

# Controlled Document

**Table B.1 Lattice Reactivity Comparisons  
 (REBOL, Bounding, and Limiting)**

Case Description	Lattice Description	Maximum In-Rack $k_{\infty}$ (CASMO-4 @ 4 °C)
<b>Top Lattices</b>		
REBOL, Top Lattice [            ]	XMLCT-3.38 (no Gad)	0.8934
<b>Reference Bounding Top Lattice</b> [            ]	<b>XMLCT-470UL-8G35</b>	<b>0.8797*</b>
Limiting As-Fabricated Top Lattice [            ]	GE14 (from Table B.4) †	0.8452
Margin to Reference Bounding Lattice (Reference - Limiting)		0.0345 $\Delta k$
<b>Bottom Lattices</b>		
REBOL, Bottom Lattice [            ]	XMLCB-3.21 (no Gad)	0.8935
<b>Reference Bounding Bottom Lattice</b> [            ]	<b>XMLCB-470UL-8G3919</b>	<b>0.8790*</b>
Limiting As-Fabricated Bottom Lattice [            ]	GE14 (from Table B.4) †	0.8410
Margin to Reference Bounding Lattice (Reference - Limiting)		0.0380 $\Delta k$

\* For direct comparison with the legacy fuel, this value also includes the effects of lumped fission products. Without lumped fission products the  $k_{\infty}$  value increases to 0.8825 as reported in Table 7.1.

† Lattice descriptions for non-AREVA supplied fuel are not provided in this document since they have been identified as proprietary by that vendor.

## **B.2 Previously Manufactured Lattices**

Monticello has loaded a number of different product lines including GE7x7, GE8x8 (GE7 thru GE10), GE9x9 (GE11), and GE10x10 (GE12 and GE14) fuel. Some lead use assemblies have also been loaded.

Initial operation of the Monticello reactor transitioned from initial 12 month nominal cycle lengths to the current 24 month cycles. The reactor power level has also increased with the later cycles operating at 106.3% of the original licensed thermal power level\*. As a consequence of the movement towards longer cycles and higher operating power levels, the fuel designs have transitioned to higher U-235 enrichment and Gadolinia loadings. The general trend is that the later high enrichment fuel designs bound the earlier low enrichment designs.

### **B.2.1 Current Inventory and Initial Screening**

The previously manufactured fuel inventory is summarized in Table B.2 and Table B.3. An initial screening of the previously manufactured fuel assemblies was performed based upon U-235 enrichment and gadolinia loading. It was determined that explicit calculation of in-rack  $k_{\infty}$  is not required for lattices with gadolinia and with initial peak average enrichment at or below the lowest REBOL lattice enrichment of 3.21 wt% U-235. These fuel assemblies are identified in Table B.2. This criterion is based upon the recognition that a lattice without gadolinia (such as the REBOL lattices) will always exhibit a higher reactivity than a lattice having the same enrichment and gadolinia (this condition is illustrated in Figure D.4 of Appendix D). While it is noted that the application of enrichment only screening does not specifically address changes in lattice geometry (i.e., 7x7 or 8x8 versus later 9x9 and 10x10 designs), these lattice geometry impacts are small compared to the conservatism established with the non-gadolinia REBOL lattice, as discussed above. Furthermore, Table B.3 shows that similar lattices with higher U-235 enrichment levels have significant reactivity margin to the limiting lattices. Application of this criterion immediately screens out the GE 7x7 fuel and many of the older GE 8x8 assemblies.

---

\* Future operating cycles are planned for uprate to 120% of original licensed thermal power.



## B.2.2 Explicit Reactivity Evaluations

Table B.3 provides a comparison of the peak in-rack CASMO-4  $k_{\infty}$  values\* of the evaluated lattices. The axial zones are separated at [                      ]. These in-rack lattice k-infinity comparisons are based upon actual GE8x8, GE9x9, and GE10x10 lattice geometries and enrichment distributions.

The most reactive lattice for each axial zone and each assembly type is listed in Table B.4. This comparison supports the comparison in Table B.1 which establishes that the lattices of all previously manufactured Monticello fuel assemblies are less reactive than the lattices of the ATRIUM 10XM reference bounding assembly. As such, the ATRIUM 10XM reference bounding assembly design forms the basis for demonstrating that the  $k_{95/95}$  for the spent fuel pool storage array remains less than 0.95.

---

\* [                      ]

]

# Controlled Document

**Table B.2 Low U-235 Enrichment Fuel Assemblies**

Assembly Description	Peak Planar Enrichment	Array
7D225 (Initial Core)	2.25	7x7
7D230	2.30	7x7
8D262-4G1.5	2.62	8x8
8D250-4G1.5	2.50	8x8
8D219-3G40	2.19	8x8
8D262-4G1.5	2.62	8x8
8DRB265-6G20	2.82	8x8
8DRB282-7G30	3.01	8x8
P8DRB265-6G20	2.82	8x8
P8DRB282-7G30	3.01	8x8
P8DRB284-5G30	3.02	8x8
P8DRB299-7G30-80M-145	3.19	8x8

# Controlled Document

Monticello Nuclear Plant Spent Fuel Storage Pool  
 Criticality Safety Analysis for ATRIUM™ 10XM Fuel

ANP-3113(NP)  
 Revision 0  
 Page B-6

**Table B.3 In-Rack Reactivity Comparison (by product line)**

Assembly Description	Bottom	Top	Peak In-Rack K-infinity			
			[ Depletion ]	[ Depletion ]	[ Depletion ]	
<b>GE8B - 8x8 Array</b>						
	1	x		0.8119	0.8124	0.8123
GE8B-P8DRB319-9GZ1-80M-4WR-145	2	x	x	<b>0.8302</b>	0.8299	0.8288
	3		x	0.8036	0.8032	0.8025
	4		x	<b>0.8302</b>	0.8299	0.8288
Max. Bottom Lattice				<b>0.8302</b>	0.8299	0.8288
Max. Top Lattice				<b>0.8302</b>	0.8299	0.8288

Assembly Description	Bottom	Top	Peak In-Rack K-infinity			
			[ Depletion ]	[ Depletion ]	[ Depletion ]	
<b>GE9B - 8x8 Array</b>						
	1	x		0.7834	0.7842	0.7855
GE9B-P8DWB312-9GZ-80M-145-T	2	x	x	0.7938	0.7941	0.7941
	3		x	0.7867	0.7861	0.7846
	4		x	0.8007	0.8015	0.8014
GE9B-P8DWB313-10GZ-80M-145-T	1	x		0.8020	0.8027	0.8023
	2	x	x	<b>0.8124</b>	0.8117	0.8103
	3		x	0.7977	0.7970	0.7950
	4		x	0.8206	<b>0.8212</b>	0.8191
Max. Bottom Lattice				<b>0.8124</b>	0.8117	0.8103
Max. Top Lattice				0.8206	<b>0.8212</b>	0.8191

# Controlled Document

Monticello Nuclear Plant Spent Fuel Storage Pool  
 Criticality Safety Analysis for ATRIUM™ 10XM Fuel

ANP-3113(NP)  
 Revision 0  
 Page B-7

**Table B.3 In-Rack Reactivity Comparison (by product line) (Continued)**

Assembly Description	Bottom	Top	Peak In-Rack K-infinity			
			[ Depletion ]	[ Depletion ]	[ Depletion ]	
<b>GE10 - 8x8 Array</b>						
	1	x		0.7951	0.7964	0.7985
GE10-P8DXB324-10GZ-70M-145.24-C	2	x	x	0.8228	0.8226	0.8222
	3		x	0.8083	0.8083	0.8077
	4		x	0.8122	0.8131	0.8138
<b>GE10-P8DXB324-11GZ-70M-145.24-C</b>						
	1	x		0.7951	0.7965	0.7984
GE10-P8DXB324-11GZ-70M-145.24-C	2	x	x	0.8225	0.8223	0.8219
	3		x	0.7990	0.7988	0.7981
	4		x	0.8125	0.8129	0.8135
<b>GE10-P8DXB324-10GZ1-70M-145.24-C</b>						
	1	x		0.7996	0.8009	0.8024
GE10-P8DXB324-10GZ1-70M-145.24-C	2	x	x	0.8256	0.8264	0.8258
	3		x	0.8107	0.8104	0.8097
	4		x	0.8144	0.8166	0.8173
<b>GE10-P8DXB333-10GZ-70M-145.24-C</b>						
	1	x		0.8028	0.8038	0.8053
GE10-P8DXB333-10GZ-70M-145.24-C	2	x	x	<b>0.8296</b>	0.8293	0.8286
	3		x	0.8133	0.8129	0.8119
	4		x	0.8181	0.8184	0.8187
Max. Bottom Lattice				<b>0.8296</b>	0.8293	0.8286
Max. Top Lattice				<b>0.8296</b>	0.8293	0.8286

Assembly Description	Bottom	Top	Peak In-Rack K-infinity			
			[ Depletion ]	[ Depletion ]	[ Depletion ]	
<b>SPC IX QFA - 9x9 Array</b>						
	1	x		0.8024	0.8047	0.8072
SPC 9x9-IX QFA	2	x	x	0.8297	0.8315	<b>0.8323</b>
	3		x	0.8019	0.8040	0.8061
	4		x	0.8080	0.8113	0.8141
Max. Bottom Lattice				0.8297	0.8315	<b>0.8323</b>
Max. Top Lattice				0.8297	0.8315	<b>0.8323</b>

# Controlled Document

Monticello Nuclear Plant Spent Fuel Storage Pool  
 Criticality Safety Analysis for ATRIUM™ 10XM Fuel

ANP-3113(NP)  
 Revision 0  
 Page B-8

**Table B.3 In-Rack Reactivity Comparison (by product line) (Continued)**

Assembly Description	Bottom	Top	Peak In-Rack K-infinity			
			[ Depletion ]	[ Depletion ]	[ Depletion ]	
<b>GE11 - 9x9 Array</b>						
	1	x		0.8026	0.8035	0.8040
GE11-P9DUB348-10GZ-100T-141-T	2	x	x	0.8220	0.8224	0.8223
	3		x	0.8139	0.8154	0.8166
	4		x	0.8258	0.8258	0.8249
GE11-P9DUB347-10GZ-100T-141-T	1	x		0.8011	0.8024	0.8036
	2	x	x	0.8163	0.8168	0.8169
	3		x	0.8204	0.8212	0.8214
GE11-P9DUB366-16GZ-100T-141-T	1	x		0.8086	0.8099	0.8117
	2	x	x	0.8234	0.8252	0.8270
	3		x	0.8123	0.8132	0.8135
	4		x	0.8278	0.8303	0.8331
GE11-P9DUB366-17GZ-100T-141-T	1	x		0.8032	0.8054	0.8074
	2	x	x	0.8133	0.8157	0.8178
	3		x	0.8038	0.8045	0.8050
	4		x	0.8173	0.8201	0.8230
GE11-P9DUB380-17GZ-100T-141-T	1	x		0.8207	0.8226	0.8230
	2	x	x	0.8242	0.8285	<b>0.8324</b>
	3		x	0.8249	0.8273	0.8277
	4		x	0.8290	0.8339	<b>0.8383</b>
GE11-P9DUB380-16GZ-100T-141-T	1	x		0.8182	0.8198	0.8197
	2	x	x	0.8237	0.8279	0.8314
	3		x	0.8273	0.8291	0.8286
	4		x	0.8286	0.8333	0.8375
Max. Bottom Lattice				0.8242	0.8285	<b>0.8324</b>
Max. Top Lattice				0.8290	0.8339	<b>0.8383</b>

# Controlled Document

**Table B.3 In-Rack Reactivity Comparison (by product line) (Continued)**

Assembly Description	Bottom	Top	Peak In-Rack K-infinity			
			[ Depletion ]	[ Depletion ]	[ Depletion ]	
<b>GE12 - 10x10 Array</b>						
	1	x		0.8013	0.8022	0.8031
GE12-P10DSB330-12GZ-100T-145-T	2	x	x	0.8158	<b>0.8159</b>	0.8156
	3		x	0.8213	0.8227	<b>0.8237</b>
Max. Bottom Lattice				0.8158	<b>0.8159</b>	0.8156
Max. Top Lattice				0.8213	0.8227	<b>0.8237</b>

Assembly Description	Bottom	Top	Peak In-Rack K-infinity			
			[ Depletion ]	[ Depletion ]	[ Depletion ]	
<b>GE14 - 10x10 Array</b>						
	1	x		0.8328	0.8297	0.8249
GE14-P10DNAB391-14GZ-100T-145-T-a	2	x	x	<b>0.8410</b>	0.8380	0.8336
	3		x	0.8214	0.8195	0.8162
	4		x	<b>0.8452</b>	0.8431	0.8394
	1	x		0.8251	0.8219	0.8172
GE14-P10DNAB391-14GZ-100T-145-T-b	2	x	x	<b>0.8410</b>	0.8380	0.8336
	3		x	0.7966	0.7963	0.7954
	4		x	0.8193	0.8190	0.8180
	1	x		0.8145	0.8119	0.8076
GE14-P10DNAB393-17GZ-100T-145-T-a	2	x	x	0.8296	0.8266	0.8220
	3		x	0.8126	0.8102	0.8060
	4		x	0.8370	0.8343	0.8294
	1	x		0.8145	0.8119	0.8076
GE14-P10DNAB393-17GZ-100T-145-T-b	2	x	x	0.8296	0.8266	0.8220
	3		x	0.8158	0.8139	0.8107
	4		x	0.8398	0.8377	0.8339
	1	x		0.7991	0.7977	0.7954
GE14-P10DNAB392-16GZ-100T-145T-T-a	2	x	x	0.8136	0.8118	0.8090
	3		x	0.8003	0.7996	0.7983
	4		x	0.8234	0.8226	0.8210

# Controlled Document

Monticello Nuclear Plant Spent Fuel Storage Pool  
 Criticality Safety Analysis for ATRIUM™ 10XM Fuel

ANP-3113(NP)  
 Revision 0  
 Page B-10

**Table B.3 In-Rack Reactivity Comparison (by product line) (Continued)**

Assembly Description	Bottom	Top	Peak In-Rack K-infinity			
			[ Depletion ]	[ Depletion ]	[ Depletion ]	
<b>GE14 - 10x10 Array (cont.)</b>						
	1	x		0.7988	0.7974	0.7951
GE14-P10DNAB392-16GZ-100T-145T-T-b	2	x	x	0.8133	0.8115	0.8087
	3		x	0.7999	0.7993	0.7980
	4		x	0.8230	0.8223	0.8206
	1	x		0.8142	0.8116	0.8074
GE14-P10DNAB392-17GZ-100T-145T-T	2	x	x	0.8292	0.8263	0.8218
	3		x	0.8154	0.8135	0.8104
	4		x	0.8394	0.8373	0.8336
	1	x		0.8045	0.8031	0.8001
GE14-P10DNAB424-14GZ-100T-145-T	2	x	x	0.8192	0.8170	0.8129
	3		x	0.8048	0.8036	0.8006
	4		x	0.8286	0.8272	0.8235
	1	x		0.7812	0.7805	0.7796
GE14-P10DNAB375-16GZ-100T-145-T	2	x	x	0.7952	0.7940	0.7925
	3		x	0.7798	0.7801	0.7807
	4		x	0.8010	0.8014	0.8021
	1	x		0.7988	0.7974	0.7951
GE14-P10DNAB392-16GZ-100T-145-T	2	x	x	0.8059	0.8047	0.8030
	3		x	0.7910	0.7909	0.7905
	4		x	0.8137	0.8135	0.8127
	1	x		0.8009	0.8003	0.7992
GE14-P10DNAB391-12GZ-100T-145-T	2	x	x	0.8075	0.8067	0.8055
	3		x	0.7933	0.7934	0.7933
	4		x	0.8162	0.8161	0.8156
	1	x		0.7801	0.7794	0.7785
GE14-P10DNAB373-16GZ-100T-145-T	2	x	x	0.7887	0.7881	0.7873
	3		x	0.7724	0.7730	0.7739
	4		x	0.7935	0.7941	0.7952
	1	x		0.7922	0.7899	0.7864
GE14-P10DNAB391-16GZ-100T-145-T	2	x	x	0.7974	0.7957	0.7932
	3		x	0.7815	0.7818	0.7816
	4		x	0.8035	0.8038	0.8037

# Controlled Document

Monticello Nuclear Plant Spent Fuel Storage Pool  
 Criticality Safety Analysis for ATRIUM™ 10XM Fuel

ANP-3113(NP)  
 Revision 0  
 Page B-11

**Table B.3 In-Rack Reactivity Comparison (by product line) (Continued)**

Assembly Description	Bottom	Top	Peak In-Rack K-infinity			
			[ Depletion ]	[ Depletion ]	[ Depletion ]	
<b>GE14 – 10x10 Array (Cont.)</b>						
	1	x		0.7961	0.7943	0.7914
GE14-P10DNAB391-15GZ-100T-145-T	2	x	x	0.7987	0.7966	0.7933
	3		x	0.7828	0.7827	0.7814
	4		x	0.8052	0.8051	0.8051
	1	x		0.7988	0.7984	0.7978
GE14-P10DNAB391-12GZ-100T-145-T	2	x	x	0.8033	0.8025	0.8014
	3		x	0.7879	0.7889	0.7894
	4		x	0.8103	0.8112	0.8117
	1	x		0.7804	0.7802	0.7796
GE14-P10DNAB372-17GZ-100T-145-T6	2	x	x	0.7941	0.7938	0.7933
	3		x	0.7777	0.7790	0.7806
	4		x	0.7992	0.8005	0.8022
	1	x		0.7886	0.7869	0.7845
GE14-P10DNAB386-16GZ-100T-145-T6a	2	x	x	0.7978	0.7973	0.7969
	3		x	0.7818	0.7830	0.7848
	4		x	0.8031	0.8048	0.8069
	1	x		0.7864	0.7851	0.7834
GE14-P10DNAB386-16GZ-100T-145-T6b	2	x	x	0.7964	0.7957	0.7946
	3		x	0.7808	0.7819	0.7829
	4		x	0.8024	0.8035	0.8048
	1	x		0.8039	0.8049	0.8057
GE14-P10DNAB389-11GZ-100T-145-T6	2	x	x	0.8142	0.8141	0.8139
	3		x	0.7932	0.7948	0.7967
	4		x	0.8151	0.8168	0.8189
	Max. Bottom Lattice			<b>0.8410</b>	0.8380	0.8336
Max. Top Lattice			<b>0.8452</b>	0.8431	0.8394	



# Controlled Document

**Table B.4 Limiting In-Rack Reactivity Comparison (by product line)**

Product Line	Array	Max In-Rack $k_{\infty}$ (CASMO-4 @ 4 °C)
<b>Limiting Top Lattices by Product Line</b>		
<b>GE14</b>	<b>10x10</b>	<b>0.8452</b>
GE12	10x10	0.8237
GE11	9x9	0.8383
SPC IX	9x9	0.8323
GE10	8x8	0.8296
GE9B	8x8	0.8212
GE8B	8x8	0.8302
<b>Limiting Bottom Lattices by Product Line</b>		
<b>GE14</b>	<b>10x10</b>	<b>0.8410</b>
GE12	10x10	0.8159
GE11	9x9	0.8324
SPC IX	9x9	0.8323
GE10	8x8	0.8296
GE9B	8x8	0.8124
GE8B	8x8	0.8302

The limiting lattice for each axial zone is indicated by **bold italic font**.

# Controlled Document

## **B.2.4 Evaluation of Modified, Abnormal, and Damaged Assemblies**

The preceding evaluation of previously supplied fuel is based upon nominal assembly designs. The potential exists that assemblies that have been damaged or modified may have a configuration that is more reactive than the nominal design.

One of the primary issues that could affect in-rack reactivity is the removal of one or more fuel rods from an assembly. Some BWR lattices are under moderated in the storage rack configuration; therefore, removal of a fuel rod without replacement would introduce additional moderator which could result in an increase in the lattice reactivity. This would also apply to the case where a rod has been broken and a portion of the broken fuel rod removed from the bundle.

Reconstitution of assemblies involves the replacement of one or more fuel rods. Replacement rods can be from a donor assembly, inert rods (such as stainless steel rods), or newly manufactured rods (containing either natural or enriched uranium). Assemblies in which a fuel rod has been replaced with either an inert rod or a natural uranium rod would represent a reduction in reactivity from the nominal design since the fissile material content is reduced and no change in the amount of moderator would occur. An assembly with a matched reactivity replacement rod would represent a configuration in which the resulting assembly does not significantly deviate from the nominal design. The Monticello pool contains 4 reconstituted assemblies (RMTB01 to RMTB04) where the replacement fuel rods have higher BOL U-235 enrichments levels. These have been considered and are dispositioned as part of this evaluation.

The existing inventory of fuel in the Monticello spent fuel pool includes a number of bundles that have experienced damage. Table B.5 provides a listing of the fuel assemblies that have been damaged or modified into a configuration different than the original design. Assemblies with missing fuel rods, with replacement fuel rods, or with broken fuel rods are of special interest.

Regarding the GE8x8 assemblies with missing fuel rods, a calculation for the GE8x8 lattice geometry with 4 empty rod locations produced a reactivity increase of less than  $0.005 \Delta k$ . This has relevance for assemblies MTB048 and MTB072 that have missing rod locations. Given

# Controlled Document

their low U-235 enrichment level it is apparent that these assemblies remain less limiting than the reference bounding assembly.

Assemblies MTB001, MTB048, MTB072, and MTB099 have had fuel rods removed and other GE8x8 fuel rods put in their place. Given the low enrichment level (~2.6 wt% U-235) and high burnup level (>23 GWd/STU) of these assemblies it is apparent that they are less limiting than the reference bounding assembly.

GE8x8 assemblies RMTB01, RMTB02, RMTB03, and RMTB04 were reconfigured to provide 4 extra water rod locations and to increase their BOL lattice average enrichment from 2.62 to 2.76 wt% U-235. Given the low U-235 enrichment level and the small reactivity worth of the additional water rods it is apparent that these assemblies remain less limiting than the reference bounding assembly.

Assembly JYA764 is of interest because of its low burnup and high U-235 enrichment level. Without damage, the maximum in-rack  $k_{\infty}$  for the lattices of this assembly are less than 0.84. Given the substantial margin of the reference bounding lattices ( $k_{\infty} \approx 0.879$ ), reactivity increases due to small geometry changes or potential missing pellets are not sufficient to make this a limiting assembly.

All damaged and modified assemblies are less reactive than the lattices of the reference bounding assembly.

# Controlled Document

Monticello Nuclear Plant Spent Fuel Storage Pool  
 Criticality Safety Analysis for ATRIUM™ 10XM Fuel

ANP-3113(NP)  
 Revision 0  
 Page B-15

**Table B.5 Summary of Damaged and Modified Bundles**

Bundle ID	Product Line	Peak Lattice Enrichment	Discharge Burnup (MWd/STU)	Description
MT422	7x7 Initial Core	2.25	15987	Damaged*
MT411	7x7 Initial Core	2.25	11399	Damaged
MT379	7x7 Initial Core	2.25	12053	Damaged
MT393	7x7 Initial Core	2.25	11045	Damaged
MT400	7x7 Initial Core	2.25	15913	Damaged
MT442	7x7 Initial Core	2.25	18270	Damaged
MT455	7x7 Initial Core	2.25	18108	Damaged
MT436	7x7 Initial Core	2.25	13353	Damaged
MT423	7x7 Initial Core	2.25	11456	Damaged
MT435	7x7 Initial Core	2.25	13324	Damaged
MT174	7x7 Initial Core	2.25	7196	Damaged
MT178	7x7 Initial Core	2.25	11457	Damaged
MT165	7x7 Initial Core	2.25	9727	Damaged
MT106	7x7 Initial Core	2.25	15171	Damaged
MT161	7x7 Initial Core	2.25	15908	Damaged
MT245	7x7 Initial Core	2.25	15204	Damaged
MT252	7x7 Initial Core	2.25	15191	Damaged
MT243	7x7 Initial Core	2.25	13089	Damaged
MT187	7x7 Initial Core	2.25	18001	Damaged
MT188	7x7 Initial Core	2.25	17966	Damaged
MT037	7x7 Initial Core	2.25	10624	Damaged
MT039	7x7 Initial Core	2.25	10605	Damaged
MT019	7x7 Initial Core	2.25	15440	Damaged

\* Damaged indicates that the cladding integrity has been compromised and therefore gaseous fission products and some fuel material has been removed. It does not mean that the geometry of these assemblies has changed in a significant way or that pellets have been removed.

# Controlled Document

**Table B.5 Summary of Damaged and Modified Bundles (Continued)**

Bundle ID	Product Line	Peak Lattice Enrichment	Discharge Burnup (MWd/STU)	Description
MT001	7x7 Initial Core	2.25	14722	Damaged
MT072	7x7 Initial Core	2.25	17406	Damaged
MT073	7x7 Initial Core	2.25	11360	Damaged
MT071	7x7 Initial Core	2.25	14750	Damaged
MT049	7x7 Initial Core	2.25	18108	Damaged
MT063	7x7 Initial Core	2.25	11823	Damaged
MT366	7x7 Initial Core	2.25	15124	Damaged
MT344	7x7 Initial Core	2.25	11505	Damaged
MT290	7x7 Initial Core	2.25	13336	Damaged
MT296	7x7 Initial Core	2.25	15378	Damaged
MT343	7x7 Initial Core	2.25	7679	Damaged
MT312	7x7 Initial Core	2.25	15712	Damaged
MT337	7x7 Initial Core	2.25	16140	Damaged
MT342	7x7 Initial Core	2.25	11325	Damaged
MT304	7x7 Initial Core	2.25	13624	Damaged
MT367	7x7 Initial Core	2.25	12026	Damaged
MT274	7x7 Initial Core	2.25	12248	Damaged
MT270	7x7 Initial Core	2.25	13618	Damaged
MT256	7x7 Initial Core	2.25	11365	Damaged
MT285	7x7 Initial Core	2.25	13565	Damaged
MT287	7x7 Initial Core	2.25	16587	Damaged
MT292	7x7 Initial Core	2.25	10904	Leaker
MT453	7x7 Initial Core	2.25	11305	Leaker
MTB001	GE4	2.62	23805	Segmented and regular rods, Spare rods and segments added to fill locations. No empty locations.

# Controlled Document

Monticello Nuclear Plant Spent Fuel Storage Pool  
 Criticality Safety Analysis for ATRIUM™ 10XM Fuel

ANP-3113(NP)  
 Revision 0  
 Page B-17

**Table B.5 Summary of Damaged and Modified Bundles** *(Continued)*

Bundle ID	Product Line	Peak Lattice Enrichment	Discharge Burnup (MWd/STU)	Description
MTB048	GE4	2.62	40323	3 rods removed, Miscellaneous rod added, 2 empty rod locations.
MTB071	GE4	2.62	34742	24 rods punctured for fission gas sample, No empty rod locations.
MTB072	GE4	2.62	29624	Used as repository for BOC-9 reconstitution, Holds 9 rods from that project, 3 empty rod locations.
MTB099	GE4	2.62	40333	9 rods removed, Miscellaneous rods added, No empty rod locations.
RMTB01	Reconstituted	2.76	28102	These bundles were reconstituted using rods from 8 assemblies. Original GE4 bundles. The average enrichment is based on the original BOL enrichment of the rods. Each bundle has 4 extra water rods.
RMTB02	GE4 Bundles	2.76	28751	
RMTB03		2.76	28751	
RMTB04		2.76	26863	
LJX637	GE6/7	3.02	29680	Damaged
LY2417	GE5/6	2.82	26520	Damaged
LY2442	GE6/7	3.02	30167	Damaged
LY5986	GE6/7	3.02	26612	Damaged
JYA764	GE14C	4.36	10369	Damaged

## Appendix C KENO V.a Bias and Bias Uncertainty Evaluation

The purpose of this Appendix is to determine the bias of the  $k_{\text{eff}}$  calculated with the SCALE 4.4a computer code for spent fuel pool criticality analysis. A statistical methodology is used to evaluate criticality benchmark experiments that are appropriate for the expected range of parameters. The scope of this report is limited to the validation of the KENO V.a module and CSAS25 driver in the SCALE 4.4a code package for use with the 44 energy group cross-section library 44GROUPNDF5 for spent fuel criticality analyses.

This calculation is performed according to the general methodology described in Reference C.2 (NUREG/CR-6698) that is also briefly described in Section C.1. The critical experiments selected to benchmark the computer code system are discussed in Section C.3. The results of the criticality benchmark calculations, the trending analysis, the basis for the statistical technique chosen, the bias, and the bias uncertainty are presented in Sections C.4 - C.7. Final results are summarized in Section C.8.

### C.1 Statistical Method for Determining the Code Bias

As presented in Reference C.2 (NUREG/CR-6698), the validation of the criticality code must use a statistical analysis to determine the bias and bias uncertainty in the calculation of  $k_{\text{eff}}$ . The approach involves determining a weighted mean of  $k_{\text{eff}}$  that incorporates the uncertainty from both the measurement ( $\sigma_{\text{exp}}$ ) and the calculation method ( $\sigma_{\text{calc}}$ ). A combined uncertainty can be determined using Equation 3 from Reference C.2, for each critical experiment:

$$\sigma_t = \sqrt{\sigma_{\text{calc}}^2 + \sigma_{\text{exp}}^2}$$

The weighted mean  $k_{\text{eff}}$ , the variance about the mean ( $s^2$ ), and the average total uncertainty of the benchmark experiments ( $\bar{\sigma}^2$ ) can be calculated using the weighting factor  $1/\sigma_i^2$  (see Eq. 4, 5, and 6 in Reference C.2). The final objective is to determine the square root of the pooled variance, defined as (Eq. 7 from Reference C.2):

$$S_p = \sqrt{s^2 + \bar{\sigma}^2}$$

# Controlled Document

Determination of the  $k_{\text{eff}}$  bias and uncertainty requires evaluation of the distribution of data and investigation of possible trends. Trends are identified by regression analysis to determine key parameters including the slope, intercept, coefficient of determination, the T-value associated with the Student's T-distribution, and a check for normality of the distribution of residuals in order to evaluate goodness-of-fit. These key parameters are used to establish the statistical significance of the calculated trend. If a trend is found to have statistical significance, then a one-sided lower tolerance band may be used to determine the bias and uncertainty. This method provides a fitted curve ( $K_L(x)$ ), above which 95% of the true population of  $k_{\text{eff}}$  is expected to lie, with a 95% confidence level.

If no trends of statistical significance are found and the data is normally distributed, then the bias and uncertainty can be based on a single-sided lower tolerance limit technique. This method defines a lower tolerance limit ( $K_L$ ) above which 95% of the true population of  $k_{\text{eff}}$  is expected to lie, with a 95% confidence level. The  $K_L$  is defined in terms of the weighted-average of the data ( $\overline{k_{\text{eff}}}$ ), the 95/95 single-sided lower tolerance factor ( $C_{95/95}$  – dependent on the size of the observed population), and the square-root of the pooled variance ( $S_p$ ), as shown below.

$$K_L = \overline{k_{\text{eff}}} - C_{95/95} S_p$$

In this case, the statistical bias and uncertainty are defined as shown below.

$$\text{Bias} = \overline{k_{\text{eff}}} - 1, \text{ for } \overline{k_{\text{eff}}} < 1, \text{ otherwise, Bias} = 0$$

$$\text{Uncertainty} = C_{95/95} S_p$$

Finally, if the data is not normally distributed, then a nonparametric analysis can be employed. This method considers the size of the observed population and determines the  $m^{\text{th}}$  lowest value ( $k_{\text{eff}}^m < 1$ ) and the associated uncertainty ( $\sigma^m$ ) to determine a limiting value ( $K_L$ ), above which 95% of the true population of  $k_{\text{eff}}$  is expected to lie, with a 95% confidence level. Here, the sample size must exceed 59 in order to attain a 95/95 confidence interval, otherwise additional Non-Parametric Margin (NPM – defined by NUREG/CR-6698, see Reference C.2) must be included in the  $K_L$ , as shown below.



# Controlled Document

$$K_L = k_{\text{eff}}^m - \sigma^m - \text{NPM}$$

$$\text{Bias} = k_{\text{eff}}^m - 1$$

$$\text{Uncertainty} = \sigma^m + \text{NPM}$$

Regardless of the method employed, the Area of Applicability (AOA) must also be defined based on evaluation of key parameters of the criticality experiments that are included in the validation. Key parameters fall into three categories: materials, geometry, and neutron energy spectrum. In general, use of the criticality evaluation is restricted to the range of parameters identified in the AOA.

## C.2 Area of Applicability Required for the Benchmark Experiments

Commercial reactor spent fuel pools will primarily contain nuclear fuel in metal rods in a square array. This fuel is characterized by the parameter values provided in Table C.1. These typical values were used as primary tools in selecting the benchmark experiments appropriate for determining the code bias.

Benchmark calculations have been made on selected critical experiments, chosen, in so far as possible, to bound the range of variables in the spent fuel rack analysis. In rack designs, the most significant parameters affecting criticality are: (1) the fuel enrichment, (2) the neutron absorbing material, and (3) the lattice spacing. Other parameters have a smaller effect but have also been included in the analysis.

One possible way of representing the data is through a spectral parameter that incorporates influences from the variations in other parameters. The energy of the average lethargy causing fission (EALF) is this type of parameter and it is computed by KENO V.a. The range for this parameter is also included in Table C.1.

**Table C.1 Range of Values for Key Spent Fuel Pool Parameters**

Parameter	Range of Values
Fissile material – Physical/Chemical Form	UO <sub>2</sub> rods
Enrichment	2.35 to 4.74 wt% U-235
Moderation/Moderator	Heterogeneous/Water
Lattice	Square, Rectangular
Pitch	1.26 to 2.54 cm
Clad	Zircaloy, Aluminum
Anticipated Absorber/Materials	Boron, Stainless Steel, Water
Moderating Ratio (H/X)	110 to >400
Reflection	Water, Stainless Steel
Neutron Energy Spectrum (Energy of the Average Lethargy Causing Fission)	0.060 to 0.247 eV

# Controlled Document

## **C.3 Description of the Criticality Experiments Selected**

The set of criticality benchmark experiments has been constructed to accommodate large variations in the range of parameters of the rack configurations and also to provide adequate statistics for the evaluation of the code bias.

Sixty eight (68) critical configurations were selected from various sources. These benchmarks include configurations performed with lattices of UO<sub>2</sub> fuel rods in water having various enrichments and moderating ratios (H/X). The area of applicability (AOA) is established within this range of benchmark experiment parameter values.

A brief description of the selected benchmark experiments is presented in Table C.2. The table includes the references where detailed descriptions of the experiments are presented.

# Controlled Document

Monticello Nuclear Plant Spent Fuel Storage Pool  
 Criticality Safety Analysis for ATRIUM™ 10XM Fuel

ANP-3113(NP)  
 Revision 0  
 Page C-6

**Table C.2 Descriptions of the Critical Benchmark Experiments**

Experiment Case Name	Measured $k_{eff}$	$\sigma_{exp}$	Brief Description	Neutron Absorber	Reflector			
LEU-COMP-THERM-007 (Reference C.1)								
CEA-001-001	1.0000	0.0014	Square pitch fuel rod arrays with varying rod pitch configurations. Each fuel rod is aluminum clad with UO <sub>2</sub> fuel at 4.738 wt% U-235. Performed at CEA Valduc Critical Mass Laboratory.	None	Water			
CEA-001-002	1.0000	0.0008						
CEA-001-003	1.0000	0.0007						
CEA-001-004	1.0000	0.0008						
LEU-COMP-THERM-0034 (Reference C.1)								
CEA-003-003	1.0000	0.0039	A 2x2 array UO <sub>2</sub> fuel rod clusters with 4.738 wt% U-235 surrounded by plates of neutron absorbing material. Each fuel rod cluster is comprised of an 18x18 array of aluminum clad fuel rods with a square lattice pitch of 1.6 cm. Performed at CEA Valduc Critical Mass Laboratory.	Borated Stainless Steel	Water			
CEA-003-004	1.0000	0.0039						
CEA-003-005	1.0000	0.0039						
CEA-003-006	1.0000	0.0039						
CEA-003-007	1.0000	0.0039						
CEA-003-008	1.0000	0.0039						
CEA-003-010	1.0000	0.0048		Boral				
CEA-003-011	1.0000	0.0048						
CEA-003-012	1.0000	0.0048						
CEA-003-013	1.0000	0.0048						
CEA-003-014	1.0000	0.0043						
CEA-003-015	1.0000	0.0043						
LEU-COMP-THERM-039 (Reference C.1)								
CEA-005-001	1.0000	0.0014				Square pitch (pitch = 1.26 cm) fuel rod arrays without fuel rods in all positions. Each fuel rod is aluminum clad with UO <sub>2</sub> fuel at 4.738 wt% U-235. Performed at CEA Valduc Critical Mass Laboratory.	None	Water
CEA-005-002	1.0000	0.0014						
CEA-005-003	1.0000	0.0014						
CEA-005-004	1.0000	0.0014						
CEA-005-005	1.0000	0.0009						
CEA-005-006	1.0000	0.0009						
CEA-005-007	1.0000	0.0012						
CEA-005-008	1.0000	0.0012						
CEA-005-009	1.0000	0.0012						
CEA-005-010	1.0000	0.0012						
CEA-005-011	1.0000	0.0013						
CEA-005-012	1.0000	0.0013						
CEA-005-013	1.0000	0.0013						
CEA-005-014	1.0000	0.0013						
CEA-005-015	1.0000	0.0013						
CEA-005-016	1.0000	0.0013						
CEA-005-017	1.0000	0.0013						

# Controlled Document

Monticello Nuclear Plant Spent Fuel Storage Pool  
 Criticality Safety Analysis for ATRIUM™ 10XM Fuel

ANP-3113(NP)  
 Revision 0  
 Page C-7

**Table C.2 Descriptions of the Critical Benchmark Experiments** *(Continued)*

Experiment Case Name	Measured $k_{eff}$	$\sigma_{exp}$	Brief Description	Neutron Absorber	Reflector
<b>LEU-COMP-THERM-001 (Reference C.1)</b>					
PNL-001-001	0.9998	0.0031	UO <sub>2</sub> pellets enriched at 2.35 wt% U-235 clad in aluminum. Varying clusters of fuel rods on a 2.032 cm pitch, moderated by water. Single cluster or multiple clusters with varying separation distances.	None	Water
PNL-001-002	0.9998	0.0031			
PNL-001-003	0.9998	0.0031			
PNL-001-004	0.9998	0.0031			
PNL-001-005	0.9998	0.0031			
PNL-001-006	0.9998	0.0031			
PNL-001-007	0.9998	0.0031			
PNL-001-008	0.9998	0.0031			
<b>LEU-COMP-THERM-002 (Reference C.1)</b>					
PNL-002-001	0.9997	0.0020	UO <sub>2</sub> pellets enriched at 4.31 wt% U-235. Varying clusters of fuel rods on a 2.54 cm pitch, moderated by water. Single cluster or multiple clusters with varying separation distances.	None	Water
PNL-002-002	0.9997	0.0020			
PNL-002-003	0.9997	0.0020			
PNL-002-004	0.9997	0.0018			
PNL-002-005	0.9997	0.0019			
<b>LEU-COMP-THERM-009 (Reference C.1)</b>					
PNL-009-001	1.0000	0.0021	UO <sub>2</sub> pellets enriched at 4.31 wt% U-235 clad in aluminum. Three 15x8 clusters of fuel rods on a 2.54 cm pitch, separated by different absorber plates. Varying separation distances.	Steel	Water
PNL-009-002	1.0000	0.0021			
PNL-009-003	1.0000	0.0021			
PNL-009-004	1.0000	0.0021			
PNL-009-005	1.0000	0.0021			
PNL-009-006	1.0000	0.0021			
PNL-009-007	1.0000	0.0021			
PNL-009-008	1.0000	0.0021			
PNL-009-009	1.0000	0.0021			
PNL-009-024	1.0000	0.0021			
PNL-009-025	1.0000	0.0021			
PNL-009-026	1.0000	0.0021			
PNL-009-027	1.0000	0.0021			
<b>LEU-COMP-THERM-016 (Reference C.1)</b>					
PNL-016-008	1.0000	0.0031	UO <sub>2</sub> pellets enriched at 2.35 wt% U-235 clad in aluminum. Three variable sized clusters of fuel rods on a 2.032 cm pitch, separated by absorber plates with varying separation distances.	Stainless Steel (1.05 – 1.62 wt% Boron)	Water
PNL-016-009	1.0000	0.0031			
PNL-016-010	1.0000	0.0031			
PNL-016-011	1.0000	0.0031			
PNL-016-012	1.0000	0.0031			
PNL-016-013	1.0000	0.0031			
PNL-016-014	1.0000	0.0031			
PNL-016-031	1.0000	0.0031			
PNL-016-032	1.0000	0.0031			
				Zircaloy-4	

## C.4 Results of Calculations with SCALE 4.4a

The critical experiments described in Section C.3 were modeled with the SCALE 4.4a computer system. The resulting  $k_{\text{eff}}$  and calculational uncertainty, along with the experimental  $k_{\text{eff}}$  and experimental uncertainty are tabulated in Table C.3. The parameters of interest in performing a trending analysis of the bias are also included in the table.

In order to address situations in which the critical experiment being modeled was at other than a critical state (i.e., slightly super or subcritical), the calculated  $k_{\text{eff}}$  is normalized to the

experimental  $k_{\text{exp}}$ , using the following formula (Eq.9 from Reference C.2):  $k_{\text{norm}} = \frac{k_{\text{calc}}}{k_{\text{exp}}}$

In the following, the normalized values of the  $k_{\text{eff}}$  were used in the determination of the code bias and bias uncertainty.

# Controlled Document

Monticello Nuclear Plant Spent Fuel Storage Pool  
 Criticality Safety Analysis for ATRIUM™ 10XM Fuel

ANP-3113(NP)  
 Revision 0  
 Page C-9

**Table C.3 SCALE 4.4a Results for the Selected Benchmark Experiments**

No.	Case Name	Benchmark Values		SCALE 4.4a Calculated Values		Enrichment (wt% U-235)	Rod Pitch (cm)	H/X	EALF (eV)
		$k_{eff}$	$\sigma_{exp}$	$k_{eff}$	$\sigma_{calc}$				
1	CEA-001-001	1.0000	0.0014	0.9928	0.0009	4.74	1.26	110	0.247
2	CEA-001-002	1.0000	0.0008	0.9952	0.0008	4.74	1.6	229	0.110
3	CEA-001-003	1.0000	0.0007	0.9976	0.0009	4.74	2.1	455	0.070
4	CEA-001-004	1.0000	0.0008	0.9977	0.0008	4.74	2.52	693	0.060
5	CEA-003-003	1.0000	0.0039	1.0020	0.0009	4.74	1.6	229	0.143
6	CEA-003-004	1.0000	0.0039	0.9987	0.0009	4.74	1.6	229	0.139
7	CEA-003-005	1.0000	0.0039	0.9982	0.0009	4.74	1.6	229	0.135
8	CEA-003-006	1.0000	0.0039	1.0003	0.0009	4.74	1.6	229	0.131
9	CEA-003-007	1.0000	0.0039	0.9988	0.0008	4.74	1.6	229	0.129
10	CEA-003-008	1.0000	0.0039	0.9986	0.0008	4.74	1.6	229	0.127
11	CEA-003-010	1.0000	0.0048	0.9994	0.0008	4.74	1.6	229	0.149
12	CEA-003-011	1.0000	0.0048	1.0001	0.0009	4.74	1.6	229	0.147
13	CEA-003-012	1.0000	0.0048	0.9967	0.0008	4.74	1.6	229	0.145
14	CEA-003-013	1.0000	0.0048	0.9961	0.0009	4.74	1.6	229	0.142
15	CEA-003-014	1.0000	0.0043	0.9924	0.0009	4.74	1.6	229	0.140
16	CEA-003-015	1.0000	0.0043	0.9954	0.0008	4.74	1.6	229	0.137
17	CEA-005-001	1.0000	0.0014	0.9951	0.0009	4.74	1.26	110	0.227
18	CEA-005-002	1.0000	0.0014	0.9963	0.0010	4.74	1.26	110	0.216
19	CEA-005-003	1.0000	0.0014	0.9978	0.0009	4.74	1.26	110	0.197
20	CEA-005-004	1.0000	0.0014	0.9947	0.0008	4.74	1.26	110	0.186
21	CEA-005-005	1.0000	0.0009	0.9963	0.0008	4.74	1.26	110	0.141
22	CEA-005-006	1.0000	0.0009	0.9986	0.0009	4.74	1.26	110	0.146
23	CEA-005-007	1.0000	0.0012	0.9952	0.0009	4.74	1.26	110	0.217
24	CEA-005-008	1.0000	0.0012	0.9934	0.0010	4.74	1.26	110	0.208
25	CEA-005-009	1.0000	0.0012	0.9957	0.0009	4.74	1.26	110	0.202
26	CEA-005-010	1.0000	0.0012	0.9973	0.0008	4.74	1.26	110	0.176
27	CEA-005-011	1.0000	0.0013	0.9922	0.0008	4.74	1.26	110	0.227
28	CEA-005-012	1.0000	0.0013	0.9937	0.0009	4.74	1.26	110	0.222
29	CEA-005-013	1.0000	0.0013	0.9926	0.0009	4.74	1.26	110	0.219
30	CEA-005-014	1.0000	0.0013	0.9934	0.0009	4.74	1.26	110	0.218
31	CEA-005-015	1.0000	0.0013	0.9944	0.0009	4.74	1.26	110	0.217
32	CEA-005-016	1.0000	0.0013	0.9951	0.0009	4.74	1.26	110	0.214
33	CEA-005-017	1.0000	0.0013	0.9954	0.0009	4.74	1.26	110	0.215

# Controlled Document

Monticello Nuclear Plant Spent Fuel Storage Pool  
 Criticality Safety Analysis for ATRIUM™ 10XM Fuel

ANP-3113(NP)  
 Revision 0  
 Page C-10

**Table C.3 SCALE 4.4a Results for the Selected Benchmark Experiments** *(Continued)*

No.	Case Name	Benchmark Values		SCALE 4.4a Calculated Values		Enrichment (wt% U-235)	Rod Pitch (cm)	H/X	EALF (eV)
		$k_{eff}$	$\sigma_{exp}$	$k_{eff}$	$\sigma_{calc}$				
34	PNL-001-001	0.9998	0.0031	0.9970	0.0008	2.35	2.032	399	0.096
35	PNL-001-002	0.9998	0.0031	0.9958	0.0009	2.35	2.032	399	0.096
36	PNL-001-003	0.9998	0.0031	0.9947	0.0008	2.35	2.032	399	0.095
37	PNL-001-004	0.9998	0.0031	0.9955	0.0007	2.35	2.032	399	0.095
38	PNL-001-005	0.9998	0.0031	0.9950	0.0007	2.35	2.032	399	0.094
39	PNL-001-006	0.9998	0.0031	0.9963	0.0007	2.35	2.032	399	0.095
40	PNL-001-007	0.9998	0.0031	0.9959	0.0007	2.35	2.032	399	0.093
41	PNL-001-008	0.9998	0.0031	0.9936	0.0007	2.35	2.032	399	0.094
42	PNL-002-001	0.9997	0.0020	0.9963	0.0009	4.31	2.54	256	0.114
43	PNL-002-002	0.9997	0.0020	0.9956	0.0009	4.31	2.54	256	0.114
44	PNL-002-003	0.9997	0.0020	0.9961	0.0008	4.31	2.54	256	0.114
45	PNL-002-004	0.9997	0.0018	0.9951	0.0008	4.31	2.54	256	0.113
46	PNL-002-005	0.9997	0.0019	0.9945	0.0008	4.31	2.54	256	0.111
47	PNL-009-001	1.0000	0.0021	0.9979	0.001	4.31	2.54	256	0.114
48	PNL-009-002	1.0000	0.0021	0.9958	0.0007	4.31	2.54	256	0.113
49	PNL-009-003	1.0000	0.0021	0.9977	0.0008	4.31	2.54	256	0.114
50	PNL-009-004	1.0000	0.0021	0.9968	0.0008	4.31	2.54	256	0.114
51	PNL-009-005	1.0000	0.0021	0.9975	0.0008	4.31	2.54	256	0.115
51	PNL-009-006	1.0000	0.0021	0.9973	0.0009	4.31	2.54	256	0.114
53	PNL-009-007	1.0000	0.0021	0.9961	0.0009	4.31	2.54	256	0.115
54	PNL-009-008	1.0000	0.0021	0.9972	0.0008	4.31	2.54	256	0.114
55	PNL-009-009	1.0000	0.0021	0.9967	0.0008	4.31	2.54	256	0.115
56	PNL-009-024	1.0000	0.0021	0.9964	0.0007	4.31	2.54	256	0.114
57	PNL-009-025	1.0000	0.0021	0.9970	0.0009	4.31	2.54	256	0.114
58	PNL-009-026	1.0000	0.0021	0.9950	0.0008	4.31	2.54	256	0.113
59	PNL-009-027	1.0000	0.0021	0.9957	0.0008	4.31	2.54	256	0.113
60	PNL-016-008	1.0000	0.0031	0.9952	0.0007	2.35	2.032	399	0.097
61	PNL-016-009	1.0000	0.0031	0.9965	0.0008	2.35	2.032	399	0.096
62	PNL-016-010	1.0000	0.0031	0.9946	0.0006	2.35	2.032	399	0.097
63	PNL-016-011	1.0000	0.0031	0.9954	0.0007	2.35	2.032	399	0.096
64	PNL-016-012	1.0000	0.0031	0.9954	0.0007	2.35	2.032	399	0.097
65	PNL-016-013	1.0000	0.0031	0.9960	0.0007	2.35	2.032	399	0.096
66	PNL-016-014	1.0000	0.0031	0.9943	0.0007	2.35	2.032	399	0.097
67	PNL-016-031	1.0000	0.0031	0.9949	0.0008	2.35	2.032	399	0.095
68	PNL-016-032	1.0000	0.0031	0.9965	0.0007	2.35	2.032	399	0.095



## C.5 Trending Analysis

The next step of the statistical methodology used to evaluate the code bias for the pool of experiments selected is to identify any trend in the bias. This is done by using the following trending parameters:

- Fuel enrichment (wt% U-235)
- Fuel rod pitch
- Atom ratio of the moderator to fuel (H/X)
- Energy of the Average Lethargy causing Fission, EALF (eV)

The first step in calculating the bias uncertainty limit is to apply regression-based methods to identify any correlation of the calculated values of  $k_{\text{eff}}$  with the trending parameters. The trends show the results of systematic errors or bias inherent in the calculational method used to estimate criticality.

For the critical benchmark experiments that were slightly super or subcritical, an adjustment to the  $k_{\text{eff}}$  value calculated with SCALE 4.4a ( $k_{\text{calc}}$ ) was done as suggested in Reference C.2. This adjustment is done by normalizing the calculated ( $k_{\text{calc}}$ ) value to the experimental value ( $k_{\text{exp}}$ ). This normalization does not affect the inherent bias in the calculation due to very small differences in  $k_{\text{eff}}$ . Unless otherwise mentioned, the normalized  $k_{\text{eff}}$  values ( $k_{\text{norm}}$ ) have been used in all subsequent calculations.

The regression analysis employs the normalized  $k_{\text{eff}}$  values ( $k_{\text{norm}}$ ) and corresponding total uncertainty values ( $\sigma_i$ ), which are the values of the dependent variable and the corresponding weighting factors defined by  $1/\sigma_i^2$ , where  $\sigma_i = \sigma_i$  for the  $i^{\text{th}}$  data point. Data points consist of the ordered pairs  $(x_i, y_i)$ , where  $y_i = k_{\text{eff}}$  for the  $i^{\text{th}}$  data point. Reference C.2 suggests the use of weighting factors to reduce the importance of data with higher uncertainty. For this application, the weighted trends were evaluated and the results were verified by comparison to the non-weighted trending results.

Note that  $\sigma_i$  values are an intermediate calculational result and all downstream calculations should include all significant digits resulting from the intermediate calculation. Therefore, to be consistent with the guidance from Reference C.2, the weighting factors were evaluated as shown below with all significant digits included in later calculations.

# Controlled Document

$$\frac{1}{\sigma_i^2} = \left( \frac{1}{\sigma_{\text{exp}}^2 + \sigma_{\text{calc}}^2} \right)_i$$

The linear fitting function is defined as:  $y_i = mx_i + b$ , where  $m$  and  $b$  are the fitting coefficients, slope and intercept, respectively. The slope ( $m$ ) and intercept ( $b$ ) are determined by application of the following equations (from Reference C.2, page 8):

$$m = \frac{1}{\Delta} \left\{ \sum_i \frac{1}{\sigma_i^2} \sum_i \frac{x_i y_i}{\sigma_i^2} - \sum_i \frac{x_i}{\sigma_i^2} \sum_i \frac{y_i}{\sigma_i^2} \right\}$$

$$b = \frac{1}{\Delta} \left\{ \sum_i \frac{x_i^2}{\sigma_i^2} \sum_i \frac{y_i}{\sigma_i^2} - \sum_i \frac{x_i}{\sigma_i^2} \sum_i \frac{x_i y_i}{\sigma_i^2} \right\}$$

$$\Delta = \sum_i \frac{1}{\sigma_i^2} \sum_i \frac{x_i^2}{\sigma_i^2} - \left( \sum_i \frac{x_i}{\sigma_i^2} \right)^2$$

The weighted-average value of the dependent variable ( $\overline{k_{\text{eff}}}$ ) is calculated as follows:

$$\bar{y} = \frac{\sum_i \frac{y_i}{\sigma_i^2}}{\sum_i \frac{1}{\sigma_i^2}} = \overline{k_{\text{eff}}}$$

For the residuals, there are  $n - 2 = 66$  degrees of freedom, since there are  $n = 68$  data points.

The  $i^{\text{th}}$  value of the regression is expressed as  $\hat{y}_i = mx_i + b$  and the weighted sums of the squares for the residuals ( $SS_{\text{Residual}}$ ), for the regression ( $SS_{\text{Regression}}$ ), and for the total ( $SS_{\text{Total}}$ ) are calculated as follows:

# Controlled Document

$$SS_{\text{Residual}} = \frac{\sum_i \frac{(y_i - \hat{y}_i)^2}{\sigma_i^2}}{\sum_i \frac{1}{\sigma_i^2}}$$

$$SS_{\text{Regression}} = \frac{\sum_i \frac{(\hat{y}_i - \bar{y})^2}{\sigma_i^2}}{\sum_i \frac{1}{\sigma_i^2}}$$

$$SS_{\text{Total}} = SS_{\text{Residual}} + SS_{\text{Regression}}$$

These, in turn, allow calculation of the goodness-of-fit parameters: coefficient of correlation ( $r^2$ ), and the  $T_{\text{Value}}$  corresponding to the Student's T-distribution:

$$r^2 = \frac{SS_{\text{Regression}}}{SS_{\text{Total}}}$$

$$|T_{\text{Value}}| = \sqrt{\frac{(n-2)SS_{\text{Regression}}}{SS_{\text{Residual}}}}$$

The  $r^2$  value represents the proportion of the sum of the squares for the y-values about their mean that can be attributed to a linear relation between x and y. The closer that  $r^2$  approaches a value of 1, the better the fit of the data to the linear equation. As described in Section 10.3.2 of Reference C.3, calculated  $T_{\text{Values}}$  are compared with the critical value of the Student's T-distribution with a significance level of  $\alpha = 0.05/2 = 0.025$  and  $n - 2 = 66$  degrees of freedom (i.e., a critical value of 1.996). The null hypothesis for this test ( $H_0$ ), is that the slope is not statistically significant; thus, a statistically significant trend may exist if:  $|T_{\text{Value}}| > 1.996$ .

Alternatively, the probability of obtaining a  $T_{\text{Value}}$  of larger magnitude from a two-tailed T-distribution with the same  $n - 2 = 66$  degrees of freedom is calculated. In general, a low probability (e.g.,  $p < 0.05$ ) is necessary to confirm that a statistically significant trend exists.

In cases where a statistically significant trend is indicated by the Student's T-test, then the residuals of the regression are tested to determine if the error component is normally distributed with mean zero, which confirms that the statistical test for significance is valid (Section 10.4 of Reference C.3). The Anderson-Darling test described in Reference C.5 is employed for this

# Controlled Document

purpose; calculation of the test statistic ( $A^2$ ) proceeds by first sorting the sample into ascending order.

$$X_1 \leq \dots \leq X_n$$

Calculate the sample average  $\bar{X}$ , and standard deviation  $\sigma_x$ :

$$\bar{X} = \frac{1}{n} \sum_{i=1}^n X_i$$

$$\sigma_x = \sqrt{\frac{\sum_{i=1}^n (X_i - \bar{X})^2}{n-1}}$$

Then, compute standardized values:  $Y_i = \frac{X_i - \bar{X}}{\sigma_x}$ .

Now, the Anderson-Darling test statistic can be calculated, as shown:

$$A^2 = -\sum_{i=1}^n \left\{ (2i-1) \left[ \frac{\ln(P_i) + \ln(1-P_{n+1-i})}{n} \right] \right\} - n$$

Here,  $P_i$  is the cumulative normal probability corresponding to the standard score of  $Y_i$ , defined above. Finally, the calculated  $A^2$  value is adjusted for the size of the sample ( $n$ ):

$$A^* = A^2 \left( 1.0 + \frac{0.75}{n} + \frac{2.25}{n^2} \right)$$

The null hypothesis of normality is rejected if the value of  $A^*$  exceeds the critical value of 0.752, at a significance level of 0.05. Therefore, if  $A^* \leq 0.752$ , then the residuals are distributed normally and the statistical test for significance is valid.

Results of the weighted regression analysis and statistical tests are summarized in Table C.4 for all key parameters. This table shows that only H/X produces a valid trend. Therefore, a single-sided lower tolerance band will be used to establish the bias and uncertainty as a function of H/X. Although there is no trend for U-235 enrichment and the residuals for rod pitch

# Controlled Document

and EALF are not normally distributed (indicating an invalid trend), lower tolerance bands have also been calculated for these parameters. The intermediate results are listed in Table C.5.

Calculational details of the single-sided lower tolerance band can be found in Reference C.2 (pages 12 – 13); some details will be repeated here for the sake of convenience, clarity, and for verification of intermediate values used in the calculations. The equation for the single-sided lower tolerance band is as follows:

$$K_L(x) = K_{\text{fit}}(x) - (S_P)_{\text{fit}} \left\{ \sqrt{2F_a^{(\text{fit}, n-2)} \left[ \frac{1}{n} + \frac{(x - \bar{x})^2}{\sum_i (x_i - \bar{x})^2} \right]} + Z_{2P-1} \sqrt{\frac{(n-2)}{\chi_{1-\gamma, n-2}^2}} \right\}$$

$K_{\text{fit}}(x)$  is the function derived in the trending analysis for independent variable  $x$ . Because a positive bias may be non-conservative, the value  $K_{\text{fit}} = 1.00$  is substituted for all  $x$  where  $K_{\text{fit}}(x) > 1.00$ . Other symbols not previously introduced are defined below:

$p$  = the desired confidence level = 0.95

$F^{\text{fit}, n-2}$  = the F distribution percentile with degree of fit (2, for linear) and  $n-2$  degrees of freedom, based on the Excel function FINV with arguments (1-0.95, 2,  $n-2$ ).

$Z_{2P-1}$  = the symmetric percentile of the Gaussian (normal) distribution that contains the P fraction, based on the Excel function NORMSINV with argument (0.95).

$$\gamma = \frac{1-p}{2} = \frac{1-0.95}{2} = 0.025$$

$\chi_{1-\gamma, n-2}^2$  = the upper Chi-square percentile  
= based on the Excel function CHIINV with arguments (1-0.025,  $n-2$ ).

In addition to the constants defined above, the equations listed below are quantities that are dependent upon the type of fit and the specific independent variable (except that  $\bar{\sigma}^2$  is constant, as shown).

# Controlled Document

$$\bar{x} = \frac{\sum_i \frac{x_i}{\sigma_i^2}}{\sum_i \frac{1}{\sigma_i^2}}$$

$$\sum_i (x_i - \bar{x})^2 = \frac{\sum_i \frac{(x_i - \bar{x})^2}{\sigma_i^2}}{\frac{1}{n} \sum_i \frac{1}{\sigma_i^2}}$$

$$\bar{\sigma}^2 = \frac{n}{\sum_i \frac{1}{\sigma_i^2}}$$

$$s_{\text{fit}}^2 = \frac{\frac{1}{n-2} \sum_i \left\{ \frac{(y_i - \hat{y}_i)^2}{\sigma_i^2} \right\}}{\frac{1}{n} \sum_i \frac{1}{\sigma_i^2}}$$

$$(S_P)_{\text{fit}} = \sqrt{s_{\text{fit}}^2 + \bar{\sigma}^2}$$

Figures C.1 to C.4 show the normalized  $k_{\text{eff}}$  datasets plotted as a function of the weighted U-235 enrichment, rod pitch, H/X, and EALF data, respectively. The plotted data is overlaid with the linear trend line and the lower tolerance band. This lower tolerance band bounds 95% of the population with a confidence level of 95%.

# Controlled Document

Monticello Nuclear Plant Spent Fuel Storage Pool  
 Criticality Safety Analysis for ATRIUM™ 10XM Fuel

ANP-3113(NP)  
 Revision 0  
 Page C-17

**Table C.4 Results Summary for Weighted Trending Analysis**

Parameter	Enrichment (wt% U-235)	Rod Pitch (cm)	Moderating Ratio (H/X)	EALF (eV)
<b>Slope</b>	4.19E-05	1.14E-03	4.30E-06	-1.75E-02
<b>Intercept</b>	0.9957	0.9838	0.9949	0.9985
<b>r<sup>2</sup></b>	0.0003	0.1331	0.1429	0.3170
<b>Tcrit</b>	1.996	1.996	1.996	1.996
<b>  T-value  </b>	0.1422	3.1838	3.3175	5.5343
<b>P(T&gt;T-value)</b>	0.8874	0.0022	0.0015	5.802E-07
<b>Valid Trend?</b>	NO	YES	YES	YES
<b>A*</b>	---	1.2471	0.5916	0.8537
<b>Statistical Test Valid?</b>	---	NO	YES	NO

# Controlled Document

**Table C.5 Intermediate Results for Lower Tolerance Band Evaluation**

	$\bar{x}$	$\sum_i (x_i - \bar{x})^2$	$s_{fit}^2$	$(S_P)_{fit}$
<b>Weighted Fit</b>				
<b>Enrichment (wt% U-235)</b>	4.390	35.126	3.0529E-06	0.00270
<b>Rod Pitch (cm)</b>	1.766	20.620	2.6473E-06	0.00262
<b>Moderating Ratio H/X</b>	229.11	1.5584E+06	2.6174E-06	0.00262
<b>EALF (eV)</b>	0.1498	0.2082	2.0859E-06	0.00251



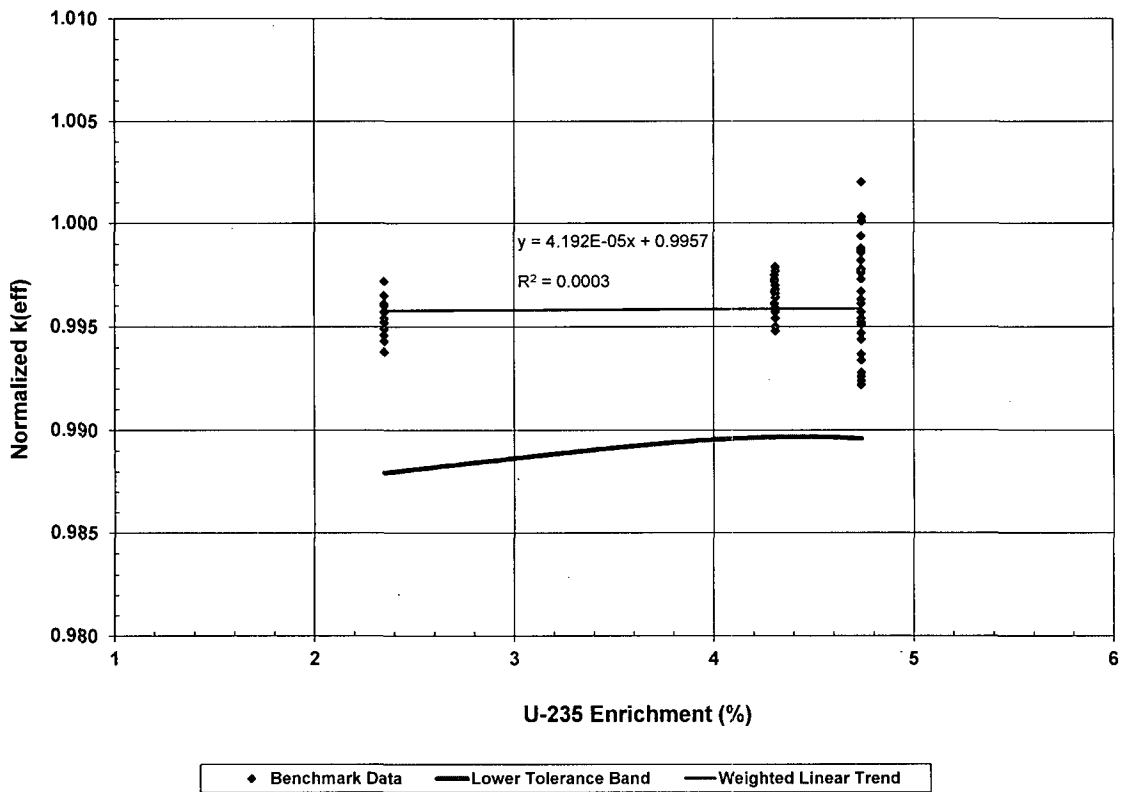


Figure C.1 Weighted U-235 Enrichment Trend Evaluation

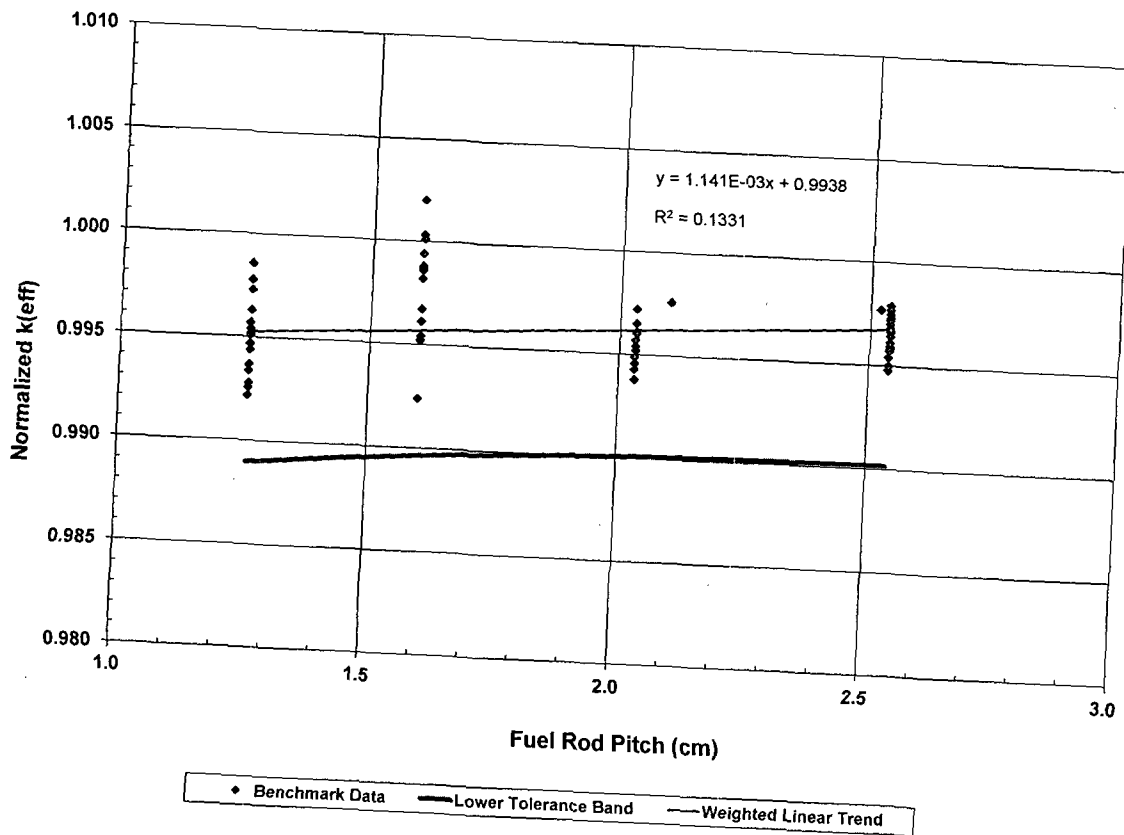


Figure C.2 Weighted Fuel Rod Pitch Trend Evaluation

# Controlled Document

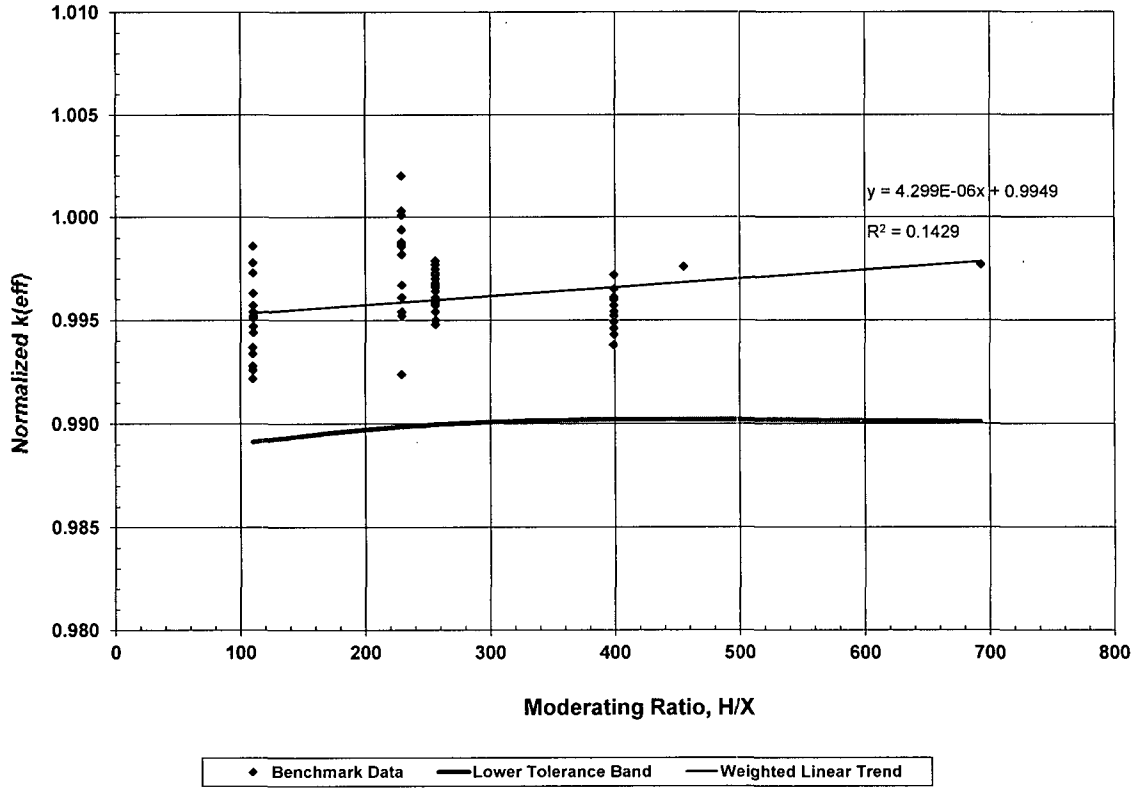


Figure C.3 Weighted H/X Trend Evaluation

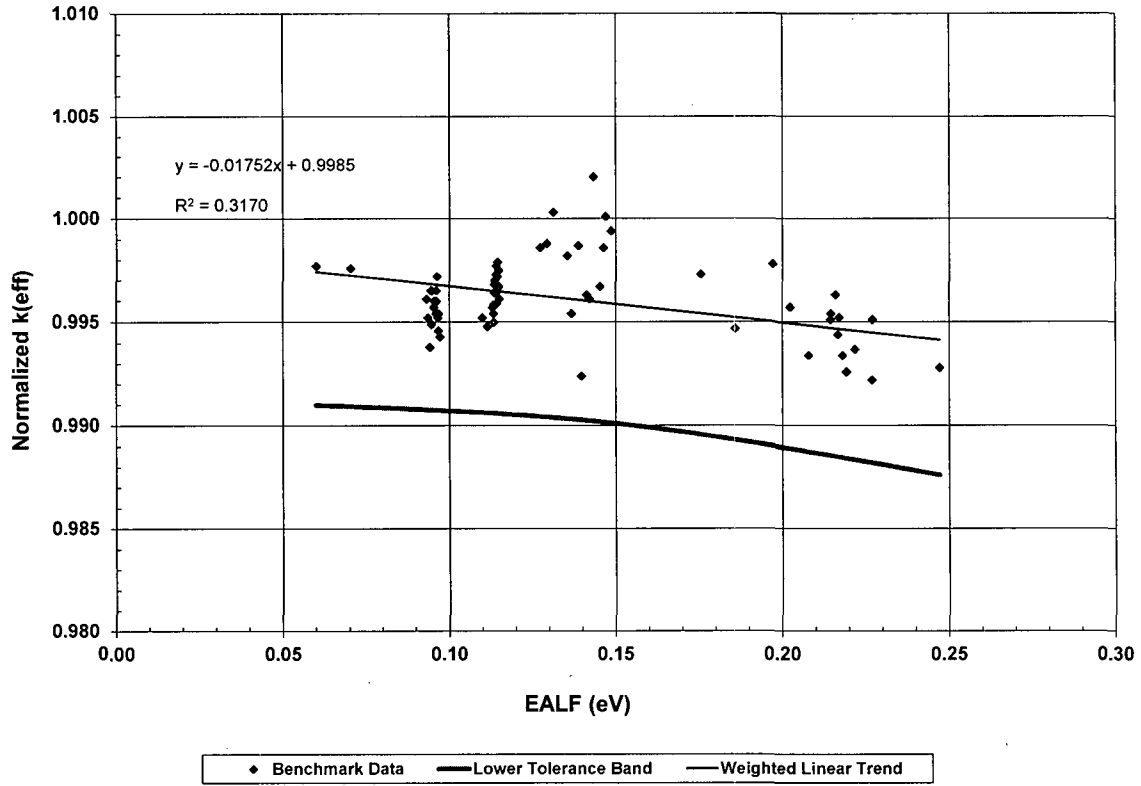


Figure C.4 Weighted EALF Trend Evaluation

**C.6 Bias and Bias Uncertainty**

For situations in which no significant trend in bias is identified the statistical methodology, presented in Reference C.2 and summarized in Section C.1 of this appendix, suggests to first check the distribution of the normalized  $k_{eff}$  dataset. The Anderson-Darling test statistic is calculated consistent with the description presented in Section C.5. The null hypothesis of normality is rejected if the value of  $A^*$  exceeds the critical value of 0.752, (based upon a significance level of 0.05). Therefore, if  $A^* \leq 0.752$ , then the data are distributed normally.

The Anderson-Darling test was completed for the 68 case benchmark set. The resulting Anderson-Darling test statistic modified from the number of data points  $A^*$  was determined to be 0.4186. A plot of the data relative to a normal distribution is provided in Figure C.5. Based on the test statistic and plot, the benchmark data can be considered normally distributed.

With the assumption of normality being validated, a single-sided lower tolerance limit can be used to determine the bias and uncertainty. For  $n = 68$ , the tolerance limit is  $C_{95/95} = 1.996$ , from Reference C.4. Results obtained for the weighted average  $k_{eff}$  ( $\overline{k_{eff}}$ ), the variance about the mean ( $s^2$ ), the average total uncertainty ( $\overline{\sigma}^2$ ), and the square-root of the pooled variance ( $S_p$ ), are shown below.

Weighted

$$\overline{k_{eff}} = \bar{y} = \frac{\sum_i y_i}{\sum_i \frac{1}{\sigma_i^2}} = 0.99585$$

$$\text{Bias} = k_{eff} - 1 = -0.00415$$

$$s^2 = \frac{\frac{1}{n-1} \sum_i \left\{ \frac{(y_i - \bar{y})^2}{\sigma_i^2} \right\}}{\frac{1}{n} \sum_i \frac{1}{\sigma_i^2}} = 3.0083 \cdot 10^{-6}$$

$$\overline{\sigma}^2 = \frac{n}{\sum_i \frac{1}{\sigma_i^2}} = 4.2355 \cdot 10^{-6}$$

# Controlled Document

$$S_p = \sqrt{s^2 + \bar{\sigma}^2} = 0.00269$$

The bias and bias uncertainty are:

$$\text{Bias} = -0.00415$$

$$\text{Uncertainty} = (C_{95/95})(S_p) = (1.996)(0.00269) = 0.00537$$

The corresponding lower tolerance limit is:

$$K_L = \bar{k}_{\text{eff}} - (C_{95/95})(S_p) = 0.99585 - 0.00537 = 0.99048$$

When this lower tolerance limit,  $K_L = 0.99048$ , is compared with the lower tolerance bands of the trended data in Figures C.1 through C.4, the lower tolerance limit is not sufficiently conservative to bound all the trended parameters. A minimum  $k_{\text{eff}}$  of 0.98761 is projected for the EALF\* trend evaluation (see Figure C.4). Based upon this minimum value, a trend corrected bias<sup>†</sup> can be calculated as follows:

$$\text{Bias}_{\text{corr}} = -0.00415 - (0.99048 - 0.98761) = -0.00702$$

If the magnitude of this corrected bias is conservatively adjusted to 0.0075 (with the pooled uncertainty rounded to 0.0027) a bounding limit is established as shown:

$$k_L = (1 - 0.0075) - (1.996)(0.0027) = 0.9871$$

These adjusted values will be used to represent this benchmark data, i.e.,  $|\text{Bias}| = 0.0075$  and  $S_p = 0.0027$ .

---

\* This is a conservative treatment because the EALF trend was shown to not be statistically valid in Table C.4.

† Including the trend correction in the bias term will result in a more conservative  $k_{95/95}$  than treating it as an increased uncertainty.

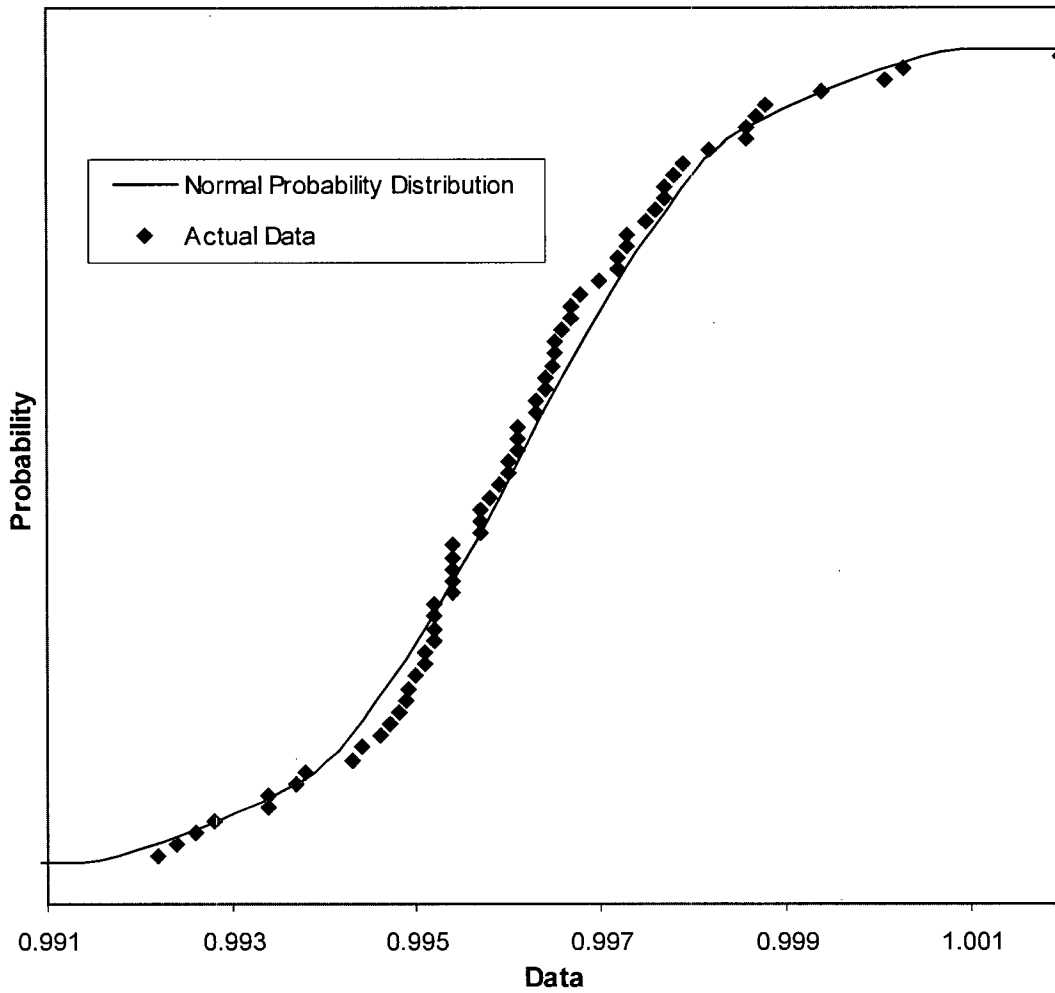


Figure C.5 Normal Probability Plot for the  $k_{eff}$  Dataset

# Controlled Document

## C.7 Area of Applicability

A brief description of the spectral and physical parameters characterizing the set of selected benchmark experiments is provided in Table C.6.

**Table C.6 Range of Values for Key Benchmark Experiment Parameters**

Parameter	Range of Values
Geometrical Shape	Heterogeneous lattices, with Square and Rectangular pitch
Fuel type	UO <sub>2</sub> fuel rods
Enrichment (for UO <sub>2</sub> fuel)	2.35 to 4.74 wt% U-235
Fuel rod pitch	1.26 to 2.54 cm
H/X	110 to >400
EALF	0.060 to 0.247 eV
Absorbers	Stainless steel, borated stainless steel, aluminum, Zircaloy-4, and Boral
Reflectors	Water Stainless Steel



## C.8 Bias Summary and Conclusions

The mixed dataset of 68 criticality safety benchmarks experiments was tested against the null hypothesis of normality and was found to be normally distributed. Thus, a parametric analysis was used to determine the bias and bias uncertainty, which resulted in a lower tolerance limit of  $K_L = 0.99048$ .

A standard trending analysis was also performed using linear regression analysis, including significance testing and goodness-of-fit evaluation. Four independent variables were examined: enrichment (wt% U-235), rod pitch, moderating ratio (H/X), and EALF (eV). The results of the trending analysis showed that the weighted trend for H/X met the criteria for statistical validity. Although most trends for the other parameters were deemed statistically insignificant, lower tolerance bands were calculated for all variables and then overlaid on the data plots to illustrate the effect.

When the lower tolerance limit,  $K_L = 0.99048$ , was compared with the lower tolerance bands of the trended data, the lower tolerance limit ( $K_L$ ) was not conservative for all trended parameters. Thus, the bias term was increased as shown below.

$$|\text{Adjusted bias}| = 0.0075$$

$$\text{Adjusted } K_L = (1 - 0.0075) - (1.996)(0.0027) = 0.9871$$

(The following adjusted values are referenced in Section 5.0 and applied in Section 7.8 of the report:  $|\text{Bias}| = 0.0075$  and  $S_p = 0.0027$ ).

# Controlled Document

## C.9 References

- C.1 Nuclear Energy Agency, "International Handbook of Evaluated Criticality Safety Benchmark Experiments," NEA/NSC/DOC(95)03, Nuclear Energy Agency, Organization for Co-operation and Development, September 2009.
- C.2 Nuclear Regulatory Commission, "Guide for Validation of Nuclear Criticality Safety Calculational Methodology", NUREG/CR-6698, January 2001.
- C.3 Rosenkrantz W.A., "Introduction to Probability and Statistics for Scientists and Engineers," The McGraw-Hill Companies Inc. 1997.
- C.4 Owen, D.B., "Factors for One-Sided Tolerance Limits and for Variables Sampling Plans," Sandia Corporation Monograph SRC-607, 1963.
- C.5 D'Agostino, R.B. and Stephens, M.A. "Goodness of Fit Techniques", *Statistics, Textbooks and Monographs*, Volume 68, New York, NY, 1986.
- C.6 Final Division of Safety Systems Interim Staff Guidance, DSS-ISG-2010-01 Revision 0, Staff Guidance Regarding The Nuclear Criticality Safety Analysis For Spent Fuel Pools, (ADAMS # ML110620086).
- C.7 NUREG/CR-6979, "Evaluation of the French Haut Taux de Combustion (HTC) Critical Experiment Data," September 2008, (ADAMS # ML082880452).

## Addendum to Appendix C

### Benchmark Extension with HTC Critical Experiments

Critical experiments with Plutonium and other actinides are outside of the area of applicability for BOL reactivity equivalent evaluations such as this one. However, item IV.4.a.i of the Reference C.6 guidance document indicates that the HTC critical experiments should be considered. This section has been created to demonstrate that it is reasonable to exclude the HTC critical experiments from the SCALE 4.4a benchmarking evaluation.

Twenty three of the 26 cases from the phase 3 experiments (Reference C.7) were added to the 68 cases shown in Tables C.2 and C.3 (producing a total of 91 cases). These cases were selected because they are similar to BWR spent fuel pool conditions and because they do not contain soluble boron or soluble gadolinia. The SCALE 4.4a results for these cases are shown in Table C.7. A statistical evaluation performed per Reference C.2 indicates that this expanded benchmark set is normally distributed with an average  $k_{eff}$  of 0.99765 with a pooled uncertainty of 0.002536. Therefore the Bias, the total uncertainty, and the parametric lower tolerance limit (see below) are less limiting for this expanded dataset than for the 68 case dataset (see Section C.6).

$$\text{Bias} = \overline{k_{eff}} - 1 = 0.99765 - 1 = -0.00235$$

$$\text{Uncertainty} = (C_{95/95})(S_p) = (1.942)(0.002536) = 0.00492$$

$$K_L = \overline{k_{eff}} - (C_{95/95})(S_p) = 0.99765 - 0.00492 = 0.99273$$

This extended dataset produced statistically significant trends for H/X and EALF. Therefore, lower tolerance bands were determined for these parameters (per Reference C.2) and the resulting comparison plots are included as Figures C.6 and C.7. These trend results show that the minimum overall value remains unchanged (about 0.988 for EALF at 0.247 eV).

From this comparison the recommended HTC critical benchmark cases can be excluded without creating non-conservative results. Since these benchmark cases are outside of the area of applicability for the BOL reactivity equivalent KENO calculations, the  $k_{95/95}$  evaluation in the main body of this report will be based upon the 68 case dataset summarized in Section C.8.

# Controlled Document

Monticello Nuclear Plant Spent Fuel Storage Pool  
 Criticality Safety Analysis for ATRIUM™ 10XM Fuel

ANP-3113(NP)  
 Revision 0  
 Page C-30

**Table C.7 SCALE 4.4a Results for the HTC Critical Benchmark Experiments**

No.	Case Name	Benchmark Values		SCALE 4.4a Calculated Values		Enrichment (wt% U-235)	Rod Pitch (cm)	H/X	EALF (eV)
		$k_{eff}$	$\sigma_{exp}$	$k_{eff}$	$\sigma_{calc}$				
<b>1 to 68 see Table C.3</b>									
69	HTC-2518	1.0000	0.0011	0.9973	0.0002	1.57	1.6	466	0.125
70	HTC-2521	1.0000	0.0011	0.9974	0.0002	1.57	1.6	466	0.131
71	HTC-2522	1.0000	0.0011	0.9975	0.0002	1.57	1.6	466	0.126
72	HTC-2523	1.0000	0.0011	0.9967	0.0002	1.57	1.6	466	0.137
73	HTC-2511	1.0000	0.0011	0.995	0.0002	1.57	1.6	466	0.131
74	HTC-2525	1.0000	0.0011	0.9955	0.0002	1.57	1.6	466	0.135
75	HTC-2526	1.0000	0.0011	0.9972	0.0003	1.57	1.6	466	0.131
76	HTC-2527	1.0000	0.0011	0.9942	0.0002	1.57	1.6	466	0.139
77	HTC-2509	1.0000	0.0008	0.999	0.0002	1.57	1.6	466	0.114
78	HTC-2531	1.0000	0.0008	0.9989	0.0002	1.57	1.6	466	0.113
79	HTC-2532	1.0000	0.0008	0.9995	0.0002	1.57	1.6	466	0.113
80	HTC-2532	1.0000	0.0008	0.999	0.0002	1.57	1.6	466	0.112
81	HTC-2533	1.0000	0.0008	0.9989	0.0002	1.57	1.6	466	0.112
82	HTC-2534	1.0000	0.0008	0.9978	0.0002	1.57	1.6	466	0.11
83	HTC-2536	1.0000	0.0008	0.9995	0.0002	1.57	1.6	466	0.107
84	HTC-2537	1.0000	0.0008	1.0003	0.0002	1.57	1.6	466	0.105
85	HTC-2538	1.0000	0.0008	1.0001	0.0002	1.57	1.6	466	0.103
86	HTC-2539	1.0000	0.0008	0.9998	0.0002	1.57	1.6	466	0.106
87	HTC-2541	1.0000	0.0008	0.9999	0.0002	1.57	1.6	466	0.108
88	HTC-2544	1.0000	0.0008	0.9985	0.0002	1.57	1.6	466	0.116
89	HTC-2547	1.0000	0.0008	0.9998	0.0002	1.57	1.6	466	0.154
90	HTC-2548	1.0000	0.0008	1.0001	0.0002	1.57	1.6	466	0.129
91	HTC-2549	1.0000	0.0008	0.9991	0.0002	1.57	1.6	466	0.117

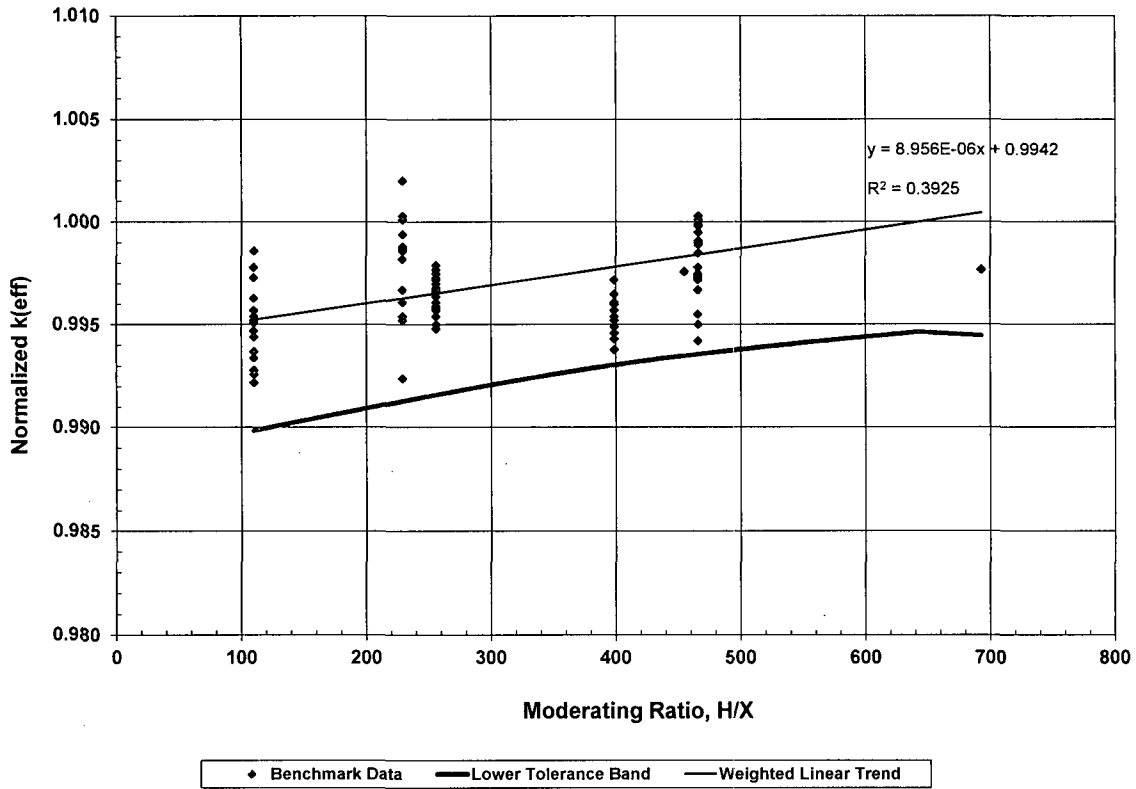


Figure C.6 Weighted H/X Trend (HTC Extended Benchmark)

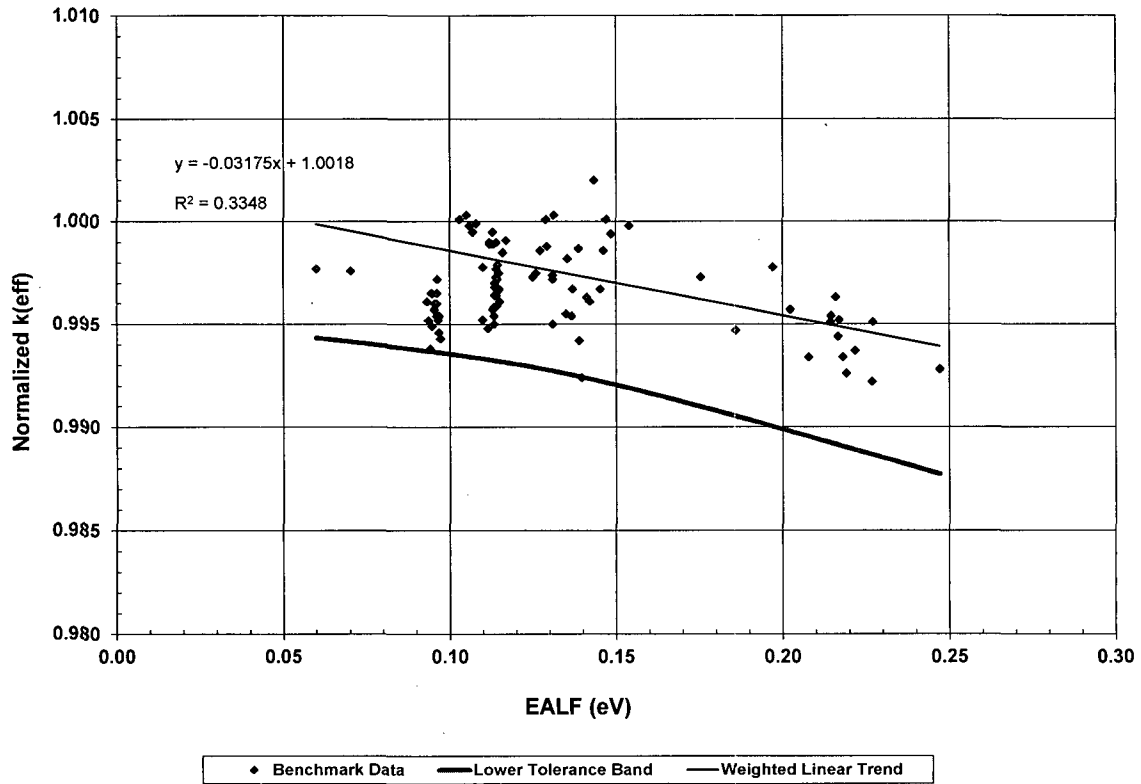


Figure C.7 Weighted EALF Trend (HTC Extended Benchmark)

## Appendix D CASMO-4 Qualification for In-Rack Modeling

### D.1 Introduction

The criticality safety analysis provided in this report is primarily a KENO V.a based analysis. However, KENO V.a does not have depletion capability so the CASMO-4 code is used for a subset of calculations that require fuel depletion. Since CASMO-4 is a two-dimensional code, it cannot provide stand-alone benchmark results of finite criticality experiments.

CASMO-4 has demonstrated acceptable isotopic depletion and nuclear library capability for reactor core related calculations in Reference D.1. It is a multi-group, two-dimensional transport theory code which also has an in-rack geometry option where typical storage rack geometries can be modeled on an infinite lattice basis. This code is used for fuel depletion in a manner that is consistent with AREVA's NRC approved CASMO-4 / MICROBURN-B2 methodology (Reference D.1). The library files used in this evaluation are the standard CASMO-4 70 group library based on ENDFB-IV. The CASMO-4 computer code and data library are controlled by AREVA procedures and the version used in this analysis meets the requirements of Reference D.1.

Within this criticality evaluation, CASMO-4 is used to:

- perform a  $k_{\infty}$  ranking of fuel lattices at peak in-rack reactivity conditions (see Appendix B)
- define reference lattices that are more reactive than all past and expected future fuel lattices (the lattices of the reference bounding assembly)
- define fresh fuel reactivity equivalent lattices\* for use in KENO V.a.

In support of this usage, this appendix will:

- compare CASMO-4  $k_{\infty}$  results with KENO V.a to demonstrate that the fuel storage rack option in CASMO-4 also produces reasonable results
- estimate the CASMO-4 depletion uncertainty
- demonstrate that the CASMO-4 depletion uncertainty combined with a CASMO-4 calculational uncertainty is smaller than the 0.010  $\Delta k$  uncertainty added that is applied when the REBOL lattice is defined.

---

\* REBOL lattices.

## D.2 $k_{\infty}$ Comparisons

These comparisons are performed in accordance with the guidance provided in References D.2. They are performed to quantify the differences in predicted  $k_{\infty}$  between CASMO-4 and KENO V.a (Section D.2.2.1) and to demonstrate that a  $\Delta k$  predicted by CASMO-4 is nearly identical to a  $\Delta k$  predicted by KENO V.a (Section D.2.2.2).

### D.2.1 Comparison Methodology

The evaluation in this appendix will compare the  $k_{\infty}$  values produced by the CASMO-4 code to the SCALE 4.4a KENO V.a code for different geometries and U-235 enrichment levels.

The validation of the CASMO-4 code in this Appendix is performed in two steps to demonstrate its acceptability for the two different ways that CASMO-4 is used in this analysis.

- Identify the relative reactivity of a lattice with the use of the storage rack geometry option. This is addressed by determining the CASMO-4 uncertainty relative to KENO V.a by comparison of calculated k-infinities from the two codes.
- Evaluate relative changes in reactivity associated with changes in geometry and U-235 enrichment. For this evaluation, the differential k-infinities from the two codes are compared based upon the same input perturbations.

These different approaches are described in more detail in the following sections.

#### D.2.1.1 CASMO-4 Uncertainty for Absolute $k_{\infty}$ Relative to KENO

The approach taken is to perform a series of calculations with varied enrichments and geometries with the two codes and then to compare the  $k_{\infty}$  results. The validation guidance of NUREG/CR-6698 (Reference D.2) is followed to determine a code uncertainty for CASMO-4 relative to KENO V.a. The KENO V.a calculations are treated as the critical experiments in this comparison. GE8x8 fuel as well as top and bottom lattices from the GE9x9, GE10x10, ATRIUM-10 (10x10), and ATRIUM 10XM (10x10) product lines are used.

#### D.2.1.2 CASMO-4 Uncertainty for $\Delta k_{\infty}$ Relative to KENO

The capability of the CASMO-4 code to predict the change in reactivity associated with a perturbation of fuel parameters is demonstrated by comparison of  $\Delta k$  values obtained with KENO V.a to those obtained with CASMO-4. The approach taken is to evaluate small



# Controlled Document

perturbations in reactivity by varying the enrichment relative to a base case. The same cases used in the evaluation of the uncertainty of the absolute multiplication factor are used in this evaluation. The  $\Delta k$  values will be determined for both KENO V.a and CASMO-4 for enrichment perturbations from the reference case.

The  $\Delta k$  values are compared between the two codes and a statistical evaluation similar to that identified in Reference D.2 is used to establish an uncertainty for the determination of  $\Delta k$  values with CASMO-4 relative to  $\Delta k$  values with KENO V.a.

### D.2.1.3 Experiment Descriptions

As noted, KENO calculations are used as the reference experiments. The evaluations are based on the Boral storage racks in the Monticello spent fuel pool. The validation is performed using GE8x8 lattices and both bottom and top lattices from the GE9x9, GE10x10, ATRIUM-10 (10x10), and ATRIUM 10XM (10x10) product lines. These lattices represent the limiting past and current fuel types for the Monticello Nuclear plant. Enrichment is varied in 0.05 increments around a base of 3.35% U-235 by weight. A total of eleven (11) enrichment levels from a minimum of 3.1 wt% to a maximum of 3.6 wt% are evaluated.

The calculations are reported for 4 °C since it represents the limiting in-rack reactivity condition for the Boral storage racks (see Table 6.1). The fuel assembly data and rack geometry are consistent with the inventory and configuration of the Monticello spent fuel pool.

**D.2.2 Analysis of Validation Results****D.2.2.1 CASMO-4 Uncertainty for Absolute k-effective Relative to KENO**

The calculated multiplication factors from KENO and CASMO were tabulated. The  $\sigma_{keno}$  terms are taken from each individual KENO calculation and the  $\sigma_{casmo}$  terms are set to the CASMO-4 convergence criterion for the individual case. (Use of the CASMO convergence is consistent with footnote 1 on page 6 of Reference D.2.) A combined uncertainty  $\sigma_{tot}$  was determined consistent with equation 3 of Reference D.2.

$$\sigma_{tot} = \sqrt{\sigma_{keno}^2 + \sigma_{casmo}^2}$$

The tabulated results are provided in Table D.1 for variations of geometry and enrichment. The geometry is specified by product line. A suffix of 'B' or 'T' is used to describe bottom or top lattice geometry, respectively. For example, 'A10XMT' specifies ATRIUM 10XM top lattice geometry. The GE8x8 fuel contains only one geometry configuration and therefore does not have this suffix. The differences of the calculated multiplication factor values along with the components used in the statistical evaluation are provided in Table D.2.

The weighted average difference ( $\Delta k_{bar}$ ), the variance about the mean ( $s^2$ ), and the average total uncertainty ( $\sigma^2$ ) are calculated using the weighting factor  $1/\sigma_i^2$ . The square root of the pooled variance is determined per Equation 7 of Reference D.2 as shown. These results are listed below.

$$S_p = \sqrt{s^2 + \sigma^2}$$

[

]

# Controlled Document

Monticello Nuclear Plant Spent Fuel Storage Pool  
Criticality Safety Analysis for ATRIUM™ 10XM Fuel

ANP-3113(NP)  
Revision 0  
Page D-5

The simple average and standard deviation values were also tabulated by lattice geometry type:

[

]

A data normality test was completed using the Anderson-Darling test (see section 9.5.4.1 of Reference D.3). (The Anderson-Darling test is described in Section C.5 of Appendix C). The AD test statistic was calculated to be 0.8143 and the criterion is 0.746 \*. Since the AD test statistic is greater than the test criterion one can conclude that the data is not from a normal distribution.

A distribution free one sided tolerance limit evaluation was also performed for this data set of 99 values. This was performed for both the upper and lower bounds. This evaluation indicated that on a 95/95 basis the more limiting  $k_{\alpha}$  difference boundary is [            ]. For the weighted mean difference of [            ] and the limiting boundary value (above), the limiting effective uncertainty<sup>†</sup> term is [            ].

---

\* In Appendix C the AD test statistic was adjusted for the number of data points and compared to the criteria of 0.752. In this appendix, the criterion was adjusted for the number of data points.

† As indicated by equation 20 of Reference D.2, the uncertainty component is effectively the difference between the limiting boundary and the mean value.

# Controlled Document

Monticello Nuclear Plant Spent Fuel Storage Pool  
Criticality Safety Analysis for ATRIUM™ 10XM Fuel

ANP-3113(NP)  
Revision 0  
Page D-6

---

## Area of Applicability

The fuel and rack geometries as well as representative fuel enrichments were selected to be consistent with the Monticello GE High density Boral storage racks. It is recognized that spent fuel pool storage tube modeling simplifications are included in the CASMO model relative to the more explicit model used with KENO, see Section 6.1. This difference in the modeling technique is included in this comparison. The REBOL lattice enrichment and geometries used in the  $k_{95/95}$  determination for the Monticello Spent Fuel Pool are within the area of applicability of this comparison.

# Controlled Document

Monticello Nuclear Plant Spent Fuel Storage Pool  
Criticality Safety Analysis for ATRIUM™ 10XM Fuel

ANP-3113(NP)  
Revision 0  
Page D-7

---

## Table D.1 CASMO-4 and KENO V.a Validation Case Information

[

]

# Controlled Document

Monticello Nuclear Plant Spent Fuel Storage Pool  
Criticality Safety Analysis for ATRIUM™ 10XM Fuel

ANP-3113(NP)  
Revision 0  
Page D-8

---

**Table D.1 CASMO4 and KENO Validation Case Information** *(Continued)*

[

]

# Controlled Document

Monticello Nuclear Plant Spent Fuel Storage Pool  
Criticality Safety Analysis for ATRIUM™ 10XM Fuel

ANP-3113(NP)  
Revision 0  
Page D-9

---

## Table D.1 CASMO4 and KENO Validation Case Information *(Continued)*

[

]

# Controlled Document

Monticello Nuclear Plant Spent Fuel Storage Pool  
Criticality Safety Analysis for ATRIUM™ 10XM Fuel

ANP-3113(NP)  
Revision 0  
Page D-10

**Table D.2 CASMO - KENO Difference and Statistical Parameters**

[

]

---

\*  $\Delta k$  is  $k_{\text{CASMO}} - k_{\text{KENO}}$



# Controlled Document

Monticello Nuclear Plant Spent Fuel Storage Pool  
Criticality Safety Analysis for ATRIUM™ 10XM Fuel

ANP-3113(NP)  
Revision 0  
Page D-11

**Table D.2 CASMO - KENO Difference and Statistical Parameters** *(Continued)*

[

]

---

\*  $\Delta k$  is  $k_{\text{CASMO}} - k_{\text{KENO}}$

# Controlled Document

Monticello Nuclear Plant Spent Fuel Storage Pool  
Criticality Safety Analysis for ATRIUM™ 10XM Fuel

ANP-3113(NP)  
Revision 0  
Page D-12

**Table D.2 CASMO - KENO Difference and Statistical Parameters** *(Continued)*

[

]

---

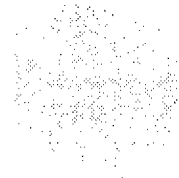
\*  $\Delta k$  is  $k_{\text{CASMO}} - k_{\text{KENO}}$

# Controlled Document

Monticello Nuclear Plant Spent Fuel Storage Pool  
Criticality Safety Analysis for ATRIUM™ 10XM Fuel

ANP-3113(NP)  
Revision 0  
Page D-13

[



1

**Figure D.1 Normality Plot for CASMO-KENO k-infinity Comparison**

# Controlled Document

## D.2.2.2 CASMO-4 Uncertainty for $\Delta k$ -effective

The actual KENO and CASMO calculations used in this  $\Delta k$  evaluation are those used in Section D.2.2.1. In this evaluation, the relative reactivity change is evaluated by taking the delta with respect to the reference case. A difference is then determined between the  $\Delta k$  values obtained with KENO and the  $\Delta k$  values obtained with CASMO-4 for the same perturbation.

The Anderson-Darling goodness of fit for normality test was also completed with the AD test statistic calculated to be 0.7425 with the criterion of 0.7456. Based on these results and the comparison in Figure D.2, it is determined that the data is normally distributed.

The magnitude of the average difference between the  $\Delta k$  values was [ ] with a standard deviation of [ ]. For the data sample of 50 the single sided tolerance factor is 2.065 from Table 2.1 of Reference D.2. This is conservatively applied for 90 data samples. Therefore the 95/95 bias uncertainty is: [ ] when rounded to four decimal places.

### Area of Applicability

The fuel and rack geometries as well as representative fuel enrichments were selected to be consistent with the Monticello GE High density Boral storage racks. It is recognized that spent fuel pool storage tube modeling simplifications are included in the CASMO model relative to the more explicit model used with KENO, see Section 6.1. This difference in the modeling technique is included in this comparison. The REBOL lattice enrichment and geometries used in the  $k_{95/95}$  determination for the Monticello Spent Fuel Pool are within the area of applicability of this comparison.

# Controlled Document

Monticello Nuclear Plant Spent Fuel Storage Pool  
Criticality Safety Analysis for ATRIUM™ 10XM Fuel

ANP-3113(NP)  
Revision 0  
Page D-15

---

[ **Table D.3 CASMO versus KENO Relative Reactivity Differences at 4°C**

]

# Controlled Document

Monticello Nuclear Plant Spent Fuel Storage Pool  
Criticality Safety Analysis for ATRIUM™ 10XM Fuel

ANP-3113(NP)  
Revision 0  
Page D-16

**Table D.3 CASMO versus KENO Relative Reactivity Differences at 4°C** *(Continued)*

[

]

# Controlled Document

Monticello Nuclear Plant Spent Fuel Storage Pool  
Criticality Safety Analysis for ATRIUM™ 10XM Fuel

ANP-3113(NP)  
Revision 0  
Page D-17

---

**Table D.3 CASMO versus KENO Relative Reactivity Differences at 4°C** *(Continued)*

[

]

# Controlled Document

Monticello Nuclear Plant Spent Fuel Storage Pool  
Criticality Safety Analysis for ATRIUM™ 10XM Fuel

ANP-3113(NP)  
Revision 0  
Page D-18

[

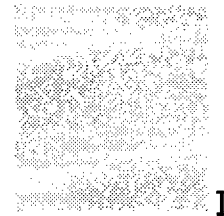


**Figure D.2 Normality Plot for  $\Delta k_{\text{CASMO}}$  -  $\Delta k_{\text{KENO}}$   $\Delta k$ -infinity Comparison**



## D.3 Depletion Uncertainty Estimates

Depletion uncertainty estimates from EMF-2158(P) (Reference D.1) and from the interim staff guidance document (Reference D.5) will be described in this section.

### D.3.1 EMF-2158 Based Depletion Uncertainty

The CASMO-4 depletion uncertainty is derived from the AREVA licensing topical report based on the extensive benchmarking that is documented within Reference D.1. Comparisons against critical experiments were performed by Studsvik with results reported in Table 2.1 of AREVA's CASMO-4/MICROBURN-B2 licensing topical report (Reference D.1). In addition, the beginning of cycle cold critical calculations reported in Table 2.2 of this same licensing topical report also provide comparisons to critical data. Results of these comparisons indicate that CASMO-4 results will have a standard deviation of [ ]  $\Delta k$  (Table 2.1 of Reference D.1) without depletion and a standard deviation of [ ]  $\Delta k$  (Table 2.2 of Reference D.1) when the majority of assemblies have been depleted\*.

### D.3.2 ISG Based Depletion Uncertainty

Five percent of the reactivity difference from BOL (without gadolinia) to peak reactivity is used to estimate the isotopic uncertainty associated with depletion to peak reactivity, (i.e., the uncertainty in the uranium depletion, fission product production, and actinide production). The approach presented here is a conservative application of the 5% reactivity decrement approach originally suggested in Section 5.A.5.d of the Kopp memo (Reference D.4) and currently addressed in DSS-ISG-2010-01 (Reference D.5).

The reference bounding and limiting lattices used in this comparison are identified in Table B.1. All lattices are depleted in-core and then evaluated at the limiting moderator temperature (4 °C) in the fuel storage rack configuration. Figure D.3 illustrates the two reactivity decrement values used.

---

\* The uncertainty of cold critical benchmarks effectively includes a depletion uncertainty since the majority of the bundles in the core have some depletion. It is noted, that an in-sequence critical has significant similarities to an in-rack calculation since the majority of the control blades remain inserted effectively surrounding the majority of the fuel with a strong neutron absorber on two sides.

# Controlled Document

A BOL no gad solution for each lattice was completed by removing the gadolinium and maintaining the same uranium number density in the lattice.\* The depletion reactivity reactivity decrement is determined by subtracting the peak in-rack  $k_{\infty}$  from the BOL no gad in-rack  $k_{\infty}$ . A second reactivity decrement representing the uncertainty in gadolinia content was also determined by subtracting the peak in-rack  $k_{\infty}$  from a value similar to the gadolinia free  $k_{\infty}$  at the peak reactivity exposure†.

Based on the calculation process illustrated in Figure D.3, five percent of the burn-up reactivity decrement ( $\Delta k_{bu}=0.05*\Delta k$ ) and five percent of the residual gadolinia reactivity change ( $\Delta k_{gd}=0.05*\Delta k_{g}$ ) are tabulated in Table D.4 for the limiting lattices. This assessment produces a maximum depletion uncertainty of 0.0055  $\Delta k$  for the reference bounding lattices.

It is noted that this process will produce a larger penalty as the gadolinia content increases (either the number of rods or the concentration). However, increasing the gadolinia content within a given lattice will substantially decrease the peak in-rack  $k_{\infty}$  of the lattice as shown in Figure D.4.

---

\* This is accomplished by setting the gadolinia number densities to zero with the CASMO GNU input.

† The peak  $k_{\infty}$  values with no gadolinia assume an in-core depletion with gadolinia to the maximum reactivity exposure, all gadolinia is then removed and an in-rack calculation is performed.

# Controlled Document

Monticello Nuclear Plant Spent Fuel Storage Pool  
Criticality Safety Analysis for ATRIUM™ 10XM Fuel

ANP-3113(NP)  
Revision 0  
Page D-21

**Table D.4 Depletion Uncertainty Values for Limiting Lattices**

	Peak $k_{\infty}$	BOL $k_{\infty \text{ nogad}}$	Peak $k_{\infty \text{ nogad}}^*$	$\Delta k_{bu}$ ( $0.05 \cdot \Delta k$ )	$\Delta k_{gd}$ ( $0.05 \cdot \Delta k_{gd}$ )	$\Delta k_{bu} +$ $\Delta k_{gd}$
<b>Top Zone</b>						
limiting legacy lattice	0.8452	0.9554	0.8616	0.0055	0.0008	0.0063
<b>Bounding Lattice</b>	<b>0.8797</b>	<b>0.9638</b>	<b>0.8931</b>	<b>0.0042</b>	<b>0.0007</b>	<b>0.0049</b>
<b>Bottom Zone</b>						
limiting legacy lattice	0.8410	0.9508	0.8565	0.0055	0.0008	0.0063
<b>Bounding Lattice</b>	<b>0.8790</b>	<b>0.9733</b>	<b>0.8954</b>	<b>0.0047</b>	<b>0.0008</b>	<b>0.0055</b>

\* The Peak k-infinity values with no gadolinia assume in-core depletion with gadolinia to the maximum reactivity exposure, all gadolinia is then removed and an in-rack calculation is performed.

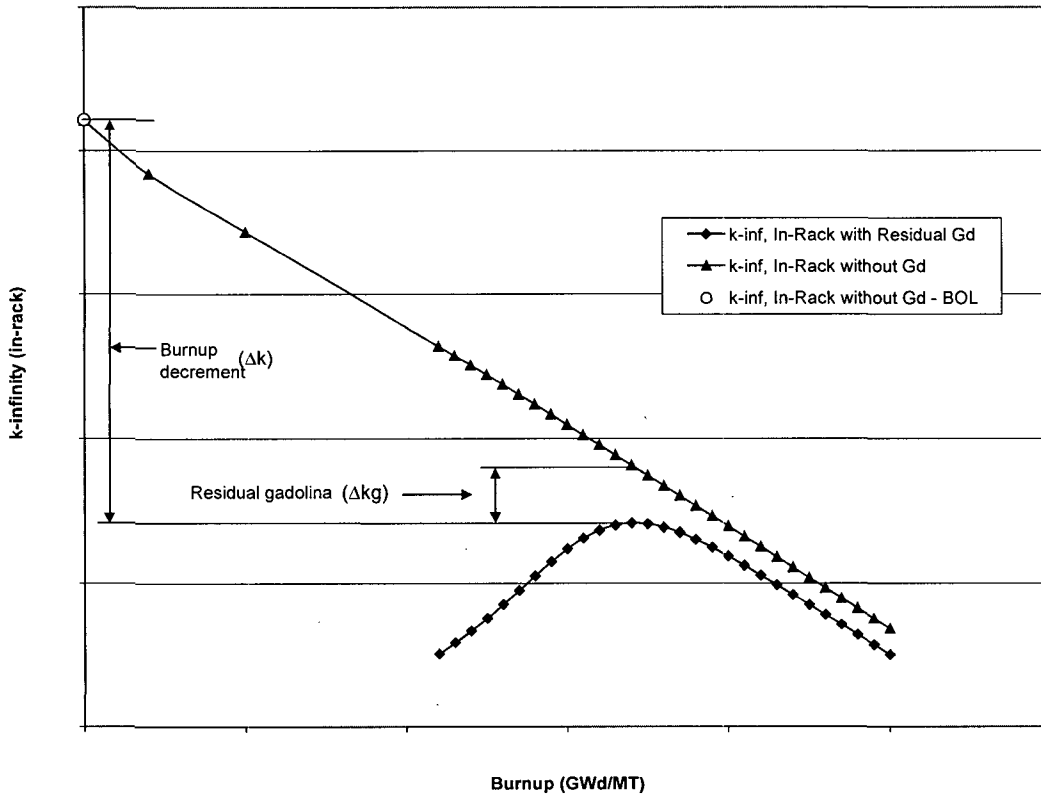


Figure D.3 Representation of the ISG Depletion Uncertainty Assessment

# Controlled Document

[

Figure D.4 Gadolinia Concentration Sensitivity

]

**Figure D.4 Gadolinia Concentration Sensitivity**

# Controlled Document

## D.4 Conclusions and Overall Uncertainty

The evaluation of GE8x8 fuel lattices as well as top and bottom lattices from the GE9x9, GE10x10, ATRIUM-10 (10x10), and ATRIUM 10XM (10x10) product lines demonstrated that the CASMO-4 fuel storage rack calculations will produce reasonable results for these types of geometries. In addition, it has been demonstrated that reasonable results can be obtained for U-235 enrichment levels between 3.1 and 3.6 wt% U-235. These comparisons also indicate that [

].

When applied on a differential basis a  $\Delta k$  predicted by CASMO-4 agrees with the KENO V.a based  $\Delta k$  with a standard deviation of [ ]  $\Delta k$ , (see Section D.2.2.2). This can be combined with uncertainty estimates from EMF-2158(P) (Section D.3.1) or the estimated depletion uncertainty determined with the method from the interim staff guidance document (Section D.3.2) to produce a maximum combined value. A 95/95 uncertainty result is obtained by multiplying these uncertainty values by an appropriate multiplier. Since these values are independent they will be combined using the square root of the sum of the squares as shown below. This process results in a maximum combined uncertainty of [ ]. The 0.010  $\Delta k$  adder used when defining the REBOL lattices conservatively bounds this CASMO-4 uncertainty value.

Uncertainty Value	$\sigma$	95/95 Multiplier	95/95 Uncertainty	Combined Uncertainty
Calculational ( $\Delta k_{\infty}$ based)	[ ]	2.065	[ ]	
EMF-2158 Depletion	[ ]	2.0	[ ]	[ ]
Calculational ( $\Delta k_{\infty}$ based)	[ ]	2.065	[ ]	
ISG Depletion	---	---	0.0055*	[ ]

\* This is not necessarily a 95/95 value; however, it is acceptable per Section IV.2.a of Reference D.5.

# Controlled Document

## D.5 References

- D.1 EMF-2158(P)(A) Revision 0, *Siemens Power Corporation Methodology for Boiling Water Reactors: Evaluation and Validation of CASMO-4/MICROBURN-B2*, Siemens Power Corporation, October 1999.
- D.2 NUREG/CR-6698, "Guide for Validation of Nuclear Criticality Safety Computational Methodology," USNRC, January 2001.
- D.3 MIL-HDBK-5J, "Metallic Materials and Elements for Aerospace Vehicle Structures," Department of Defense Handbook, January 2003.
- D.4 Memorandum L. Kopp to T. Collins, "Guidance on the Regulatory Requirements for Criticality Analysis of Fuel Storage at Light-Water Reactor Power Plants," NRC, August 19, 1998. (NRC –ADAMS Accession Number ML072710248)
- D.5 Final Division of Safety Systems Interim Staff Guidance, DSS-ISG-2010-01 Revision 0, Staff Guidance Regarding The Nuclear Criticality Safety Analysis For Spent Fuel Pools, (NRC - ADAMS Accession Number ML110620086).